

# **Characterization of protein complexes associated with TRP channels in the context of nociception**

Dissertation

for the award of the degree

*“Doctor rerum naturalium”*

of the Georg-August-Universität Göttingen

within the doctoral program Sensory and Motor Neuroscience  
of the Göttingen Graduate School for Neurosciences, Biophysics, and  
Molecular Biosciences (GGNB)  
of the Georg-August University School of Science (GAUSS)

submitted by

**Luca Avenali**

From Jesi, Italy

Göttingen 2015

## **Thesis committee**

### **Dr. Manuela Schmidt**

Somatosensory Signaling group  
Max Planck Institute of Experimental Medicine, Göttingen

### **Prof. Dr. Martin C. Göpfert**

Dept. of Cellular Neurobiology  
Schwann-Schleiden Research Centre, Georg-August-Universität, Göttingen

### **Prof. Dr. Klaus-Armin Nave**

Dept. of Neurogenetics  
Max Planck Institute of Experimental Medicine, Göttingen

## **Members of the Examination Board**

### **Referee: Dr. Manuela Schmidt**

Somatosensory Signaling group  
Max Planck Institute of Experimental Medicine, Göttingen

### **2<sup>nd</sup> Referee: Prof. Dr. Martin C. Göpfert**

Dept. of Cellular Neurobiology  
Schwann-Schleiden Research Centre, Georg-August-Universität, Göttingen

## **Further members of the Examination Board**

### **Prof. Dr. Klaus-Armin Nave**

Dept. of Neurogenetics  
Max Planck Institute of Experimental Medicine, Göttingen

### **Prof. Dr. Michael W. Sereda**

AG Molecular and Translational Neurology  
Max Planck Institute of Experimental Medicine, Göttingen

### **Prof. Dr. Ralf Heinrich**

Dept. of Cellular Neurobiology  
Schwann-Schleiden Research Centre, Georg-August-Universität, Göttingen

### **Prof. Dr. Luis A. Pardo**

Dept. of Molecular Biology of Neuronal Signals  
Max Planck Institute of Experimental Medicine, Göttingen

Date of oral examination: 29<sup>th</sup> January 2016

**Declaration:**

I hereby declare that this doctoral thesis is my own work and has been written independently, with no other sources and aids than quoted.

Göttingen, 1<sup>st</sup> December 2015

Luca Avenali

# Table of Contents

List of figures.....	4
Abbreviations.....	5
<b>1. INTRODUCTION.....</b>	<b>6</b>
1.1 Pain .....	6
1.2 Nociception and the pain pathway.....	7
1.3 The nociceptor in chronic pathological pain .....	10
1.4 Transient receptor potential (TRP) ion channels.....	11
1.4.1 General information .....	11
1.4.2 Role in sensory transduction .....	12
1.4.3 TRP channels and pain .....	14
1.4.3.1 TRPV1.....	14
1.4.3.2 TRPM8 .....	15
1.5 TRPA1.....	16
1.5.1 Gene and protein structure .....	16
1.5.2 Activation .....	17
1.5.3 Expression .....	19
1.5.4 Role in pain .....	19
1.5.5 Regulation .....	20
1.6 Protein complexes as modulators of receptor function in pain.....	21
1.7 Aims of the study.....	23
<b>2. MATERIALS AND METHODS .....</b>	<b>24</b>
Reagents .....	24
Methods.....	25
2.1 Annexin A2 (AnxA2) regulates TRPA1-dependent nociception.....	25
2.1.1 Protein identification by mass spectrometry analysis and database search.....	25
2.1.2 Cloning of the AnxA2 N-term deletion construct ( $\Delta$ AnxA2).....	25
2.1.3 HEK293T cell culture and transfection .....	26
2.1.4 Protein affinity purification from tissue lysates and coimmunoprecipitation from cell lysates.....	27
2.1.5 Western blotting.....	27

2.1.6 Dissociated mouse dorsal root ganglion neuron culture .....	28
2.1.7 Nucleofection of DRG cultures .....	28
2.1.8 Electrophysiology .....	29
2.1.9 Ratiometric calcium imaging .....	29
2.1.10 Immunohistochemistry .....	30
2.1.11 Image acquisition and analysis of immunohistochemistry .....	31
2.1.12 RNA isolation and quantitative PCR (qPCR) .....	31
2.1.13 TRPA1 live labeling .....	32
2.1.14 Mouse behavior.....	32
2.1.15 Statistical analysis .....	33
2.2 TRPA1 interactome undergoes dramatic changes during inflammatory pain .....	33
2.2.1 Inflammatory pain paradigm and TRPA1 immunoprecipitation from tissue lysates .....	33
2.2.2 Protein identification by mass spectrometry analysis and database search .....	34
2.2.3 Data analysis .....	35
2.3 NIPSNAP1 and Nocistatin modulate TRPA1 channels .....	36
2.3.1 HEK293T cell culture and transfection .....	36
2.3.2 Dissociated mouse dorsal root ganglion neuron culture .....	36
2.3.3 Nucleofection of DRG cultures .....	36
2.3.4 RNA isolation and quantitative PCR (qPCR) .....	37
2.3.5 Immunocytochemistry .....	37
2.3.6 Immunohistochemistry .....	38
2.3.7 Image acquisition and analysis of immunostainings.....	38
2.3.8 Ratiometric calcium imaging .....	39
2.3.9 TRPA1 live labeling .....	39
2.3.10 Statistical analysis.....	40
<b>3. RESULTS.....</b>	<b>41</b>
3.1 Annexin A2 (AnxA2) regulates TRPA1-dependent nociception.....	41
3.1.1 AnxA2 is a binding partner of TRPA1 in mouse sensory neurons .....	41
3.1.2 AnxA2 coimmunoprecipitates with TRPA1 in a heterologous expression system..	42
3.1.3 AnxA2 does not affect biophysical properties of recombinant TRPA1 channels ....	44
3.1.4 AnxA2 is coexpressed with TRPA1 in nociceptors .....	46

3.1.5 AnxA2 <sup>-/-</sup> mice exhibit increased TRPA1 expression in sensory neurons.....	48
3.1.6 TRPA1 responses are sensitized in a subset of AnxA2 <sup>-/-</sup> sensory neurons .....	49
3.1.7 AnxA2 limits TRPA1 plasma membrane expression in sensory neurons .....	51
3.1.8 TRPA1-dependent nocifensive behaviors are enhanced in AnxA2 <sup>-/-</sup> mice .....	53
3.2 TRPA1 interactome undergoes dramatic changes during inflammatory pain .....	56
3.2.1 Identification of TRPA1-protein complexes in different conditions.....	56
3.2.2 Mass spectrometry screening reveals significant changes in TRPA1-protein complexes during inflammatory pain .....	58
3.3 NIPSNAP1 and Nocistatin modulate TRPA1 channels .....	63
3.3.1 NIPSNAP1 is abundantly expressed in nociceptors of mouse DRGs .....	63
3.3.2 Overexpression of NIPSNAP1 decreases TRPA1 expression in sensory neurons ....	65
3.3.3 NIPSNAP1 decreases TRPA1 expression and activity in a heterologous expression system .....	67
3.3.4 Nocistatin specifically sensitizes TRPA1 responses in sensory neurons.....	69
3.3.5 Nocistatin does not alter TRPA1 cell surface expression .....	70
3.3.6 Nocistatin's effect on TRPA1 does not require NIPSNAP1 .....	71
<b>4. DISCUSSION.....</b>	<b>73</b>
4.1 Annexin A2 (AnxA2) regulates TRPA1-dependent nociception.....	73
4.2 TRPA1 interactome undergoes dramatic changes during inflammatory pain .....	76
4.2.1 Potential relevance of these findings .....	79
4.3 NIPSNAP1 and Nocistatin modulate TRPA1 channels .....	79
<b>5. SUMMARY.....</b>	<b>83</b>
<b>6. REFERENCES .....</b>	<b>85</b>
<b>Acknowledgments .....</b>	<b>103</b>
<b>Appendix .....</b>	<b>104</b>
<b>Curriculum vitae .....</b>	<b>107</b>

## List of figures

<b>Figure 1.</b> The pain pathway.....	<b>9</b>
<b>Figure 2.</b> Thermosensitive transient receptor potential channels (thermoTRPs) .....	<b>13</b>
<b>Table 1.</b> Transient receptor potential (TRP) ion channels known to be involved in mammalian nociception .....	<b>14</b>
<b>Figure 3.</b> A schematic view of TRPA1 structure and activation modalities .....	<b>18</b>
<b>Figure 4.</b> AnxA2 coimmunoprecipitates with native TRPA1 from mouse sensory neurons ....	<b>42</b>
<b>Figure 5.</b> AnxA2 coimmunoprecipitates with TRPA1 in a heterologous expression system ...	<b>43</b>
<b>Figure 6.</b> AnxA2 neither affects TRPA1 voltage dependence nor cellular responses to the TRPA1 agonist MO.....	<b>45</b>
<b>Figure 7.</b> AnxA2 is coexpressed with TRPA1 in nociceptors .....	<b>47</b>
<b>Figure 8.</b> AnxA2 <sup>-/-</sup> mice exhibit more TRPA1-positive DRG neurons .....	<b>49</b>
<b>Figure 9.</b> TRPA1 responses are sensitized in a subset of AnxA2 <sup>-/-</sup> sensory neurons.....	<b>51</b>
<b>Figure 10.</b> AnxA2 restricts TRPA1 membrane levels in cultured DRG neurons.....	<b>52</b>
<b>Figure 11.</b> Enhanced TRPA1-dependent nocifensive behaviors in AnxA2 <sup>-/-</sup> mice.....	<b>55</b>
<b>Figure 12.</b> Identification of TRPA1-protein complexes during inflammatory pain .....	<b>57</b>
<b>Figure 13.</b> TRPA1 interactome undergoes dramatic changes during inflammatory pain .....	<b>59</b>
<b>Figure 14.</b> STRING association networks of single datasets .....	<b>60</b>
<b>Figure 15.</b> Volcano plot of quantitative proteomics data .....	<b>61</b>
<b>Figure 16.</b> Alternative scatter plots of quantitative proteomics data .....	<b>62</b>
<b>Figure 17.</b> NIPSNAP1 is abundantly expressed in nociceptive neurons of mouse DRGs.....	<b>64</b>
<b>Figure 18.</b> Validation of NIPSNAP1 antibody specificity .....	<b>65</b>
<b>Figure 19.</b> DRG neuron cultures show less TRPA1-positive cells upon NIPSNAP1 overexpression.....	<b>66</b>
<b>Figure 20.</b> NIPSNAP1 decreases TRPA1 expression and activity in HEK293T cells .....	<b>68</b>
<b>Figure 21.</b> Nocistatin specifically modulates TRPA1-mediated calcium response in DRG neurons.....	<b>69</b>
<b>Figure 22.</b> Nocistatin does not alter TRPA1 cell surface expression in cultured DRG neurons	<b>70</b>
<b>Figure 23.</b> NIPSNAP1 siRNA effectively knocks down the expression of NIPSNAP1 in DRG sensory neurons .....	<b>71</b>
<b>Figure 24.</b> NIPSNAP1 knock-down does not affect Nocistatin's enhancement of TRPA1-mediated calcium response in DRG neuron cultures.....	<b>72</b>

## Abbreviations

AMPA	$\alpha$ -amino-3-hydroxy-5-methyl-4-isoxazolepropionic acid
AU	Arbitrary unit
BDNF	Brain-derived neurotrophic factor
Cap	Capsaicin
CFA	Complete Freund's Adjuvant
COX	Cyclooxygenase
DRG	Dorsal root ganglion
EGFP	Enhanced green fluorescent protein
GAPDH	Glyceraldehyde-3-phosphate dehydrogenase
GDNF	Glial cell line-derived neurotrophic factor
GFP	Green fluorescent protein
GO	Gene ontology
HIV	Human immunodeficiency virus
IP	Immunoprecipitation
kDa	KiloDalton
LC-MS	Liquid chromatography-mass spectrometry
MO	Mustard oil
MS	Mass spectrometry
NGF	Nerve growth factor
NMDA	N-Methyl-D-aspartate
NT-3	Neurotrophin-3
NT-4	Neurotrophin-4
OE	Overexpression
PCR	Polymerase chain reaction
PKA	Protein kinase A
PLC	Phospholipase C
ROS	Reactive oxygen species
TG	Trigeminal ganglion
TRP	Transient receptor potential
UPLC	Ultra performance liquid chromatography
VEH	Vehicle
WT	Wild type
YFP	Yellow fluorescent protein

# 1. INTRODUCTION

## 1.1 Pain

The ability to sense the world is essential for adequate response to environmental stimuli, which determines survival of the organism and, consequently, drives evolution. Different sensory modalities enable the detection of specific stimuli, with the traditionally recognized five senses, also known as sound, sight, touch, smell, and taste, operating continuously and oftentimes even “unperceived” to decode any input and therefore direct essentially any response and action. Among them, the most primitive and indeed the most essential to survival is the sense of touch, better referred to as somatosensation. The somatosensory system is complex and encompasses different submodalities, namely:

- Touch: detection of mechanical stimulation of the body;
- Proprioception: detection of mechanical displacement of muscles and joints; it contributes to sense the position of the body and limbs;
- Thermosensation: detection of a wide range of temperatures, from cold to heat;
- Nociception: detection of noxious (painful) stimuli, of mechanical, thermal and chemical nature;

Nociception is probably the most enigmatic of these submodalities, mainly because of the dual nature that is associated to pain. On the one hand in fact, pain has, as the other submodalities, a fundamental physiological role, as it is protective against stimuli that have the potential to harm the body, and triggers protective and defensive mechanisms aimed at ceasing the threatening condition. Because this pain is involved with the sensing of noxious stimuli, it is referred to as nociceptive or acute pain, a high-threshold pain only activated in response to stimuli intense enough to potentially create damage (Basbaum et al., 2009; Woolf, 2010). The paramount importance of acute pain is exemplified in people born with congenital insensitivity to pain, which is caused by rare mutations in the genes coding for the voltage-gated sodium channels Nav1.7 (Cox et al., 2006), Nav1.9 (Leipold et al., 2013) or neurotrophin receptor TrkA (Indo et al., 1996). These individuals experience harmful conditions without any protective reaction, undergoing bone fractures, self-mutilations, amputations, and often die early in life as a result of injuries. The importance of acute pain is also revealed in cases of peripheral neuropathy, where sensory denervation of joints leads to severe damage and deformities due to lack of pain sensitivity (Haus et al., 2010; Mabileau and Edmonds, 2010).

On the other hand however, pain is also the first reason that people seek medical attention. Pain can extend beyond its protective usefulness, becoming pathological and chronic. In this case, pain is maladaptive and is believed to result from abnormal functioning of the nervous system, becoming a disease state in its own right (Costigan et al., 2009). In Europe, chronic pain of moderate to severe intensity is estimated to affect almost 20% of the adult population, which results in serious damage to the quality of the patients’ social and working

life, in addition to a huge economic burden (Breivik et al., 2006). Effective treatment of many chronic pathological pain conditions has not been achieved so far and faces major challenges. Current pain therapeutics are either not effective in some clinical settings, or they are too often characterized by extremely narrow safety windows and intolerable side effects. In the light of these difficulties, it is of primary importance finding new therapeutic targets for the development of novel, more effective, and better-targeted analgesics. A special focus is needed in order to identify ways to interfere selectively with the pathological side of pain, while preserving the physiological function of acute pain, and therefore an individual's ability to detect noxious stimuli.

## **1.2 Nociception and the pain pathway**

In order to figure out how to potentially target pain, we need to understand how the sensation of pain is generated. In 1986, the International Association for the Study of Pain (IASP) defined pain as “a sensory and emotional experience associated with actual or potential tissue damage, or described in terms of such damage” (Merskey, 1994). Pain is a complex experience made up of sensory, affective, motivational and cognitive dimensions, which is physiologically associated, but different from, nociception. Nociception refers to the neurophysiological consequences induced by a noxious stimulation, and starts with the detection of such stimulus through specialized primary afferent neurons which innervate both the skin and internal organs, the so-called nociceptors.

The term nociceptor was coined in the early 1906 by Sir Charles Scott Sherrington, whose pioneering studies led him to the conclusion that the skin is provided with a set of nerve endings with the specific function of sensing potentially harmful stimuli (Sherrington, 1903). Sherrington's “specificity theory” was contrasting the then widely believed notions that pain was caused by a central summation upon excessive sensory stimulation, and that nerve endings were all alike (Woolf and Ma, 2007). The nociceptor is nowadays widely recognized for its specific function in triggering the nociceptive process, and extensive knowledge has been developed about the different properties and specific characteristics that mark distinct populations. Nociceptors, like other primary somatosensory neurons, show a pseudounipolar morphology, with their cell bodies located in dorsal root ganglia (DRG, for most of the trunk and limbs innervation), trigeminal ganglia (TG, for cephalic innervation), jugular ganglia and nodose ganglia (vagal innervation of head and viscera)(Kollarik et al., 2010). They possess a single process that originates from the cell body and bifurcates into a peripheral axon that innervates the target tissue, and a central axon that synapses on second-order neurons in the dorsal horn of the spinal cord (for DRG neurons) or in the trigeminal subnucleus caudalis (for TG neurons)(Basbaum et al., 2009; Dubin and Patapoutian, 2010). Nociceptive neurons are rather heterogeneous and can be classified based on different properties, for instance the diameter of the axon, which correlates well

with the speed of transmission of action potentials and whether the fiber is myelinated. This aspect is also reflected in the specific qualities of pain signaled. The initial fast-onset pain, usually perceived as burning, pricking and well-localized, is mediated by medium-diameter A $\delta$ -fiber nociceptors, whose axons are thinly myelinated with conduction velocities of approximately 5–30 m/s (Djouhri and Lawson, 2004). Most nociceptors, however, have small diameter non-myelinated axons, called C-fibers (Woolf and Ma, 2007) with conduction velocities of 0.4–1.4m/s (Djouhri and Lawson, 2004). They signal a slower-onset pain, with throbbing, burning and poorly localized qualities.

Nociceptors are unique in their ability to sense noxious stimuli of physical and chemical nature, which is possible because they express specific receptors and ion channels that are the real primary detectors of the noxious stimulus. The range of stimuli they respond to is also a direct reflection of the specific receptors they express. Such molecular transducers act in free nerve endings to encode the noxious stimulus into a signal that is then transmitted to the somata of the neurons (in DRGs or TGs) and eventually conveyed to second-order neurons and local interneurons in the dorsal horn of the spinal cord (Fig.1). Here, different fibers terminate in anatomically and electrophysiologically distinct laminae (Basbaum and Jessell, 2000). Specifically, A $\delta$  nociceptors project to lamina I as well as to the deeper lamina V, whereas C-fiber nociceptors synapse more superficially mainly to laminae I and II (Snider and McMahon, 1998). Projection neurons within laminae I and V constitute the main output from the dorsal horn to higher order systems, travelling through five major ascending pathways: the spinothalamic, spinoreticular, spinomesencephalic (or spinoparabrachial), cervicothalamic, and spinohypothalamic tracts (Basbaum and Jessell, 2000). These nociceptive pathways convey the information to different cervical structures, with the different nuclei of the thalamus representing the principal relay structures of sensory information. The lateral and medial nuclear thalamic groups are involved in the reception, integration, and transfer of the signal primarily to the somatosensory cortices and other cortical structures (Basbaum and Jessell, 2000). The insula receives impulses from several pathways and its projections are directed at the limbic system, mainly amygdala and some areas of the prefrontal cortex (PFC). The anterior cingulate cortex (ACC) coordinates inputs from parietal areas with frontal cortical regions that integrate the perception of bodily threats and contributes to the response priorities of pain behavior (Almeida et al., 2004).

In general, there does not seem to be a single brain region essential for pain perception (Apkarian et al., 2005). Instead, pain seems to be the result of complex activation of a wide number of structures, some of which contribute to the sensory-discriminative components (as the somatosensory cortex) while others are more associated with the affective-emotional aspects (such as the insula, the anterior cingulate cortex and the limbic system) (Basbaum and Jessell, 2000). These structures work in an orchestrated way in the deconvolution of the sensory stimulation, but also in its modulation, which then affects pain response. Several mechanisms of descending pain regulation have been discovered, among which a serotonergic and a monoaminergic systems which originate in the periaqueductal

grey matter and the locus ceruleus (and other medullar nuclei), respectively. But the best known is definitely the endogenous opioid system: opioid peptides and their receptors are widely distributed throughout the body and constituted the major target of exogenous pain suppression from the ancient Sumerians in 3300 BC to our times (Basbaum and Jessell, 2000). Clearly such a strategy of targeting widely expressed molecules involved in several functions is inevitably linked to a cascade of side-effects, to which we can add a dangerous addictive potential (Ueda and Ueda, 2009).

A seemingly more reasonable strategy to target pain is to target cellular processes and mechanisms that are as much as possible specific for pain, so that interfering with such mechanisms would ideally spare other physiological functions from unwanted consequences. From looking at the different steps in the pain pathway, the nociceptor clearly stands out for its unique ability in sensing the noxious stimulus and triggering the nociceptive process, and is therefore a desirable target where to find mechanisms that are as much as possible nociception-specific.

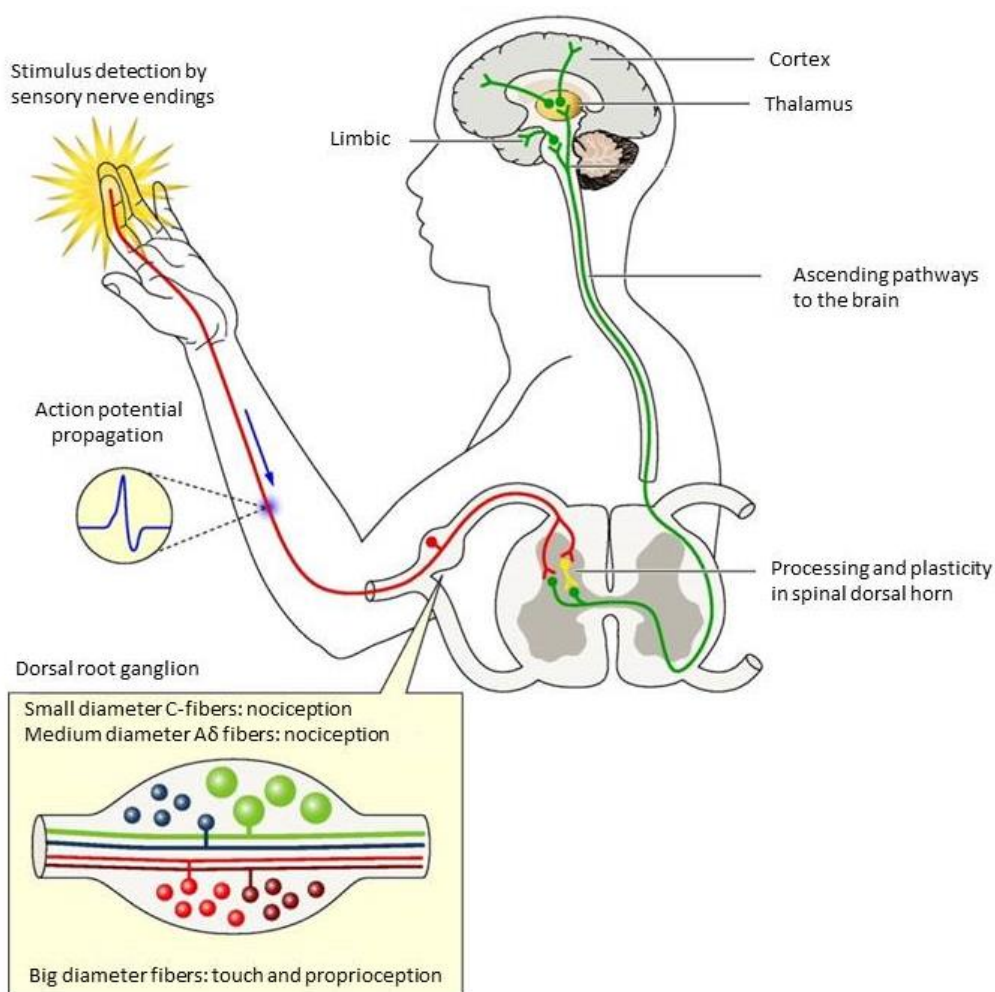


**Figure 1. The pain pathway.**

Noxious stimuli of physical and chemical nature are detected by primary afferent nociceptors, which encode them into a signal that is transmitted first to their somata and then to second-order neurons in the dorsal horn of the spinal cord. DRGs harbor the cell bodies of these neurons, many of which are small diameter non-

myelinated C-fibers, with low conduction velocities. Thinly-myelinated afferents correspond to faster-signaling A $\delta$  nociceptors, while big-diameter myelinated neurons mainly convey touch and proprioception signals. In the spinal cord, the sensory information is integrated locally and then conveyed to higher-order circuitry in the brain, primarily the thalamus and then cortical structures. Adapted from (Bourinet et al., 2014).

### **1.3 The nociceptor in chronic pathological pain**

A great number of cases of chronic pain are associated with altered excitability and activity of primary afferent neurons, potentially caused by pathological processes that follow inflammation (inflammatory pain) or nerve injury (neuropathic pain). The etiology of such processes can be diverse, including physical trauma, metabolic disease, infections and chemotherapy. (Sousa-Valente et al., 2014). Made for distinguishing innocuous from noxious stimuli, nociceptors exhibit a high threshold of activation. However, in response to injury and inflammation the nociceptors' activation characteristics can be modulated in a process known as peripheral sensitization, which represents a form of functional plasticity of the nociceptor (Woolf and Ma, 2007). Basically, at the site of inflammation/injury a variety of signaling molecules and cellular mediators are released as a result of disruption of cells, infiltration and activation of immune cells and induction of enzymes, which together make up an "inflammatory soup" that acts on primary afferent neurons to modify their response properties. Cytokines, chemokines, growth factors, prostaglandins, proteases, all contribute to changes in the chemical milieu of the nociceptor resulting in a reduced threshold of activation and increased responsiveness to stimuli. These phenomena translate respectively into allodynia (response to innocuous stimuli) and hyperalgesia (exaggerated pain response to noxious activation), which are thought to contribute to the etiology of clinically relevant chronic pain syndromes (Patapoutian et al., 2009). As a consequence, activity-dependent changes in the spinal cord lead to increased neurotransmitter release and enhanced excitability of second-order sensory neurons which may promote central sensitization (Ji et al., 2003).

The wide variety of sensitizing agents acting in parallel in this process makes potential blockage of their effects a rather poor option for the reduction of pain (analgesia). Nonetheless, blockage of prostaglandin synthesis by inhibition of cyclooxygenase (COX) enzymes has been the basis of most non-steroidal anti-inflammatory drugs (NSAIDs). Whilst non-selective inhibition of COX produces a significant analgesic effect, they are molecules widely expressed in the body and therefore, their clinical use is limited by serious side effects (Kidd and Urban, 2001). Many other pharmacological agents designed to achieve analgesia by either decreasing neuronal excitation or increasing inhibition suffer from the same issues and a strategy targeting molecules and their molecular scaffolds, which are selectively expressed or highly enriched in the primary detectors of noxious stimuli is highly desirable. As already mentioned, the nociceptor houses specialized receptors and ion channels that endow it with the unique ability to sense physical and chemical stimuli and

translate them into a signal that will then be propagated along the pain neuraxis and culminate into pain perception. These molecules are the real primary detectors of the noxious stimulus and are highly enriched in nociceptive neurons (Basbaum et al., 2009). In fact, to date many of these receptors and ion channels have become important targets in the search for new pain therapies (Wood et al., 2004) and the biggest advances in understanding their identity and function were certainly led by the discovery of Transient Receptor Potential (TRP) ion channels as the largest superfamily of sensors for temperature and chemesthesis (Bandell et al., 2007; Dhaka et al., 2006).

## **1.4 Transient receptor potential (TRP) ion channels**

### **1.4.1 General information**

TRP channels are present in a large variety of multicellular organisms, and the mammalian TRP channel superfamily encompasses 28 members, which are subdivided into 6 subfamilies based on their sequence homology: TRPA (ankyrin), TRPC (canonical), TRPM (melastatin), TRPML (mucolipin), TRPP (polycystin) and TRPV (vanilloid) (Benemei et al., 2015). A more distant TRPN group (also known as no mechanoreceptor potential C or NOMPC) has not been found in mammals, but is expressed in flies, worms and cold-blooded vertebrates (Moiseenkova-Bell and Wensel, 2011; Montell, 2001). In addition, even yeasts and other fungi have been reported to express a TRP channel subfamily known TRPY (yeast) (Moiseenkova-Bell and Wensel, 2011). TRP proteins share a common structure, which consists of six putative transmembrane domains (TM) with a pore-forming loop (P) between the fifth (S5) and sixth segments (S6) (Nilius et al., 2007). The N- and C-termini are both intracellular and seem to contribute to the regulation of channel assembly and function. Functional TRP channels are constituted of four pore-forming subunits that have been shown to potentially assemble as both homo-tetramers and hetero-tetramers (Benemei et al., 2015; Zheng, 2013). Several specific properties have been used to differentiate and classify TRP subfamilies, among which the number of ankyrin repeats, coiled-coil regions and TRP signature motifs. TRP proteins form ion channels that are mostly non-selective for monovalent and divalent cations, but several exceptions have been reported such as TRPM4 and TRPM5, which show a great selectivity for monovalent cations, and TRPV5 and TRPV6 that are instead highly selective for Ca<sup>2+</sup> ions (Smani et al., 2015).

To date, much evidence has accumulated demonstrating an important role of TRP channels in cellular processes in both a physiological and pathophysiological context. They function as ligand-gated, second messenger-operated or receptor-operated channels coupling such events to the transmembrane flow of ions down their electrochemical gradients. The influx of Na<sup>+</sup> and Ca<sup>2+</sup> ions inside the cell may in turn contribute to membrane depolarization and the activation of Ca<sup>2+</sup>-dependent pathways in a variety of systems and organs (Clapham, 2003). In excitable cells, variations in transmembrane potential determine in fact action

potential generation and muscle contraction (Ramsey et al., 2006). Furthermore, dysregulation of TRP channel activity and function, which might be linked to abnormal expression levels, impaired trafficking or mutations, has been associated with a large number of disorders, thus revealing the crucial biological relevance of these channels (Smani et al., 2015).

#### **1.4.2 Role in sensory transduction**

Many TRP channels are peculiar in their functional properties that allow them to function as cellular sensors (Clapham, 2003). The first clue that they could be involved in sensory transduction emerged from the first identification of a TRP ion channel in *Drosophila melanogaster* (Montell and Rubin, 1989). It was observed that a fly mutant displayed a transient instead of sustained response to stimulation with bright light, hence the name of the protein family. Among different organisms, TRP channels show disparate functions, which are partially shared among closely related species. For instance, yeasts use a TRP channel to perceive and respond to hypertonicity (Zhou et al., 2003). Nematodes like *C. elegans* instead possess TRP channels in their 'noses' at the tips of neuronal dendrites where they are needed for detection and avoidance of noxious chemicals (de Bono et al., 2002). In mammals TRP channels have demonstrated a clear role as major players in chemesthesis, osmoregulation and thermosensation.

Thermosensation is a fascinating chapter which advances have been precipitated by the identification of seven highly temperature-sensitive ion channels (the so-called thermoTRPs) as candidate temperature sensors. They are expressed in sensory nerve endings and in the skin, where they couple activation by distinct thermal ranges to transmembrane ion flow (Ferrandiz-Huertas et al., 2014). So far, five heat-activated channels (TRPV1-4 and TRPM3) and two cold-activated channels (TRPM8 and TRPA1) have been reported to contribute to mammalian thermosensation, even though the debate is still open (Dhaka et al., 2006; Ferrandiz-Huertas et al., 2014; Patapoutian et al., 2003). All seven, when expressed in heterologous expression systems (like HEK293 cells or *Xenopus* oocytes), showed the amazing property of making the cells temperature-sensitive within their specific activation window. Each thermoTRP has in fact unique characteristics, as indicated by different thresholds of activation, which combined cover the whole spectrum of temperature sensation in mammals (Fig.2). While the precise molecular determinants of temperature detection are still unknown, the identification of structural elements in these channels indicates an important role of the intracellular N- and C- termini in determining the temperature range of activation (Bandell et al., 2007). The ability to sense internal and environmental temperatures thanks to these channels are fundamental not only for maintenance of homeostasis, but also for avoidance of harmful noxious temperatures. (Dhaka et al., 2006; Lumpkin and Caterina, 2007).

Several TRP channels (among which most of the thermoTRPs) have also shown a clear role in chemesthesis, here referred to as the chemical sensitivity of the skin and membranes to endogenous and exogenous molecules and that is perceived as pungency, irritation, cooling, warmth, or heat. Examples of chemesthesis include the irritating effects of concentrated saline solutions on the nasal mucosa, or painful sensations evoked by inhaling vehicle exhaust gas. Other examples are the irritation and pain caused by eating hot chili peppers, due to the active ingredient capsaicin, which is known to directly activate the TRPV1 channel (Caterina et al., 1997).

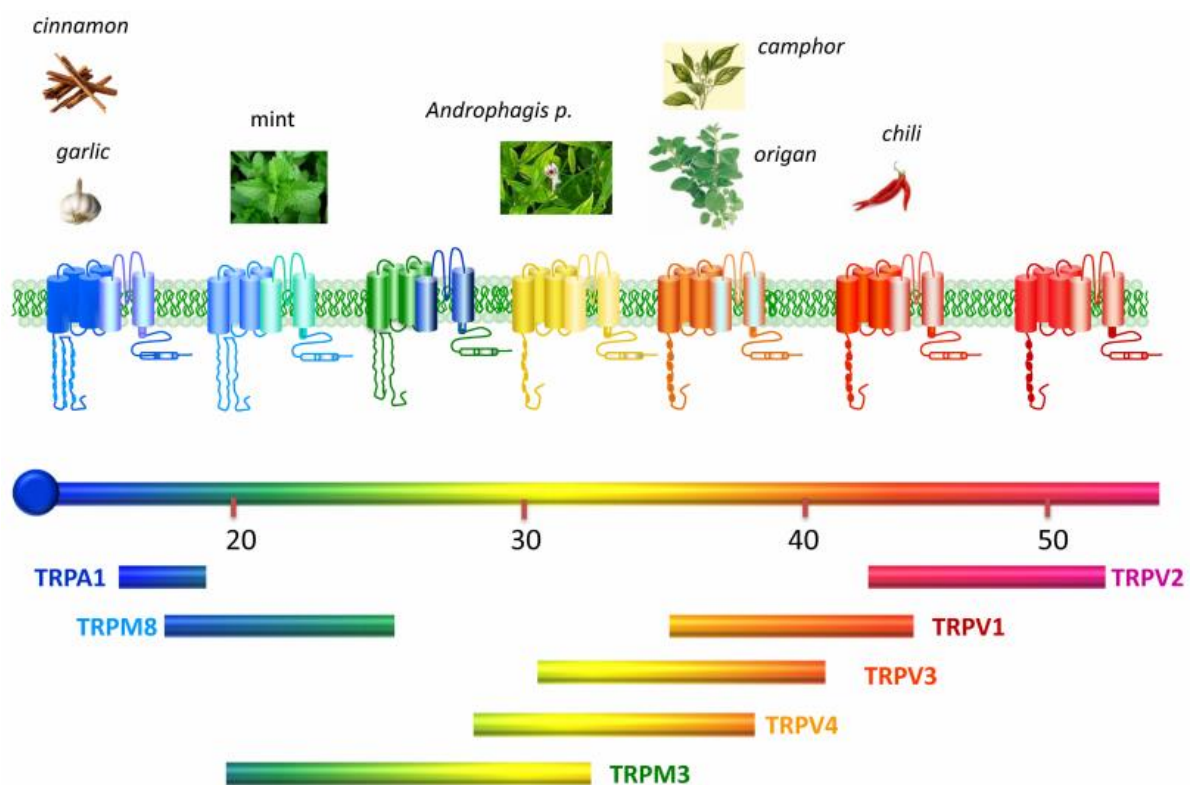


**Figure 2. Thermosensitive transient receptor potential channels (thermoTRPs).**

Several members of the TRP channels superfamily showed to mediate temperature sensation by coupling activation by temperature to flow of ions through the membrane. They all share a common topology with six transmembrane domains (S1–S6) and a pore loop between S5 and S6. N- and C-termini are intracellular and four subunits associate into functional channels. ThermoTRPs show distinct thermal activation ranges from noxious cold (TRPA1) to potentially harmful heat (TRPV1 and TRPV2). Most thermoTRPs showed also a role in chemesthesis, sensing a variety of natural chemicals known to induce the respective thermal sensations in humans. Adapted from (Ferrandiz-Huertas et al., 2014).

### 1.4.3 TRP channels and pain

The superfamily of TRP channels constitutes the largest group of molecular sensory transducers so far known to be involved in pain signaling in mammals, with ten members (TRPV1to4, TRPA1, TRPM2-3-8, TRPC1-6) that showed a clear role in nociceptive processing, as listed in table 1.

TRP channel	References
TRPV1	(Caterina et al., 2000; Caterina et al., 1997)
TRPV2	(Caterina et al., 1999; Nagy and Rang, 1999)
TRPV3	(Peier et al., 2002b; Smith et al., 2002)
TRPV4	(Alessandri-Haber et al., 2003; Liedtke et al., 2000)
TRPA1	(Obata et al., 2005; Story et al., 2003)
TRPM2	(Haraguchi et al., 2012; Kudoh et al., 1997)
TRPM3	(Lee et al., 2003; Vriens et al., 2011)
TRPM8	(Bautista et al., 2007; Knowlton et al., 2010)
TRPC1	(Alessandri-Haber et al., 2009; Zitt et al., 1996)
TRPC6	(Alessandri-Haber et al., 2009; Boulay et al., 1997)

**Table 1. Transient receptor potential (TRP) ion channels known to be involved in mammalian nociception.**

Among these channels, some of them as TRPV1, TRPM8 and TRPA1 have drawn special attention because they have been shown to be highly expressed in nociceptors, where they play major roles as transducers of noxious stimuli and modulators of nociceptive signaling. Activation of these channels is involved in acute pain signaling and furthermore their regulation and sensitization significantly contribute to pathological pain conditions (Sousa-Valente et al., 2014).

#### 1.4.3.1 TRPV1

In the elucidation of the molecular mechanisms of noxious temperature sensation, limited progress was made until 1997, when the TRPV1 channel was cloned by the Julius' lab (Caterina et al., 1997). TRPV1 is a member of the vanilloid subfamily of TRP channels that showed a clear enrichment in nociceptive neurons, and reported properties of a noxious heat-activated channel with a thermal activation threshold close to 43°C (Caterina et al., 1997; Julius, 2013). TRPV1 is also responsible for the irritation and pain caused by hot chili peppers, due to the active ingredient capsaicin, which is a direct and specific agonist. Indeed TRPV1-deficient (knock out) mice showed partial deficits in the detection of acute thermal stimuli, which confirms a role for this channel in heat-evoked pain, and complete

abolishment of capsaicin-induced pain responses (Caterina et al., 2000; Caterina et al., 1997). In addition to heat and natural compounds, TRPV1 can be activated and modulated by lipids, voltage and phosphorylation (Pingle et al., 2007).

Importantly, many cellular mediators produced in the context of tissue injury and inflammation (components of the mentioned inflammatory soup) can dramatically affect TRPV1 function, reducing its threshold of activation and, as a result, increase nociceptor excitability. TRPV1 is therefore a fundamental component of the cellular mechanisms that lead to peripheral sensitization and, consequently, drive the clinically relevant manifestations of pain hypersensitivity (hyperalgesia and allodynia) (Basbaum et al., 2009; Caterina et al., 2000; Davis et al., 2000). TRPV1-deficient mice indeed showed attenuated thermal hyperalgesia induced by inflammatory molecules such as bradykinin and nerve growth factor (NGF) (Caterina et al., 2000; Chuang et al., 2001; Davis et al., 2000). In addition, injection of oleoylethanolamide, an endogenous TRPV1 agonist, induces nocifensive (pain-related) behavior in mice that is absent in TRPV1-deficient animals and can be blocked by the TRPV1 antagonist capsazepine (Wang et al., 2005). Modulation of TRPV1 has therefore clear potential for pain therapy and pharmacological blockade or knock-down of TRPV1 displayed analgesic activity in different animal pain models (Chu et al., 2011; Szabo et al., 2005). In 2010 capsaicin patches (Qutenza®) have been approved in the USA for the treatment of post-herpetic neuralgia and a recent study involving a total of over 2000 participants claimed that high-concentration capsaicin patches could be effective even for the treatment of HIV-induced neuropathy (Derry et al., 2013). However, since TRPV1 inhibition lowers the sensitivity to noxious heat, this might lead to an increased susceptibility to injury and it has been associated to a risk of increased body temperature (hyperthermia) (Brederson et al., 2013; Gavva et al., 2008).

#### **1.4.3.2 TRPM8**

TRPM8 has been shown to respond to a variety of natural and synthetic cooling agents, such as menthol, eucalyptol and icilin, as well as to cold stimuli, with an activation temperature proximal to 26°C (Dhaka et al., 2006). TRPM8 shares TRPV1 topology, forming a homotetrameric nonselective cation channel permeable to calcium ions (McCoy et al., 2011; Peier et al., 2002a). In sensory neurons TRPM8 is enriched in a subpopulation of primary afferents which, interestingly, does not overlap the neuronal subset which instead expresses TRPV1 and TRPA1, suggesting the existence of “labelled lines” in sensory transduction and signaling. (Almaraz et al., 2014). TRPM8-deficient mice exhibited profound deficits in their ability to discriminate between cold and warm surfaces, or to respond to evaporative cooling, demonstrating the essential role of TRPM8 in thermosensation (Bautista et al., 2007). Furthermore, injury-evoked cold hypersensitivity is impaired in animal models of both inflammatory and neuropathic pain, advancing the prospect that therapeutic modulation of

TRPM8 may provide relief to patients who suffer from altered sensitivity to cold (Colburn et al., 2007). TRPM8 antagonism showed analgesic potential in a rat model of neuropathic pain (Calvo et al., 2012; Parks et al., 2011) and has been associated with a reduction of cold hypersensitivity following tissue injury (Knowlton et al., 2010). Nonetheless, to date no TRPM8 modulator has advanced to clinical trials.

TRPA1 will be covered in more detail as it is the main focus of this study.

## **1.5 TRPA1**

### **1.5.1 Gene and protein structure**

TRPA1 was for the first time identified in 1999 by Jaquemar and colleagues and originally baptized ANKTM1 by the Patapoutian lab as it contains multiple ankyrin repeats in the N-terminal part (Jaquemar et al., 1999; Story et al., 2003). The *Trpa1* gene is well conserved and several TRPA1 homologues have been discovered in the animal kingdom. In addition to mammals, it is present in many vertebrates and invertebrates, including rodents, flies and worms. However, in contrast to mammals that contain only one *Trpa1* gene, many other classes from the animal kingdom express different TRPA1 homologues (Nilius et al., 2012). TRPA1 is a protein of about 1,100 aminoacids (120–130 kDa), with only one splice variant identified in mouse (Zhou et al., 2013). TRPA1 shows a topology similar to the other TRP channels, with six transmembrane domains and a pore loop between S5 and S6 and cytoplasmic N- and C- termini (Fig.3). The peculiarity of TRPA1 is an exceptionally long region within the N-terminus containing 14-18 ankyrin repeat domains (ARs), which could be involved in protein–protein interactions and channel trafficking to the plasma membrane (Nilius and Flockerzi, 2014). Deletions of TRPA1 ARs have been shown, in fact, to negatively affect the insertion of the channel into the plasma membrane (Nilius et al., 2011). The N-terminal region contains also several important cysteine residues, which can interact and form disulfide bridges within and between monomers (Cvetkov et al., 2011). In its functional configuration, four TRPA1 subunits associate into tetramers, usually homo-tetramers. (Nassini et al., 2014). Recently, the Julius' lab determined a ~4 Å resolution of TRPA1 obtained by Cryo-electron microscopy, which furnished important structural insights, as well as shedding some lights on potential regulatory mechanisms, much needed for the design of selective channel modulators (Paulsen et al., 2015). Like most family members, TRPA1 is a non-selective cation channel with an inward depolarizing current mainly due to Na<sup>+</sup> and Ca<sup>2+</sup> ions (Nilius et al., 2007).

### 1.5.2 Activation

Mammalian TRPA1 is a promiscuous channel that can be activated by a plethora of endogenous mediators and natural compounds. Environmental chemicals that target TRPA1 include allyl isothiocyanate, better known as mustard oil (MO), cinnamaldehyde, and allicin, which are the pungent active ingredients that characterize mustard seeds, cinnamon, and garlic, respectively. Many airborne irritants also directly activate TRPA1, among them heavy metals and isocyanates produced during industrial manufacturing (Bautista et al., 2013). Another TRPA1 agonist is acrolein, that in addition to be found in tear gas, cigarette smoke and vehicle exhaust gas, it can be formed endogenously under conditions of inflammation (Bautista et al., 2006).

TRPA1 is targeted also by a wide number of endogenous metabolites and inflammatory molecules. One example is reactive oxygen species (ROS), which levels dramatically increase in response to tissue damage and can initiate lipid peroxidation (Bautista et al., 2013). These processes lead to the formation of different reactive carbonyl species, among which 4-oxononanal (4-ONE) and 4-hydroxynonanal (4-HNE), which in turn target TRPA1 directly (Taylor-Clark et al., 2008a; Trevisani et al., 2007). Another characteristic of inflammatory states is the formation of reactive nitrogen species (RNS). Among RNS, nitric oxide (NO) is the most potent TRPA1 activator and it is an important component of the mechanisms that underlie pain sensitization upon inflammation and injury (Nilius et al., 2012). At sites of injury and inflammation COX enzymes mediate the production of a variety of prostaglandins, which mediate inflammatory responses. One prostaglandin D2 derivative, 15d-PGJ2, specifically activates TRPA1 expressed in HEK cells as well as in mouse sensory neurons (Cruz-Orengo et al., 2008; Taylor-Clark et al., 2008b). Interestingly, also some commonly used anesthetics, both general (as isoflurane) and local (as lidocaine), are able to activate TRPA1 (Leffler et al., 2011; Matta et al., 2008).

Several studies indicated for TRPA1 a gating model involving both voltage-dependent activation and inactivation of TRPA1, with the pore helix playing an essential role in the process (Samad, 2011; Wan et al., 2014). TRPA1 activation is coupled to influx of calcium (among other ions) into the cells, which itself has been shown to modulate the channel. Calcium plays two opposing roles in regulating TRPA1 activity. TRPA1 currents in response to pungent chemicals like mustard oil are rapidly potentiated and subsequently inactivated in the presence of extracellular calcium (Doerner et al., 2007; Wang et al., 2008b; Zurborg et al., 2007). On the other hand, TRPA1 activity can be blocked by intracellular calcium (Akopian et al., 2007; Nagata et al., 2005; Wang et al., 2008b; Zurborg et al., 2007) Several reports showed that TRPA1 contributes to acute cold responses (Karashima et al., 2009; Kwan et al., 2006; Story et al., 2003) even though its role as an acute cold sensor has not been always confirmed (Caspani and Heppenstall, 2009). A recent report demonstrated that human TRPA1 expressed in artificial membranes is intrinsically cold sensitive and supports

the hypothesis that TRPA1 plays a role in cold perception also in humans (Moparthi et al., 2014).

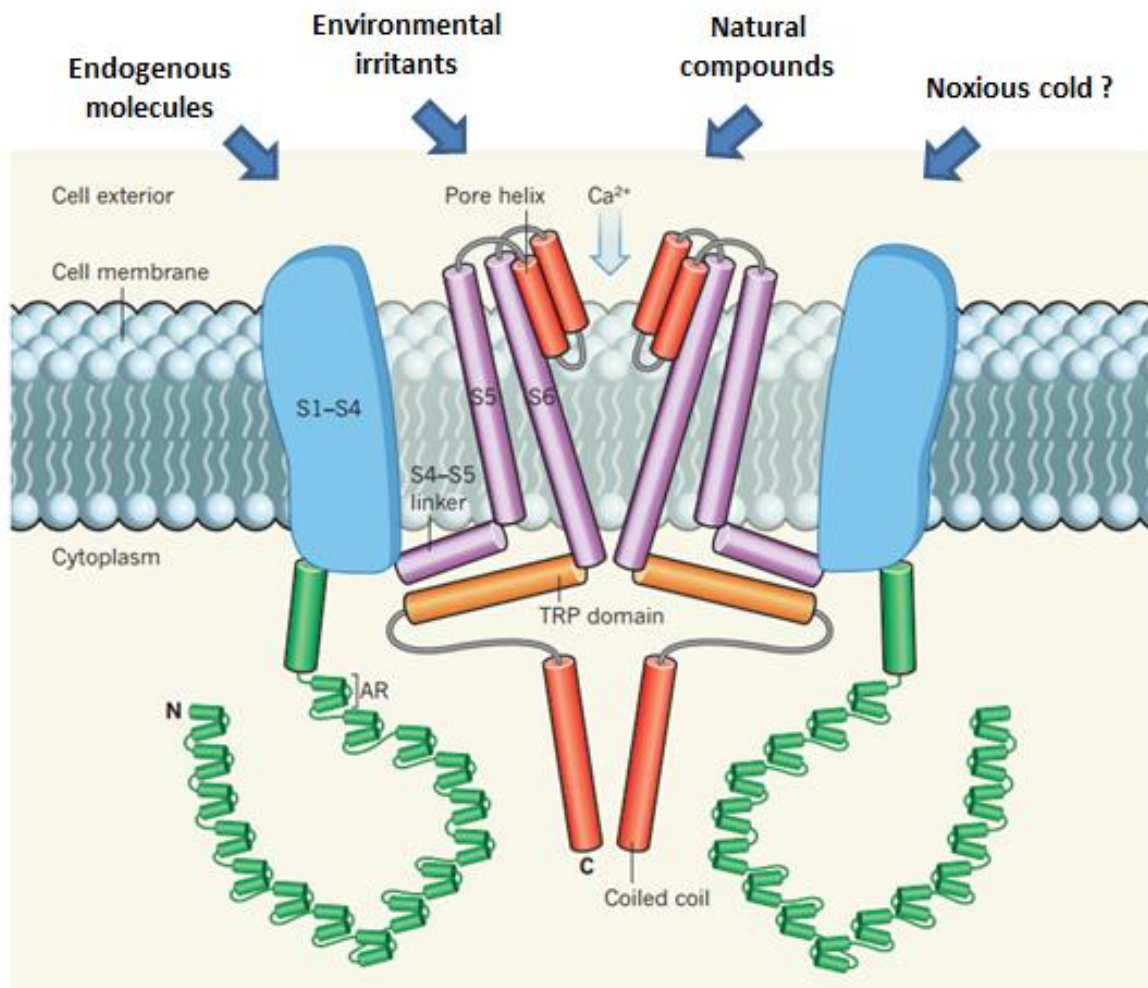


**Figure 3. A schematic view of TRPA1 structure and activation modalities.**

Two TRPA1 subunits are shown, although the channel is comprised of four. Each subunit contains six transmembrane domains (S1-S6) with a pore helix between S5 and S6. Ankyrin repeats (AR) characterize the N-terminal region, and a coiled-coil structure the C-terminus. TRPA1 is targeted by a variety of endogenous molecules with pro-inflammatory properties, environmental irritants, a plethora of natural compounds and potentially noxious cold. Channel activation is coupled to pore opening and transmembrane calcium flow. Adapted from (Clapham, 2015).

### **1.5.3 Expression**

TRPA1 is localized to both neuronal and non-neuronal tissues as the inner ear, skin and pancreas. Among them, TRPA1 shows a high enrichment in sensory neurons of dorsal root ganglia (DRG), trigeminal ganglia (TG), and nodose ganglia, where it functions as a major player in nociception (Nilius et al., 2012). In DRGs, TRPA1 is expressed in unmyelinated (C-fiber) and thinly-myelinated (A $\delta$ ) primary afferents, with only occasional identification in large myelinated axons. More than 25 % of TRPA1 containing neurons are peptidergic and release Substance P and Calcitonin gene-related peptide (CGRP), while the remaining neurons were identified as non-peptidergic neurons by immunoreactivity with the plant lectin Isolectin B4 (IB4; ~45 %). The dorsal horn of the spinal cord and trigeminal sensory nuclei are immunoreactive for TRPA1, indicating the location of nociceptive synapses into second-order neurons (Nilius et al., 2012). In sensory neurons, TRPA1 is also usually coexpressed with TRPV1 channels, in Peripherin-positive small diameter neurons of DRGs and TGs (Kobayashi et al., 2005; Story et al., 2003). In fact, ablation of TRPV1 neurons with resiniferatoxin (a superpotent TRPV1 agonist) in mice results in loss of response to both capsaicin and mustard oil (Pecze et al., 2009), suggesting a high degree of colocalization of TRPA1 and TRPV1 in sensory neurons.

### **1.5.4 Role in pain**

There is now widespread agreement that TRPA1 plays an important role as a primary detector of noxious stimuli, by sensing a wide variety of exogenous and endogenous molecules with pro-inflammatory and pro-algesic properties. (Andrade et al., 2012; Bautista et al., 2013). The creation of TRPA1-deficient animals and the development of specific antagonists have confirmed TRPA1 as a major player in acute and inflammatory pain. Several studies in TRPA1-deficient mice identified clear behavioral deficits in response to mustard oil, formaldehyde and profound deficiencies in some models of inflammatory hyperalgesia and airway irritation (Bautista et al., 2006; Kwan et al., 2006). TRPA1 has been implicated in the development and maintenance of hypersensitivity in a number of animal pain models. In models of inflammatory pain, rodents treated with TRPA1 antagonists or TRPA1-deficient animals have displayed a clear attenuation of mechanical hyperalgesia evoked by injection of tumor necrosis factor  $\alpha$  (TNF $\alpha$ ), Complete Freund's Adjuvant (CFA), or monoiodoacetate (Fernandes et al., 2011; Laing and Dhaka, 2015; McGaraughty et al., 2010). To further claim the importance of TRPA1 in pain signaling, gain of function mutations in the gene coding for TRPA1 have been associated with the only human channelopathy with pain phenotype so far linked to the TRP superfamily. This rare disease, called familial episodic pain syndrome (FEPS), is characterized by bouts of excruciating pain especially in the upper body, triggered by mild stress and cold temperatures (Kremeyer et al., 2010). It is now well established that TRPA1 contributes to the pathophysiology of headache by dural mechanisms. TRPA1 on meningeal nerve endings is involved in headache episodes induced by exposure to

environmental irritants, but it has also a potential role in migraine. TRPA1 is expressed in a population of dural primary neurons and activation of meningeal TRPA1 produces behaviors that recapitulate those observed in migraine attacks (Edelmayer et al., 2012; Nassini et al., 2014). While a clear-cut role for TRPA1 in acute noxious cold sensation cannot be unambiguously demonstrated yet, several studies have demonstrated TRPA1 contributions to the state of hypersensitivity to cold temperature (cold allodynia) that occurs in the settings of tissue and nerve injury. TRPA1 antagonism specifically reduced cold hypersensitivity in rodent models of inflammatory and neuropathic pain (del Camino et al., 2010; Karashima et al., 2009). TRPA1 is also critically involved in pain induced by anticancer treatment with platinum-based compounds, as cisplatin and oxaliplatin, which oftentimes lead to cold and mechanical hypersensitivity (Nassini et al., 2011). Antimitotic drugs, such as paclitaxel, are also known to induce peripheral neuropathy. Application of paclitaxel has been shown to stimulate ROS formation that in turn potentiates TRPA1 activation. These effects could be prevented by TRPA1 inhibition with specific antagonists (Materazzi et al., 2012). Furthermore, TRPA1 antagonism has proved effective in attenuating the mechanical allodynia and cutaneous nerve fiber loss in a rat model of streptozotocin-induced diabetes (Koivisto et al., 2012).

Together, these findings advocate a role for TRPA1 in the mechanisms underlying peripheral neuropathy, and in general support TRPA1 as an interesting therapeutic target for pharmacological intervention aimed at quelling pain. Inhibition of TRPA1 with HC-030031, a specific TRPA1 antagonist, effectively inhibited formalin-induced pain (McNamara et al., 2007) and displayed analgesic potential in a rat model of neuropathic pain (Eid et al., 2008). Several companies have showed interest in TRPA1 and reported diverse selective antagonists, among them Abbott, Merck and Janssen. Abbott for instance developed a molecule named A-967079, which inhibited spontaneous and mechanically evoked firing of neurons in uninjured, inflamed, and osteoarthritic rats (McGaraughty et al., 2010), in preclinical studies. However, as for TRPV1, direct inhibition of channel function would result in deficits also in acute pain sensation that is undesirable and asks for better-targeted interventions able to specifically regulate and fine-tune TRPA1 activity.

### **1.5.5 Regulation**

Beyond direct activation by its ligands, TRPA1 function can be sensitized or modulated via mechanisms implicated in phenomena of hypersensitivity, which in turn contribute to clinically-relevant chronic pain conditions (Hucho and Levine, 2007; Patapoutian et al., 2009). Modulators are diverse and include the inflammatory mediators mentioned above, lipid metabolites and intracellular signaling pathways (Hucho and Levine, 2007). Among them, it has been reported that NGF participates in the functional up-regulation of TRPA1 in sensory neurons (Diogenes et al., 2007) and that bradykinin and proteinase-activated

receptor 2 (PAR2) can sensitize TRPA1 via phosphorylation and via activation of PLC, which in turn releases TRPA1 from phosphatidylinositol-4,5-bisphosphate (PIP<sub>2</sub>)-mediated inhibition (Chen et al., 2011; Dai et al., 2007; Wang et al., 2008a). A recent study reported on the modulation of TRPA1 by the extracellular miRNA let7-b which, via functional coupling to the toll-like receptor-7 (TLR7), induced direct activation and excitation of nociceptive sensory neurons to evoke pain (Park et al., 2014).

In addition, the abundance of TRPA1 channels at the plasma membrane of sensory neurons has been identified as a crucial contributor to TRPA1 signaling; in this line the induction of TRPA1 membrane trafficking has been described upon activation of the channel by MO, or PKA/PLC signaling, which might contribute to the sensitization of TRPA1-mediated nocifensive behaviors of mice upon acute activation and inflammatory signals, respectively (Schmidt et al., 2009). TRPA1 membrane abundance is also affected by the coexpression with TRPV1, which seems to counteract pharmacological desensitization of TRPA1 by preventing channel internalization (Akopian et al., 2007; Ruparel et al., 2008). Recently, a TRPA1 splice isoform named TRPA1b has been identified and showed to colocalize, interact and furthermore increase the expression of TRPA1 channels to the plasma membrane and, consequently, affect mouse pain behavior (Zhou et al., 2013).

These studies highlight the impact the regulation of TRPA1 channels can exert on neuronal activity. In general, comprehensive knowledge on the mechanisms of TRPA1 regulation is still missing, especially about the potentially relevant contribution of the whole network of proteins interacting with TRPA1.

## **1.6 Protein complexes as modulators of receptor function in pain**

Among the mechanisms of regulation of ion channels and receptors, a special focus is due to the major contribution of protein-protein interactions. Diverse cellular processes and molecular mechanisms are brought about by the concerted organization of dynamic interactions among proteins, which crucially modulates the properties of the single binding partners. Assembly into multi-protein complexes has indeed been shown also for different ion channels in the pain pathway, and it has been linked to modifications of intrinsic channels properties (e.g. open-probability, activation threshold, (in)activation kinetics), trafficking, expression and post-translational modifications (Rouwette et al., 2015). These events then translate in altered neuronal excitability as well as facilitation and inhibition of synaptic transmission, which ultimately contribute to modulate pain perception and response in both physiological and pathophysiological contexts (Costigan et al., 2009; Gold et al. 2006). For example, membrane trafficking, synaptic targeting and degradation of AMPA-type glutamate receptors are regulated by a network of protein interactions, which ultimately effects synaptic plasticity (Anggono and Huganir, 2012; Schwenk et al., 2012). In

analogy, protein complexes associated with NMDA-type glutamate receptors are critically involved in the pathophysiology of chronic inflammatory pain (Tappe et al., 2006), and targeting such interactions showed therapeutic potential (Liu et al., 2008). In this context it is worth mentioning the interaction of GASP1 with type 1 cannabinoid receptor (CB1), which mediates cannabinoid-induced internalization and exposes a molecular basis of analgesic tolerance to cannabinoids (Tappe-Theodor et al., 2007). These studies advocate a major contribution of protein-protein interactions to the function of key players in nociceptive signaling, which ultimately contributes to determine pain response.

Among TRP channels involved in nociception, much relevant literature is now available about dozens of protein complexes associated with TRPV1. Many of these interactors have been reported to modulate TRPV1 activity, and interfering with the binding proved in some cases to effectively attenuate hypersensitivity in animal pain models (Fischer et al., 2013; Kim et al., 2008). The most recent work from Hanack and colleagues on the complex between TRPV1 and the GABA<sub>B1</sub> receptor subunit suggested that modulating the interaction has the impressive potential to selectively revert the sensitized state of TRPV1 channels implicated in pathological pain, while preserving TRPV1 acute pain signaling (Hanack et al., 2015).

In the case of TRPA1 however, much less is known about the network of associated protein complexes. Curiously, the still most relevant physical and functional interaction reported is with TRPV1, which largely coexpresses with TRPA1 in sensory neurons. (Salas et al., 2009; Staruschenko et al., 2010). The functional properties of the two channels are mutually modulated by the association (Akopian et al., 2007) and, on top of that, they have also been reported to form heteromers (Fischer et al., 2014). Very recently, a transmembrane adaptor protein called Tmem100 has been described to bind both TRPA1 and TRPV1 channels in sensory neurons. Mechanistically, Tmem100 seems to weaken their association and selectively potentiate TRPA1 activity; strikingly, a Tmem100 mutant showed the opposite effect, inhibiting TRPA1 response and attenuating both inflammatory pain and chemotherapy-induced neuropathy (Weng et al., 2015). In addition to TRPV1, TRPA1 has been reported to bind the PKA anchor protein AKAP5 and the human tumor suppressor CYLD (Stokes et al., 2006; Zhang et al., 2008). The latter is a ubiquitin hydrolase that seems to control TRPA1 cellular levels by a potential post-translational mechanism (Stokes et al., 2006). In conclusion, it is indeed surprising that up to date only little is known about TRPA1-associated protein complexes, and the lack of knowledge in this respect represents a clear call to action.

## **1.7 Aims of the study**

A thorough understanding of the mechanisms underlying nociception is paramount to interpret the maladaptive changes that characterize chronic and pathological pain states. Much evidence now advocates TRPA1 as a major player in noxious stimuli transduction and pain signaling in vertebrates. Being highly enriched in nociceptors, where they serve as primary sensors to integrate polymodal stimuli and trigger nociceptive signaling, TRPA1 channels represent ideal targets for developing new therapeutic strategies for pain conditions. While relevant literature is already available about TRPA1 activation modalities, still very little has been reported about the regulation of this channel, which ultimately affects its activity and function in both physiological and pathophysiological contexts. While several mechanisms have been proposed to affect protein function, the molecular network of protein interactions regulating TRPA1 (the so-called TRPA1 interactome) is only poorly understood.

This study was therefore aimed at shedding some lights on the mechanisms of TRPA1 regulation, with a special focus on identifying and characterizing novel TRPA1-protein complexes, as potentially crucial modulators of TRPA1 function and nociceptive signaling. The valuable knowledge we obtained contributes not only to a better understanding of TRPA1 channels in more detail, but also to nociceptive signaling in general; ultimately, this study might even contribute to reveal novel therapeutic targets for specific TRPA1-related pain conditions.

## 2. MATERIALS AND METHODS

### Reagents

Product	Company
10X PBS (Phosphate-buffered saline) pH 7.4	Life Technologies
10X HBSS (Hank's balanced salt solution)	Life Technologies
HEPES (4-(2-hydroxyethyl)-1-piperazineethanesulfonic acid)	Life Technologies
DMEM (Dulbecco's modified eagle medium), GlutaMAX	Life Technologies
DMEM (Dulbecco's modified eagle medium)/F-12, GlutaMAX	Life Technologies
OPTIMEM medium	Life Technologies
RPMI (Roswell Park Memorial Institute) medium	Life Technologies
Growth factors (NGF, GDNF, BDNF, NT-3, NT-4)	R&D Systems
Poly-D-lysine	Millipore
Papain	Worthington
Penicillin/Streptomycin	Life Technologies
Laminin	Life Technologies
Collagenase	Worthington
Horse serum	Life Technologies
FBS (fetal bovine serum)	Life Technologies
Donkey serum	Dianova
Goat serum	Dianova
BSA (bovine serum albumin)	Sigma-Aldrich
Mustard oil (allyl isothiocyanate, AITC, MO)	Sigma-Aldrich
Capsaicin	Sigma-Aldrich
CFA (Complete Freund's Adjuvant)	Sigma-Aldrich
ATP (adenosine 5'-triphosphate) magnesium salt	Sigma-Aldrich
DMSO (dimethyl sulfoxide)	Sigma-Aldrich
Nocistatin	Tocris
PFA (paraformaldehyde)	Science Services
NP-40 (IGEPAL CA-630)	Sigma-Aldrich
DDM (Dodecyl- $\beta$ -D-maltoside)	Roth
Triton X-100	Roth
Sodium deoxycholate	Roth
Complete protease inhibitor cocktail tablets	Roche
Fura-2 AM	Life Technologies
DTT (DL-Dithiothreitol)	Sigma-Aldrich
OCT (optimal cutting temperature) compound	Sakura
Agarose	Roth
Sucrose	Merck

EDTA (ethylenediaminetetraacetic acid)	Roth
EGTA (ethylene glycol tetraacetic acid)	Roth
Glycerol	Roth
Milk powder	Roth
NaCl	Roth
Tris-HCl	Roth
CsCl	Sigma-Aldrich
NaOH	Roth
KCl	Roth
MgCl <sub>2</sub>	Roth
Glucose	Roth
CaCl <sub>2</sub>	Roth

## Methods

### 2.1 Annexin A2 (AnxA2) regulates TRPA1-dependent nociception

The gross part of the text relative to this section is based on (Avenali et al., 2014).

#### 2.1.1 Protein identification by mass spectrometry analysis and database search

Proteins were identified by MS using an LTQ-Orbitrap mass spectrometer (Thermo Fisher Scientific) essentially as described previously (Gomez-Varela et al., 2012) except that tandem MS data were used to search a mouse-specific database with an appended reverse sequence copy (EBI-IPI database version 3.32). Proteins were only considered if they were identified by two or more peptides in both independent TRPA1 affinity purifications from trigeminal ganglia (TG) lysates and were absent in the two independent replicates of the control experiment (IgG). Scaffold (version Scaffold\_4.0.5; Proteome Software) was used to validate MS/MS-based peptide and protein identifications. Peptide identifications were accepted if they could be established at >95% probability by the Peptide Prophet algorithm (Keller et al., 2002). Protein identifications were accepted if they could be established at >95% probability and contained at least two identified peptides. The mass spectrometry-based identification and data analysis were performed before the start of my PhD project by the Genomics Institute of the Novartis Research Foundation (GNF), La Jolla, CA.

#### 2.1.2 Cloning of the AnxA2 N-term deletion construct ( $\Delta$ AnxA2)

The cDNA of mouse AnxA2 was used as a template for a PCR designed to delete the first 15 aa of the N terminus of AnxA2 using the following primers: GATCATTCTACACCCCAAG and TCAGTCATCCCCACCACACAG. Primers were designed with BamHI and EcoRV restriction sites

to insert the PCR product into pcDNA3-PV-IRES-EGFP (a kind gift from Nils Brose, Max Planck Institute of Experimental Medicine, Göttingen, Germany). PCR reactions were performed using 150 ng template DNA, in 1X Pfx reaction buffer (Life Technologies), 300  $\mu$ M dNTP mix (Thermo Scientific), 0.3  $\mu$ M of each specific primer, 1 mM MgSO<sub>4</sub> (Invitrogen), 1 U of Platinum Pfx DNA polymerase (Life Technologies). The thermocycler (Bio-Rad T100) was programmed as indicated: an initial denaturation step of 3 minutes at 94 °C, followed by 25 cycles of amplification including 94 °C for 15 s, 55 °C for 30 s, 68 °C for 70 s, and at the end 68 °C for 10 minutes. After the PCR reaction, the products were visualized using agarose gel electrophoresis, product bands excised and DNA purified using NucleoSpin gel and PCR clean-up kit (Macherey-Nagel) following manufacturer's instructions. Digestion of vector and insert was performed by incubation with FastDigest restriction enzymes EcoRV and BamHI (Thermo Scientific) in 1X green buffer (Thermo Scientific) for 35 minutes at 37 °C. In order to prevent self-ligation, the vector was then dephosphorylated by treatment with FastAP thermosensitive alkaline phosphatase (Thermo Scientific) for 35 minutes at 37 °C. Immediately after the end of the incubation, samples were run on agarose gel to stop the alkaline phosphatase reaction and visualize the products. Bands were then excised and products purified again using NucleoSpin gel and PCR clean-up kit (Macherey-Nagel) following manufacturer's instructions. For ligation, insert and vector (molar ratio 3:1) were mixed with 1 U of T4 DNA ligase (Life Technologies) in 1X ligase buffer (Life Technologies) for 2 h at 25 °C. Subcloning efficiency DH5 $\alpha$  E. coli competent cells (Life Technologies) were used for bacterial transformation. A mix of 50  $\mu$ l cells and 5  $\mu$ l ligated DNA product was incubated for 30 minutes on ice, then heat-shock transformation was performed by incubation at 42 °C for 25 s in a water bath, followed by 2 minutes on ice. Immediately after, 950  $\mu$ l SOC medium (Invitrogen) were added, and the cells incubated at 37 °C for 1 h with shaking at 250 rpm. Cells were then centrifuged at 6000 rpm for 1 minute, the pellet resuspended in 200  $\mu$ l SOC medium and finally plated on LB agar (Roth) plates containing 100  $\mu$ g/ml ampicillin (Roth). Plates were incubated at 37 °C overnight with shaking at 250 rpm. From the LB agar plate, 6 single colonies were picked and cultured in 5 ml of LB medium containing 100  $\mu$ g/ml ampicillin. After overnight incubation at 37 °C with shaking at 250 rpm, 1 ml of the culture was used for plasmid purification using PureLink quick plasmid miniprep kit (Macherey-Nagel) following manufacturer's instruction. Amount and purity of the eluted DNA were assessed by spectrophotometric analysis, and sequences verified by sequencing.

### **2.1.3 HEK293T cell culture and transfection**

HEK293T cells were maintained at 37 °C, 5% CO<sub>2</sub> in DMEM+GlutaMAX containing 10% FBS and penicillin/streptomycin. Upon transient transfection using FuGENE HD (Promega) following manufacturer's instructions, cells were plated on coverslips (for calcium imaging and electrophysiology) or MatTek dishes (for live labeling) coated with poly-D-lysine (1

mg/ml) and laminin (20 µg/ml). Twenty-four hours after plating cells were used for biochemistry, electrophysiology, or calcium imaging.

#### **2.1.4 Protein affinity purification from tissue lysates and coimmunoprecipitation from cell lysates**

HEK293T cells were transfected with cDNA encoding for mouse TRPA1-myc, AnxA2,  $\Delta$ AnxA2, p11, TRPV1, or empty plasmid (Mock) and were plated in 10 cm cell culture dishes. After 24 h cells were collected in PBS, centrifuged, and the cell pellet was resuspended in lysis buffer (150 mM NaCl, 50 mM Tris-HCl, pH 7.5, 0.5 mM EDTA, 10% glycerol, 1% NP-40, 0.5% sodium deoxycholate, complete protease inhibitor cocktail). TG were freshly extracted from male wild-type mice (6–12 weeks old), and homogenized in lysis buffer using a glass dounce homogenizer. After centrifugation (10,000 rpm, 10 minutes) the resulting supernatant from TG lysates was incubated at 4 °C for 5 h with 20 µg of TRPA1 antibodies (rabbit, E1 or E3; (Schmidt et al., 2009)) or 20 µg of rabbit IgG coupled to magnetic beads (Protein G Dynabeads; Life Technologies). The supernatant from HEK293T cell lysates was incubated at 4 °C overnight either with 20 µg of myc antibody (9E11 mouse; Santa Cruz Biotechnology), 10 µg of TRPA1 antibody (Schmidt et al., 2009), or with 20 µg of TRPV1 antibody (goat; Santa Cruz Biotechnology) coupled to magnetic beads. After five washes in lysis buffer, beads were eluted by incubation for 10 minutes at 70 °C in 40 µl of elution buffer containing the following: 1X lithium dodecyl sulfate sample buffer (Life Technologies) and 1X NuPAGE sample-reducing agent (Life Technologies). The resulting mixtures were resolved by 1D NuPAGE using the MES running buffer (Life Technologies). In case of tissue samples each resolved lane was cut into 16 equal gel slices, which were analyzed separately by mass spectrometry. In the case of cell lysates protein gels were used for western blotting followed by immunodetection.

#### **2.1.5 Western blotting**

Protein gels of cell lysates were blotted on nitrocellulose or PVDF membranes using the iBlot System (Life Technologies) and afterwards blocked for 30 minutes in 5% milk powder in PBS. Membranes were then incubated overnight at 4 °C with primary antibodies to myc (9E11 mouse; 1:100; Santa Cruz Biotechnology), Annexin A2 (rabbit; 1:100; Abcam), p11 (goat; 1:40; R&D Systems), and TRPV1 (goat; 1:100; Santa Cruz Biotechnology) in 1% milk powder in PBS. After 3 washes in PBS, membranes were incubated for 2 h at room temperature with proper secondary antibodies anti-mouse Alexa680 (donkey; 1:8000; Life Technologies), anti-rabbit Alexa680 (donkey; 1:8000; Life Technologies), anti-goat Alexa680 (donkey; 1:8000; Life Technologies) or anti-rabbit IR Dye 800 (donkey; 1:8000; Li-Cor). After 3 additional washes, detection of immunolabeled protein was performed using infrared imaging

(Odyssey; Li-Cor). Western blots were independently repeated three times. Only for presentation purposes were size, brightness, and contrast levels of paired blots (i.e., experiments done in parallel and probed with the same antibody) adjusted using Photoshop CS6 (Adobe).

### **2.1.6 Dissociated mouse dorsal root ganglion neuron culture**

Dorsal root ganglia (DRG) were isolated from all spinal levels of 6-10 weeks old, male WT C57BL/6J mice. The mice were euthanized by CO<sub>2</sub> inhalation followed by decapitation according to guidelines stated in the German Animal Welfare Act. The skin covering the spinal cord was removed and the spinal column with its adjacent connective tissue dissected out. The vertebral arches were sequentially removed to expose the spinal cord. The dorsal root ganglia were then carefully extracted from each of the intervertebral foramina. The tissue was first collected in serum free medium (DMEM/F12+GlutaMAX) then transferred into a falcon tube with 12 mg/ml collagenase. After 1 h of incubation at 37 °C, the tissue was triturated with a P1000 pipette. The DRGs were further dissociated via incubation with 10 U/ml papain for 30 minutes at 37 °C. The DRGs were then centrifuged (1000 rpm; 1 minute) following which the supernatant was removed and the mix triturated again in serum-free media. To remove cell debris, a column of 0.15 g/ml BSA was added to the cell suspension and centrifuged (1000 rpm; 10 minutes). After the centrifugation, cell debris, media and BSA layer were removed carefully with a Pasteur pipette. For WT DRG cultures, cells were directly plated on 1 mg/ml poly-D-lysine and 20 µg/ml laminin-coated coverslips following resuspension in growth medium (DMEM/F12+GlutaMAX supplemented with 10% horse serum and growth factor mix containing: 100 ng/ml NGF, 50 ng/ml GDNF, 50 ng/ml BDNF, 50 ng/ml NT-3, and 50 ng/ml NT-4). After 10 minutes incubation of the cell suspension drop at 37 °C, 1ml of growth medium was added. Cells were used 24 h after plating for calcium imaging experiments.

### **2.1.7 Nucleofection of DRG cultures**

Transfection of neurons was achieved by nucleofection of cDNA into freshly isolated DRG neurons using the P3 Primary Cell 4D Nucleofector X Kit with the 4D-Nucleofector X Unit according to the manufacturer's instructions (Lonza AG). (1) For calcium imaging rescue experiments 0.8 µg of mAnxA2-pCMVSPORT6 or empty pCMVSPORT6 were used, each in combination with 0.2 µg of pmaxGFP (Lonza AG), which was to visualize transfected neurons. (2) For live labeling 0.8 µg of mTRPA1-IRES-YFP was used and for rescue experiments an additional 1 µg of mAnxA2-pCMVSPORT6 or empty pCMVSPORT6 was used. (3) For electrophysiology 0.5 µg of mTRPA1-IRES-YFP was used. After nucleofection, neurons were allowed to recover in RPMI medium for 10 minutes at 37 °C before plating in growth

medium. Two hours after transfection half of the growth medium was exchanged with fresh medium and neurons were grown for 36–48 h.

### **2.1.8 Electrophysiology**

Whole-cell voltage-clamp recordings were performed in transfected HEK293T cells or transfected DRG cultures at room temperature with standard patch pipettes (3–5 M $\Omega$  resistance) made of borosilicate glass capillaries. Current signals were recorded with an EPC-9 patch-clamp amplifier (HEKA). Stimulus delivery and data acquisition were performed using Pulse software (HEKA). Current–voltage (*I/V*) curves were performed using voltage steps of 400 ms duration ranging from -100 to +175 mV followed by an invariant pulse at -75 mV (400 ms). The holding potential was set to 0 mV. To repress inactivation of voltage-dependent currents (Macpherson et al., 2007; Meseguer et al., 2014), these recording were made in Ca<sup>2+</sup>-free solutions [intracellular solution (in mM): 140 NaCl, 5 CsCl, 10 EGTA, and 10 HEPES, pH 7.4, adjusted with NaOH; bath solution (in mM): 140 NaCl, 3 KCl, 1.3 MgCl<sub>2</sub>, 10 HEPES, 1 EGTA, and 10 glucose]. Mustard oil (MO)-dependent currents in both TRPA1-transfected HEK293T cells and TRPA1-transfected DRG neurons were recorded using an extracellular Ca<sup>2+</sup>-containing solution to preserve and study agonist desensitization properties (Macpherson et al., 2007); intracellular solution (in mM): 135 KCl, 2 MgCl<sub>2</sub>, 2 MgATP, 5 EGTA, and 10 HEPES, pH 7.4; bath solution (in mM): 127 NaCl, 3 KCl, 1 MgCl<sub>2</sub>, 10 HEPES, 2.5 CaCl<sub>2</sub>, and 10 glucose, pH 7.3]. The effect of MO on *I/V* curves was studied using voltage ramps of 500 ms ranging from -100 to +100 mV, applied every 5 s. The holding potential was set at -70 mV. Data analysis and representation were done using FitMaster (HEKA) and Igor Pro (WaveMetrics), respectively. Electrophysiology recordings were performed by Pratibha Narayanan.

### **2.1.9 Ratiometric calcium imaging**

Ratiometric calcium imaging was performed essentially as described previously (Coste et al., 2010) using an inverted microscope (Zeiss Axio Observer Z1). Briefly, cells were washed three times with calcium imaging buffer consisting of 1 $\times$ HBSS (1.3 mM Ca<sup>2+</sup>) supplemented with 10 mM HEPES. A working solution of the ratiometric Ca<sup>2+</sup> indicator dye Fura-2 was prepared resuspending 50  $\mu$ g of Fura-2 AM cell permeant (Life Technologies) in 50  $\mu$ l DMSO and adding additional 50  $\mu$ l Pluronic F-127 (Life Technologies) and then diluting the mix 1:200 in imaging buffer. Cells were incubated with the dye for 30-60 minutes at 37 °C, according to the manufacturer's recommendations. Cells were then washed again three times prior to imaging. Fura-2 fluorescence was measured by illuminating the cells with an alternating 340/380 nm excitation light. Fluorescence intensity was measured at 510 nm for both excitation wavelengths and the intracellular Ca<sup>2+</sup> concentration expressed as the

$A_{340}/A_{380}$  ratio. All experiments were conducted at room temperature 24-48 h after plating. For experiments testing cellular response to MO upon AnxA2 overexpression, HEK293T cells were stimulated with 0.1  $\mu\text{M}$ /1  $\mu\text{M}$ /10  $\mu\text{M}$ /30  $\mu\text{M}$ /100  $\mu\text{M}$  MO for 2 minutes, followed by 2 minutes of washout and final stimulation with 100  $\mu\text{M}$  ATP to control for cellular health. For experiments testing response of DRG cultures from both genotypes, neurons were stimulated with the following protocol: 2.5 minutes with 12  $\mu\text{M}$  MO; 5 minutes washout; 2 minutes 50  $\mu\text{M}$  MO; 5 minutes washout; 1.5 minutes 0.5  $\mu\text{M}$  Capsaicin. For experiments assessing the pharmacological desensitization of TRPA1, the following stimulus protocol was applied: (1) application of 50 $\mu\text{M}$  MO for 2 minutes followed by a second 2 minutes application of 50  $\mu\text{M}$  MO 2 minutes later (homologous desensitization) and (2) application of 0.5  $\mu\text{M}$  Capsaicin for 1.5 minutes followed by 2 minutes application of 50  $\mu\text{M}$  MO 5 minutes later (heterologous desensitization; the longer interval between stimuli was necessary for recovery of intracellular calcium levels after Cap application). For data analysis, threshold for activation was set at 20% above the baseline obtained from averaging five time points immediately before addition of each stimulus. All experimental groups to be compared were processed in parallel using the same culture preparation. At least two coverslips from three independent culture preparations were analyzed per experimental paradigm.

### **2.1.10 Immunohistochemistry**

Mice (ages 6–12 weeks) and rats (ages 6–8 weeks) were killed with  $\text{CO}_2$ . DRG were carefully dissected, collected in 4% PFA/PBS, and fixed overnight at 4 °C. After cryoprotection in 30% sucrose/PBS overnight tissues were frozen in optimal cutting temperature compound, sectioned as step serial sections with a cryostat at 10  $\mu\text{m}$  width, mounted on SuperFrost Plus slides, and stored at -80 °C. Frozen slides were thawed at room temperature for 30 minutes, washed three times in PBS with 0.4% Triton X-100 (PBT), blocked for 30 minutes in PBT containing 5% goat or donkey serum, and incubated overnight at 4 °C with primary antibodies diluted in blocking solution. The following antibodies were used: 1:50 rabbit anti-TRPA1, custom-made E1 or E3 (Schmidt et al., 2009), or 1:100 rabbit anti-TRPA1 (Aviva Systems Biology); 1:100 rabbit anti-TRPV1 (Alomone Labs); 1:100 rabbit anti-Annexin A2 (Abcam); 1:40 goat anti-p11 (R&D Systems); 1:100 chicken anti-Peripherin (Abcam); and 1:200 rabbit anti-NF200 (Sigma-Aldrich). The antibody used on rat sections was 1:50 mouse anti-Annexin A2 (BD Biosciences). The sections were then washed five times in PBS and incubated for 2 h at room temperature with secondary antibodies conjugated to Alexa Fluor 488, Alexa Fluor 546 or Alexa Fluor 647 (Life Technologies) diluted 1:250 in blocking solution. Sections were then washed five times in PBS and mounted in SlowFade Gold reagent (Life Technologies).

### **2.1.11 Image acquisition and analysis of immunohistochemistry**

Digital images of stained cryosections were obtained by fluorescence microscopy (either using a Zeiss Axio Observer Z1 epifluorescence microscope or the Leica SP5 confocal laser scanning microscope). Images for all experimental groups were taken using identical acquisition parameters. All groups to be compared were processed simultaneously using the same culture or tissue preparation. Raw images were analyzed by using NIH ImageJ essentially as described previously (Schmidt et al., 2009). In cryosections neurons were considered TRPA1-positive if the mean fluorescence intensity (measured in arbitrary units, AU) was higher than the mean background fluorescence plus four times the SD measured from at least 10 random unstained cells. For TRPA1 labeling the analysis was performed using three different TRPA1 antibodies (as described above), which gave similar results. Neurons were considered positive for the other labels if the mean fluorescence intensity (measured in AU) was higher than the mean background fluorescence plus three times the SD measured from at least 10 random unstained cells. Only sections that were at least 70  $\mu\text{m}$  apart were considered to avoid double counting neurons. Only for presentation purposes were brightness, contrast, and curve levels of paired images adjusted using Photoshop CS6 (Adobe).

### **2.1.12 RNA isolation and quantitative PCR (qPCR)**

Total RNA was isolated from freshly dissociated DRG neurons of *AnxA2<sup>-/-</sup>* and WT mice by NucleoSpin RNA XS (Macherey-Nagel) according to the manufacturer's instructions. One thousand nanograms of total RNA were then used for first-strand cDNA synthesis using QuantiTect reverse transcription kit (Qiagen). First, genomic DNA (gDNA) was eliminated adding gDNA wipe-out buffer and incubating the mix at 42 °C for 6 minutes in a thermal cycler (Bio-Rad T100). Reverse transcription (RT) master mix (Quantiscript RT buffer, RT primer mix, Quantiscript reverse transcriptase) was then added, followed by incubation at 42 °C for 30 minutes and 95 °C for 3 minutes to finally obtain cDNA. TRPA1 gene expression was assessed in both genotypes by real-time qPCR using the SYBR green system (Power SYBR Green PCR Master Mix; Life Technologies) in a LightCycler 480 instrument (Roche). The melting curve analysis of amplified product was used to confirm the specificity of qPCR assay. All samples were run in triplicate and control reactions were run without template and with the reverse-transcription reaction reagents as negative controls. Threshold cycle (Ct) values, the cycle number in which SYBR green fluorescence rises above background, were normalized to two reference genes ( $\beta$ -actin and GAPDH) and recorded as a measure of initial transcript amount. Primer sequences 5'-3' are the following:

TRPA1 (fw: CCATGACCTGGCAGAATACC; rev: TGGAGAGCGTCCTTCAGAAT);  
 $\beta$ -actin (fw: GATCAAGATCATTGCTCCTCCTG; rev: CAGCTCAGTAACAGTCCGCC);  
GAPDH (fw: CAATGAATACGGCTACAGCAAC; rev: TTA CTCTTGAGGCCATGT).

### 2.1.13 TRPA1 live labeling

TRPA1 live labeling was essentially performed as described previously (Schmidt et al., 2009). Freshly dissociated neurons of AnxA2<sup>-/-</sup> mice and WT littermates were nucleofected with TRPA1-IRES-YFP, AnxA2, or empty plasmid for rescue experiments and maintained in culture for 36 h. Surface TRPA1 was live labeled by incubating neurons with TRPA1 antibodies (1:25) for 60 minutes followed by five washes in neuronal medium and incubation with secondary antibodies conjugated to Alexa Fluor 546 (Life Technologies) at a dilution of 1:200. Neurons were washed with PBS, fixed in 2% PFA/PBS for 20 minutes, and imaged on a Zeiss Axio Observer Z1 epifluorescence microscope. All groups to be compared were processed in parallel using the same culture preparation. The image analysis was performed as described previously (Schmidt et al., 2009) with the following change: as a reference for background signal we added ROIs in the non-labeled area along the ROI, which delineated the periphery of each neuron. This enabled us to determine a threshold value of intensity (in AU) above which the label was considered positive for each individual neuron. Only for presentation purposes were brightness, contrast, and curve levels of paired images (i.e., corresponding WT and AnxA2<sup>-/-</sup> cells) adjusted using Photoshop CS6 (Adobe).

### 2.1.14 Mouse behavior

All animals were housed in a temperature-controlled environment under a 12 h light/dark cycle with food and water provided *ad libitum*. Behavioral tests were performed by individuals blind to genotype. In these tests 6- to 12-week-old WT and AnxA2<sup>-/-</sup> littermates were used and the mice were matched for gender. AnxA2<sup>-/-</sup> mice were kindly provided by Katherine A. Hajjar (Ling et al., 2004). Mice were acclimatized for 30 minutes (injection paradigms) or 120 minutes (thermal and mechanical paradigm) in a transparent Plexiglas box. For injections, 10  $\mu$ l of experimental agent were injected subcutaneously into the plantar surface of one hindpaw. Nocifensive behaviors were assessed by measuring the time spent licking, flicking, or lifting the injected paw for 10 minutes. Vehicle injection (PBS) did not elicit any significant pain behavior in either genotype (data not shown). Mechanical and thermal sensitivity were measured according to standard procedures (Minett et al., 2011) and according to the manufacturer's manual (Ugo Basile).

*Mechanical sensitivity* was determined upon paw withdrawal to application of a graded force (0–10 g in 40 s for basal acute sensitivity and 0–7.5 g in 40 s for the inflammatory pain paradigm) via a dynamic aesthesiometer (Ugo Basile) to the plantar surface of both hindpaws. Paw withdrawal latencies were averaged from at least four readings per paw.

To determine thermal sensitivity two different tests were used: heat and cold sensitivity.

*Heat sensitivity.* The paw withdrawal latency to infrared heat (set at 40) was measured using a plantar test apparatus (Hargreaves apparatus; Ugo Basile). Paw withdrawal latencies for each test were averaged from at least four readings per paw.

*Cold sensitivity.* A custom-made cold plate was set at 1.5 °C and the latency to the onset of nocifensive behaviors (licking, flicking, or lifting of the injected paw) and escape behaviors (jumping) were measured. If mice did not show nocifensive behaviors (as observed often after vehicle injection) they were removed from the cold plate after 5 minutes and scored with a latency of 330 s. All groups to be compared were assessed in parallel. All animal experiments were approved and performed in compliance with the institutional guidelines and the guidelines of the Landesamt fuer Verbraucherschutz und Lebensmittelsicherheit of Lower Saxony.

### **2.1.15 Statistical analysis**

The nonparametric Mann–Whitney test or the two-tailed unpaired Student’s *t* test were used for single comparisons, and one-way ANOVA was used for multiple comparisons. All values refer to mean ± SEM; *n* indicates the sample number, *p* denotes the significance (\**p*<0.05, \*\**p*<0.01, \*\*\**p*<0.001) and refers to the respective control in each experimental group if not noted otherwise.

## **2.2 TRPA1 interactome undergoes dramatic changes during inflammatory pain**

### **2.2.1 Inflammatory pain paradigm and TRPA1 immunoprecipitation from tissue lysates**

Inflammatory pain was induced in male C57BL/6J mice (6-12 weeks old) by injection of 10 µl of Complete Freund’s Adjuvant (CFA) into the plantar surface of the left hindpaw, with PBS-injected mice serving as control. Mice were sacrificed 24 h after the injection by CO<sub>2</sub> inhalation followed by decapitation according to guidelines stated in the German Animal Welfare Act. Ipsilateral lumbar DRGs (L1 to L5) were dissected and collected in PBS with protease inhibitors. Tissue was subsequently homogenized in 500 µl/sample ice-cold solubilization buffer (100 mM NaCl, 50 mM Tris-HCl pH 7.4, 320 mM sucrose, 1mM DTT, 1% DDM, complete protease inhibitor cocktail) using first a glass dounce homogenizer and subsequently shearing the lysate passing it 10 times through a 20G needle and 10 times through a 25G needle. DRGs from 20 mice per condition were necessary for each experimental replicate, and tissue from TRPA1<sup>-/-</sup> animals (ipsilateral and contralateral lumbar DRGs from 10 non-injected mice) was processed in parallel. Lysates were then incubated for 1 h at 4 °C on a tube rotator (VWR International) followed by centrifugation for 10 minutes at 2500xg at 4 °C. A pre-clearing step was performed incubating each lysate with 50 µl magnetic beads (Protein G Dynabeads; Life Technologies) for 1 h at 4 °C on a tube rotator. Beads were then removed and the lysate incubated with 24 µg of TRPA1 antibodies (rabbit,

E1; (Schmidt et al., 2009)) for 4 h at 4 °C on a tube rotator. Magnetic beads (100 µl/sample) were then added to the lysates and incubated overnight at 4 °C on a tube rotator. After one short washing step with ice-cold solubilization buffer, beads were then eluted by incubation for 10 minutes at 70 °C in 40 µl of elution buffer containing the following: 1X TG PRiME sample buffer (Serva) and 10 mM DTT.

### **2.2.2 Protein identification by mass spectrometry analysis and database search**

Eluted proteins were separated on precast TG PRiME Tris/glycine 8-16% gradient gels (Serva) and visualized by colloidal Coomassie staining. Entire gel lanes were cut into 24 equally-sized gel pieces and subjected to automated in-gel digestion with trypsin as described previously (Schmidt et al., 2013). Tryptic peptides were dried down in a vacuum centrifuge, re-dissolved 0.1% trifluoro acetic acid and spiked with 2.5 fmol/µL of yeast enolase 1 tryptic digest standard (Waters Corporation) for quantification purposes (Silva et al., 2006). After nanoscale UPLC separation, tryptic peptides were subjected to mass spectrometry analysis using a Synapt G2-S quadrupole time-of-flight mass spectrometer equipped with ion mobility option (Waters Corporation). Positive ions in the mass range  $m/z$  50 to 2000 were acquired with a typical resolution of at least 20,000 FWHM (full width at half maximum) in the ion mobility-enhanced data-independent acquisition (DIA) mode (Geromanos et al., 2012; Silva et al., 2005) with drift time-specific collision energies (Distler et al., 2014). For protein identification, continuum LC-MS data were processed (including lock mass correction) and searched using Waters ProteinLynx Global Server version 3.0.2 (Li et al., 2009). A custom database was compiled by adding the sequence information for yeast enolase 1 and porcine trypsin to the UniProtKB/Swiss-Prot mouse proteome and by appending the reversed sequence of each entry to enable the determination of false discovery rate (FDR). UniProtKB release 2014\_10 (16,686 entries) was used for replicate experiment 1 and 2, while 2015\_01 (16,695 entries) was used for replicate experiment 3. Precursor and fragment ion mass tolerances were automatically determined by PLGS 3.0.2 and were typically below 5 ppm for precursor ions and below 10 ppm (root mean square) for fragment ions. Carbamidomethylation of cysteine was specified as fixed and oxidation of methionine as variable modification. One missed trypsin cleavage was allowed. The FDR for protein identification was set to 1% threshold. For post-identification analysis, the freely available software ISOQuant (<http://www.isoquant.net>) was used to merge the 24 LC-MS datasets per gel lane and to calculate the absolute in-sample amounts for each detected protein according to the TOP3 quantification approach (Distler et al., 2014; Kuharev et al., 2015). Based on the peptides identified in the first PLGS database search round described above, the stringency for reporting a protein was increased further by considering only peptides with a minimum length of six amino acids, which were identified with scores above or equal to 5.5. FDR for both peptides and proteins was set to 1 % threshold and only proteins reported by two and more peptides were quantified using the TOP3 method. This part was

performed by the Proteomics Group at Max Planck Institute of Experimental Medicine (Head Dr. Olaf Jahn).

### 2.2.3 Data analysis

For mass spectrometry analysis, the final volume of tryptic digestion reactions could vary based on the protein concentration of the sample, hence a first level of normalization was applied to rule out this variable. In fact, the amount of each detected protein was multiplied by the ratio between the total volume of the digest and the volume later injected into the LC-MS/MS system. For comparable analysis of the amount of all detected proteins within each single biological replicate, data were normalized to account for potential differences in the amount of bait (TRPA1) identified between the CFA and VEH samples. Specifically, in the sample where less bait was detected, the amount of each identified protein would be multiplied by the ratio of “higher bait amount/lower bait amount” between the two samples. Then, this normalized value was used to calculate the ratio of the amount in each sample (VEH or CFA) relative to the TRPA1 KO one (VEH/KO and CFA/KO), as well as the ratios CFA/VEH and VEH/CFA. Subsequently, for selection of proteins coimmunoprecipitating with TRPA1 with high specificity and strong evidence, we set the following stringent criteria: (1) detected in each of the three biological replicates; (2) in each replicate, identified with amount at least three times greater than what found in the relative TRPA1 KO sample. Only candidates fulfilling both the above criteria were considered as high confidence TRPA1-binding partners and used for further statistics and bioinformatics analysis. We then further classified such candidates as:

- Only identified in CFA: if fulfilling above criteria in three replicates in CFA samples only;
- Only identified in VEH: if fulfilling above criteria in three replicates in VEH samples only;
- Identified in both: if fulfilling above criteria in three replicates in both VEH and CFA.

Gene ontology analysis was performed by uploading gene IDs into the functional annotation tool of the DAVID (Database for Annotation, Visualization and Integrated Discovery) bioinformatics resource, to assign genes with their affiliate terms and to order them by enrichment (Huang da et al., 2009a, b). In order to visualize molecular interaction networks based on known and predicted associations among proteins we uploaded Uniprot accession numbers of all proteins in each dataset into STRING (Search Tool for the Retrieval of Interacting Genes/Proteins) (Jensen et al., 2009). The whole analysis was made by choosing datasets of mouse (*mus musculus*).

## 2.3 NIPSNAP1 and Nocistatin modulate TRPA1 channels

Most experiments were performed by Master student Oli Abate Fulas under the author's teaching and supervision; therefore part of the methods is adapted from Oli's Master thesis.

### 2.3.1 HEK293T cell culture and transfection

HEK293T cells were maintained at 37 °C, 5% CO<sub>2</sub> in DMEM+GlutaMAX containing 10% FBS and penicillin/streptomycin. Transient transfections were performed using FuGENE HD (Promega) following manufacturer's instructions, and cells plated on 1 mg/ml poly-D-lysine and 20 µg/ml laminin-coated coverslips. For testing the specificity of NIPSNAP1 antibody 0.5 µg of NIPSNAP1-myc-DKK (Origene) was used. For calcium imaging and immunocytochemistry experiments measuring the effect of NIPSNAP1 overexpression, 0.6 µg of TRPA1-myc cotransfected with 0.5 µg of either NIPSNAP1-myc-DKK or empty vector were used. Cells were used for calcium imaging or immunocytochemistry 24 h after plating.

### 2.3.2 Dissociated mouse dorsal root ganglion neuron culture

Performed exactly as reported under section 2.1.6.

### 2.3.3 Nucleofection of DRG cultures

Transfection of neurons was achieved by nucleofection of cDNA into freshly isolated DRG neurons using the P3 Primary Cell 4D Nucleofector X Kit with the 4D-Nucleofector X Unit according to the manufacturer's instructions (Lonza AG). For NIPSNAP1 knock-down a final concentration of 500 nM of NIPSNAP1 siRNA mix or scramble control siRNA were used to transfect cells. NIPSNAP1 siRNA mix details:

Name	Cat. #	Target sequence	Company
Mm_Nipsnap1_3	SI01327837	ACGAATCATGATTCCTCTGAA	Qiagen
Mm_Nipsnap1_4	SI01327844	TTCCTACATAATGTGGTTAAA	Qiagen
Mm_Nipsnap1_5	SI04919999	TCCGTCATCTCCAGGACATAA	Qiagen
Mm_Nipsnap1_6	SI04920006	CACCACTTATGGGCCTACAAA	Qiagen

For immunocytochemistry experiments testing the effect of NIPSNAP1 overexpression for TRPA1 expression, neurons were cotransfected with 0.5 µg of TRPA1-IRES-YFP and 0.5 µg of either NIPSNAP1-myc-DKK or empty vector. For live labeling experiments cultures were transfected with 0.5 µg of TRPA1-IRES-YFP. After nucleofection, neurons were allowed to recover in RPMI medium for 10 minutes at 37 °C before plating in growth medium. Two

hours after transfection half of the growth medium was exchanged with fresh medium and neurons were grown for 24-72 h, based on the experiment.

### **2.3.4 RNA isolation and quantitative PCR (qPCR)**

Total RNA extraction was performed on DRG neurons 72 h after nucleofection with NIPSNAP1 siRNA or scramble control using NucleoSpin RNA XS (Macherey-Nagel) according to the manufacturer's instruction. Two hundred and fifty nanograms of total RNA were then used for first-strand cDNA synthesis using QuantiTect reverse transcription kit (Qiagen). First, genomic DNA (gDNA) was eliminated adding gDNA wipe-out buffer and incubating the mix at 42 °C for 2 minutes in a thermal cycler (Bio-Rad T100). Reverse transcription (RT) master mix (Quantiscript RT buffer, RT primer mix, Quantiscript reverse transcriptase) was then added, followed by incubation at 42 °C for 30 minutes and 95 °C for 3 minutes to finally obtain cDNA. NIPSNAP1 gene expression was assessed by real-time qPCR using the SYBR green system (Power SYBR Green PCR Master Mix; Life Technologies) in a LightCycler 480 instrument (Roche). The melting curve analysis of amplified product was used to confirm the specificity of qPCR assay. All samples were run in triplicate and control reactions were run without template as negative controls. Threshold cycle (Ct) values, the cycle number in which SYBR green fluorescence rises above background, were normalized to two reference genes ( $\beta$ -actin and GAPDH) and recorded as a measure of initial transcript amount. Primer sequences 5'- 3' are the following:

NIPSNAP1 (fw: GGGTGCTGTGCGCTTCTATT; rev: TCCAGACATTCGGGCTTCAC);  
 $\beta$ -actin (fw: GATCAAGATCATTGCTCCTCCTG; rev: CAGCTCAGTAACAGTCCGCC);  
GAPDH (fw: CAATGAATACGGCTACAGCAAC; rev: TTA CTCTTGAGGCCATGT).

### **2.3.5 Immunocytochemistry**

DRG cultures or HEK293T cells were first fixed for 20 minutes in 4% PFA and blocked with 10% donkey serum and 0.4% Triton X-100 in PBS for 1 h at room temperature, followed by incubation with primary antibody overnight at 4 °C in 1% donkey serum 0.1% Triton X-100 in PBS. Cells were then washed five times with PBS and incubated with secondary antibodies (1:250) for 2 h at room temperature in 1% donkey serum 0.1% Triton X-100 in PBS. Cells were washed again five times with PBS before mounting with SlowFade Gold reagent (Life Technologies). For quantification of knock-down efficacy, NIPSNAP1 siRNA- and control siRNA-nucleofected DRG cultures were labeled with primary anti-NIPSNAP1 (rabbit; 1:100; Abcam) and secondary anti-rabbit Alexa488 (donkey; Life Technologies). For testing antibody specificity, HEK293T cells transfected with NIPSNAP1-myc-DKK cDNA were coimmunostained with primary anti-NIPSNAP1 (rabbit; 1:100; Abcam) and anti-myc (mouse; 1:100; Santa Cruz Biotechnology) and secondary anti-rabbit Alexa488 (donkey; Life Technologies) and anti-

mouse Alexa647 (donkey; Life Technologies). For testing effect of NIPSNAP1 overexpression for TRPA1 expression, DRG cultures transfected with TRPA1-IRES-YFP and either NIPSNAP1-myc-DKK or empty vector were costained with primary anti-TRPA1 (rabbit; 1:50) and anti-GFP (chicken; 1:500; Life Technologies) and secondary anti-rabbit Alexa546 (donkey; Life Technologies) and anti-chicken Alexa647 (goat; Life Technologies). For the same purpose, HEK293T cells cotransfected with TRPA1-myc and either NIPSNAP1-myc-DKK or empty vector were colabeled for TRPA1 with anti-TRPA1 (rabbit; 1:100) and for NIPSNAP1 with anti-Flag (mouse; 1:100; Sigma Aldrich) and secondary anti-rabbit Alexa488 (donkey; Life Technologies) and anti-mouse Alexa546 (donkey; Life Technologies).

### **2.3.6 Immunohistochemistry**

Mice (ages 6–12 weeks) were killed with CO<sub>2</sub>. DRG were carefully dissected, collected in 4% PFA/PBS, and fixed overnight at 4 °C. After cryoprotection in 30% sucrose/PBS overnight tissues were frozen in optimal cutting temperature compound, sectioned as step serial sections with a cryostat at 10 µm width, mounted on SuperFrost Plus slides, and stored at -80 °C. Frozen slides were thawed at room temperature for 30 minutes, washed three times in PBS with 0.4% Triton X-100 (PBT), blocked for 30 minutes in PBT containing 5% goat or donkey serum, and incubated overnight at 4 °C with primary antibodies diluted in antibody solution (1% donkey or goat serum and 0.1% Triton X-100 in PBS). Sections were stained with anti-NIPSNAP1 (rabbit; 1:200; Abcam) and 1:100 anti-Peripherin (chicken; 1:100; Abcam). The next day, after washing five times in PBS, corresponding secondary fluorescent antibodies: anti-rabbit Alexa488 (donkey; 1:250; Life Technologies) and anti-chicken Alexa555 (donkey; 1:250; Life Technologies) were applied and incubated for 2 h at room temperature in antibody solution. Sections were then washed five times in PBT and mounted in SlowFade Gold reagent (Life Technologies).

### **2.3.7 Image acquisition and analysis of immunostainings**

Digital images of the stained cultures and DRG cryosections were obtained by an epifluorescence microscope (Zeiss Axio Observer Z1). Images for all experimental groups were taken using identical acquisition parameters. All groups to be compared were processed simultaneously using the same culture or tissue preparation. Raw images were analyzed by using NIH ImageJ essentially as described previously (Schmidt et al., 2009). Cells were considered positive for their labeled protein (NIPSNAP1, TRPA1 or Peripherin) if the mean fluorescence intensity (measured in arbitrary units, AU) was higher than the mean background fluorescence plus three times the SD measured from at least 5 random unstained cells for the immunocytochemistry, and 10 random unstained cells for immunohistochemistry.

### **2.3.8 Ratiometric calcium imaging**

Ratiometric calcium imaging was performed essentially as described previously (Coste et al., 2010) using an inverted microscope (Zeiss Axio Observer Z1). Briefly, cells were washed three times with calcium imaging buffer consisting of 1×HBSS (1.3 mM Ca<sup>2+</sup>) supplemented with 10 mM HEPES. A working solution of the ratiometric Ca<sup>2+</sup> indicator dye Fura-2 was prepared resuspending 50 µg of Fura-2 AM cell permeant (Life Technologies) in 50 µl DMSO and adding additional 50 µl Pluronic F-127 (Life Technologies) and then diluting the mix 1:200 in imaging buffer. Cells were incubated with the dye for 30-60 minutes at 37 °C, according to the manufacturer's recommendations. Cells were then washed again three times prior to imaging. Fura-2 fluorescence was measured by illuminating the cells with an alternating 340/380 nm excitation light. Fluorescence intensity was measured at 510 nm for both excitation wavelengths and the intracellular Ca<sup>2+</sup> concentration expressed as the A<sub>340</sub>/A<sub>380</sub> ratio. All experiments were conducted at room temperature 24-72 h after plating. Experiments on the subject of examining the effect of Nocistatin on TRPA1-mediated response were performed with this protocol: 2 minutes application of 10 µM Nocistatin/vehicle followed by 2 minutes application of 10 µM Nocistatin/vehicle in 25 µM MO and then incubation for 4 minutes. Subsequently, 50 µM MO, 1 µM capsaicin and 60 mM KCl were applied in the mentioned order for 2 minutes each with 5 minutes of intervening washes between the stimuli. For experiments dealing with the influence of Nocistatin on TRPV1: pre-incubation with 10 µM Nocistatin (applied for 2 minutes) was followed by application of 10 µM Nocistatin/vehicle in 0.1 µM capsaicin and incubation for 4 minutes. After 5 minutes of washing 1 µM capsaicin was applied for 2 minutes. HEK293T cells overexpressing TRPA1 and either NIPSNAP1 or empty vector were assessed for TRPA1 response via application of 1 µM/10 µM/30 µM MO for 2.5 minutes followed by washing with imaging buffer for 5 minutes and subsequent application of 100 µM MO for 3 minutes. For data analysis, threshold for activation was set at 20% above the baseline obtained from averaging five time points immediately before addition of each stimulus. All experimental groups to be compared were processed in parallel using the same culture preparation. At least two coverslips from three independent culture preparations were analyzed per experimental paradigm.

### **2.3.9 TRPA1 live labeling**

TRPA1 live labeling was essentially performed as described previously (Schmidt et al., 2009). Freshly dissociated neurons were nucleofected with TRPA1-IRES-YFP and maintained in culture for 36 h. Cells were then incubated with 10 µM Nocistatin or vehicle for 4 minutes at room temperature, washed and immediately after surface TRPA1 was live labeled by incubation with TRPA1 antibodies (1:25) for 60 minutes followed by five washes in neuronal medium and incubation with secondary antibodies conjugated to Alexa Fluor 546 (Life Technologies) at a dilution of 1:200. Neurons were washed with PBS, fixed in 2% PFA/PBS for

20 minutes, and imaged on a Zeiss Axio Observer Z1 epifluorescence microscope. All groups to be compared were processed in parallel using the same culture preparation. The image analysis was performed as described previously (Schmidt et al., 2009) with the following change: as a reference for background signal we added ROIs in the non-labeled area along the ROI, which delineated the periphery of each neuron. This enabled us to determine a threshold value of intensity (in AUs) above which the label was considered positive for each individual neuron.

### **2.3.10 Statistical analysis**

The two-tailed unpaired Student's *t* test was used to evaluate statistical significance. All values refer to mean  $\pm$  SEM; *p* denotes the significance (\* $<p0.05$ , \*\* $<p0.01$ ) and refers to the respective control in each experimental group if not noted otherwise.

## 3. RESULTS

### 3.1 Annexin A2 (AnxA2) regulates TRPA1-dependent nociception

The gross part of the text relative to this section is based on (Avenali et al., 2014).

#### 3.1.2 AnxA2 is a binding partner of TRPA1 in mouse sensory neurons

A crucial determinant of TRPA1 activity and function could be represented by the network of protein complexes associated to the channel, the so-called TRPA1 interactome. In this line we aimed to identify TRPA1-binding candidates by affinity purification of the native TRPA1 channels from mouse sensory neurons. The choice of working with native channels was result of important considerations: on the one hand, this means dealing with the need of a significant amount of tissue, but on the other hand, it has considerable advantages with respect to, for instance, systems where the channel is overexpressed, namely a reduction of false negative hits and more reliable candidate list. In this line sensory neurons were dissected from mice and whole cell lysates obtained by mild detergent solubilization. This procedure is critical and needs to be carefully optimized in terms of the stringency of the buffer and the washing steps that will follow. We needed to obtain a reasonable amount of the bait (TRPA1) that, by its own nature and as other transmembrane proteins, is hydrophobic, and therefore difficult to isolate. On the one hand, with too harsh conditions we would end up disrupting complexes and potentially losing weak and transient interactions, likely biologically relevant. On the other hand, being too mild would result in insufficient amount of TRPA1 protein and incomplete removal of non-binding proteins, which will be then detected during mass-spectrometry analysis, making the candidate list hard to interpret. From cell lysates, TRPA1 channels were affinity purified with specific TRPA1 antibodies and rabbit IgG serving as control. An antibody with high specificity and affinity for the target protein is an essential tool for the success of coimmunoprecipitation experiments; accordingly, a custom-made antibody has been used, which performance and specificity in tissue from TRPA1-deficient mice had been already proved in previous publications (Schmidt et al., 2009). Eluates of coimmunoprecipitation were separated by 1D-PAGE, gel lanes were excised, subjected to “in-gel” digestion with trypsin, and samples submitted to mass-spectrometry analysis. This procedure enabled the detection of endogenous TRPA1 channels validating such approach (Fig. 4). In addition to the bait, a consistent list of potential interacting partner was obtained and the selection of candidates for further characterization was based on stringent criteria. We only considered proteins that: (1) appeared in both independent biological replicates of the experiment; (2) were identified with a minimum of two unique peptides; and (3) were absent in both independent control replicates. This strategy led to the identification of Annexin A2 (AnxA2) as a binding partner of TRPA1 in mouse sensory neurons (Fig. 4). AnxA2 is a member of the Annexin

superfamily of calcium-binding proteins and is involved in different membrane transport processes (Gerke et al., 2005; Rescher and Gerke, 2004).

<i>Accession number</i>	<i>Protein name</i>	<i>Identified peptides</i>	<i>No. of spectra in experimental replicates</i>	<i>No. of spectra in control replicates</i>
Q8BLA8	TRPA1	FLLSQGANPNLR CMALHFAATQGATDIVK EVIQIFQKQ IAMQVELHTNLEK LLQDISDTR	7	0
P07356	Annexin A2	DALNIETAVK DIISDTSGDFR QDIAFAYQR TNQELQEINR	5	0

**Figure 4: AnxA2 coimmunoprecipitates with native TRPA1 from mouse sensory neurons.**

The table depicts the MS/MS results (identified peptides and number of total spectra) of two independent TRPA1-affinity purifications and corresponding controls. The mass spectrometry analysis was performed by the Genomics Institute of the Novartis Research Foundation (GNF), La Jolla, CA. From (Avenali et al., 2014).

### 3.1.2 AnxA2 coimmunoprecipitates with TRPA1 in a heterologous expression system

In order to validate AnxA2 as a TRPA1-binding protein we tried to recapitulate the interaction in a well-established and widely accepted heterologous expression system, namely HEK293T cells. We transfected HEK293T cells with myc-tagged TRPA1 (TRPA1-myc) and mouse AnxA2 cDNA, and performed TRPA1 immunoprecipitation. Nicely, we could detect AnxA2 in the eluate when both anti-myc (Fig. 5A) and anti-TRPA1 antibodies (data not shown) were used for immunoprecipitation. HEK293T cells transfected with TRPA1-myc and the empty vector were used as a negative control (TRPA1+Mock; Fig. 5A). These data supports the MS results indicating that this interaction can be reproduced in a non-neuronal context and suggest that it could be potentially direct, or at least that does not involve a neuronal cell-specific mediator. To get better insights into the nature of the interaction, we attempted to identify the AnxA2 domain involved in the association with TRPA1 and therefore cloned a truncated version of AnxA2, called  $\Delta$ AnxA2. This construct lacks the first 15aa of the native protein, a region already implicated in AnxA2-protein-protein interactions, and did not immunoprecipitate with TRPA1 upon overexpression in HEK293T cells (Fig. 5A). These findings suggest that the first 15 residues of AnxA2 are critical to the binding to TRPA1 channels, either directly or via yet to be identified proteins. AnxA2 can be found associated with its best characterized binding partner p11 (also referred to as S100A10), a member of the EF-Hand superfamily of calcium-binding proteins. p11 itself has been reported to interact and modulate the activity of several ion channels (Donier et al.,

2005; Okuse et al., 2002; Svenningsson et al., 2006), among them some TRP channels, like TRPV4 (Ning et al., 2012), TRPV5, and TRPV6 (van de Graaf et al., 2003). We therefore found of interest to test whether p11 binds TRPA1 and potentially acts as a mediator of the interaction with AnxA2. However, immunoprecipitation experiments in HEK293T cells transfected with TRPA1 and p11 did not reveal any interaction between the two (Fig. 5B), and this is in line with our proteomics data in sensory neurons that did not identify p11 as a potential TRPA1-interacting protein. In sensory neurons TRPA1 is well known to be coexpressed to a large extent with the heat and capsaicin receptor TRPV1. The activity of the two channels influences each other and general nociceptor excitability, and they have also been reported to interact and form heteromers (Fischer et al., 2014; Staruschenko et al., 2010). Interestingly, immunoprecipitation in HEK293T cells expressing TRPV1 and AnxA2 did not show any physical association between the two (Fig. 5C), which points to a certain degree of specificity for the interaction of AnxA2 with TRPA1.

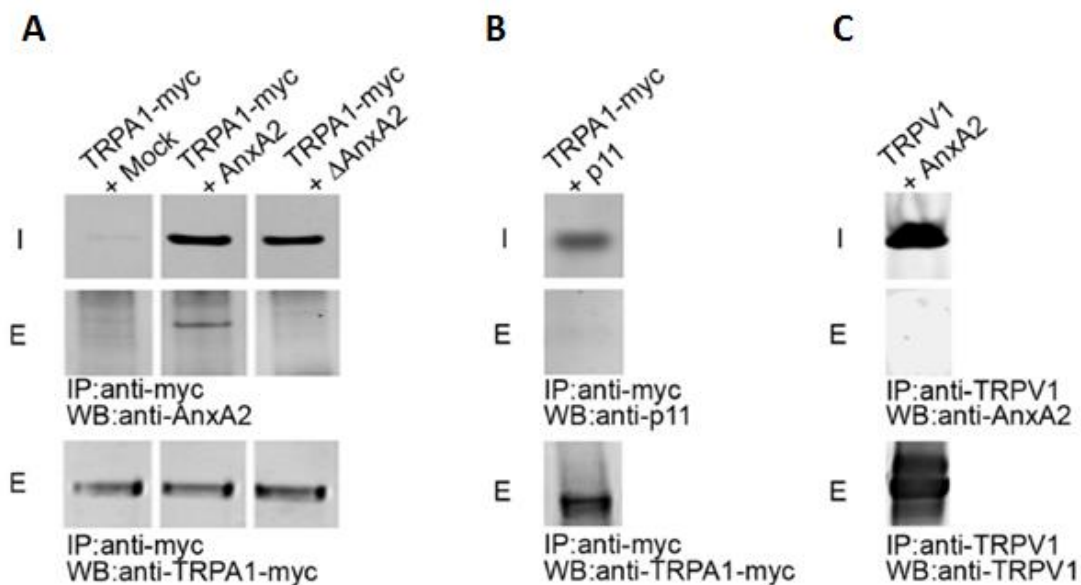


**Figure 5: AnxA2 coimmunoprecipitates with TRPA1 in a heterologous expression system.**

**A–C,** Representative Western blots (WB) of immunoprecipitation (IP) experiments in HEK293T cells recombinantly expressing the indicated constructs. **A,** AnxA2 is detected in eluates (E) of immunoprecipitations only upon cotransfection of TRPA1-myc and AnxA2 (TRPA1-myc+AnxA2) but not in control conditions (TRPA1-myc+Mock). A deletion construct of AnxA2 lacking the first 15 aa ( $\Delta$ AnxA2) did not coimmunoprecipitate with TRPA1 (TRPA1 myc+ $\Delta$ AnxA2). Immunoprecipitations were performed with myc antibodies. **B,** P11 did not coimmunoprecipitate with TRPA1 in our assay (TRPA1-myc+p11). Immunoprecipitations were performed with myc antibodies. **C,** AnxA2 did not coimmunoprecipitate with TRPV1 in cotransfected HEK293T cells (TRPV1 + AnxA2) while TRPV1 itself is readily immunoprecipitated. Immunoprecipitations were performed with TRPV1 antibodies. I, input. Western blots were probed as indicated. From (Avenali et al., 2014).

### **3.1.3 AnxA2 does not affect biophysical properties of recombinant TRPA1 channels**

The physical association of AnxA2 to TRPA1 might have functional consequences for TRPA1 activity and function. The channel might undergo conformational changes or be subjected to chemical modification (e.g. phosphorylation) that would affect its response to activating stimuli. To test this hypothesis we asked whether AnxA2 affects the biophysical properties of TRPA1 channels expressed in HEK293T cells, a well-established system to assess TRPA1 activity (Bandell et al., 2004; Jordt et al., 2004; Macpherson et al., 2007; Meseguer et al., 2014). TRPA1 is a promiscuous channel responsive to a wide variety of agonists, both endogenous and exogenous, and it is also intrinsically voltage-dependent to a certain degree. We studied both channel properties by whole-cell patch clamp recordings. First, we transfected HEK293T cells either with TRPA1 (TRPA1+Mock) or with TRPA1 and AnxA2 (TRPA1+AnxA2) and measured the voltage-dependent activation properties of TRPA1 channels upon membrane depolarization (Meseguer et al., 2014; Zhou et al., 2013). As shown in figure 6, AnxA2 expression did not change the intrinsic voltage-dependent activation profile of TRPA1 channels (Fig.6A,B). TRPA1 current density measured at -75 mV (following depolarization at +175 mV) was not affected by AnxA2 overexpression (TRPA1 + Mock:  $71.8 \pm 6.9$  pA/pF; TRPA1 + AnxA2:  $75.3 \pm 8.1$  pA/pF). Furthermore, neither activation nor inactivation time constants were different when AnxA2 was present (TRPA1 + Mock:  $19.3 \pm 4.3$  ms and  $46.7 \pm 3.1$  ms; TRPA1 + AnxA2:  $19.3 \pm 5.5$  ms and  $52.6 \pm 6.1$  ms, for activation and inactivation, respectively). We then studied TRPA1 activation properties following stimulation with mustard oil (MO), a well-known specific TRPA1 agonist (Bandell et al., 2004; Bautista et al., 2006; Macpherson et al., 2007; Zhou et al., 2013). Electrophysiological analysis showed that neither the MO-dependent I/V relationship nor activation and inactivation time constants were altered by AnxA2 overexpression (Fig.6C,D). Next, we asked whether the cellular responses to TRPA1 activation by the specific agonist MO is affected by AnxA2 overexpression (Fig.6E,F). Figure 6F shows that the dose dependency of MO-evoked increase of  $[Ca^{+2}]_i$  is very similar in both conditions, and together with the electrophysiology data show that AnxA2 overexpression does not alter properties of recombinant TRPA1 in HEK293T cells.

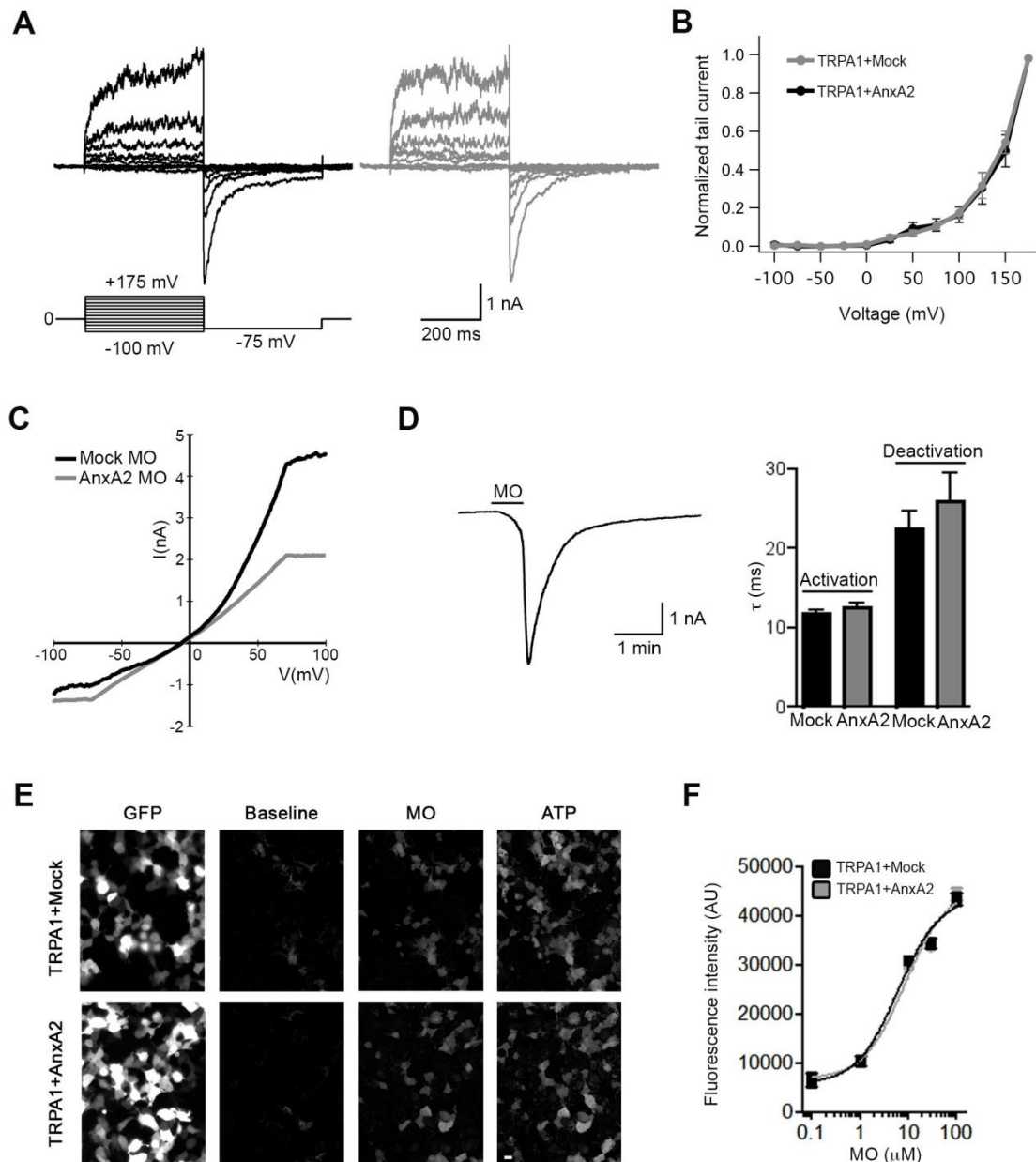


**Figure 6: AnxA2 neither affects TRPA1 voltage dependence nor cellular responses to the TRPA1 agonist MO.** **A, B,** AnxA2 does not affect the voltage dependence of TRPA1. **A,** Whole-cell currents in response to voltage steps applied to HEK293T cells expressing TRPA1 (TRPA1+Mock) or TRPA1+AnxA2. **B,** Average  $\pm$  SEM voltage dependence of TRPA1 peak tail currents at -75 mV for indicated transfections. For each transfection condition data were separately normalized to the current obtained after the maximum depolarization level (+175 mV). **C,** Representative currents elicited by I/V ramps after mustard oil (MO) application of 25  $\mu$ M MO for indicated transfections. **D,** Left, representative MO-induced current at -70 mV (holding potential). Right, Average  $\pm$  SEM time constants of MO-induced activation and inactivation measured by a mono-exponential fit to the currents obtained at -70 mV for indicated transfections ( $n > 12$  cells per condition; n.s.; Student's t-test). **E,** AnxA2 does not affect cellular responses to the TRPA1 agonist MO. Representative images of ratiometric  $[Ca^{2+}]_i$  measurements in HEK293T cells expressing TRPA1 (TRPA1+Mock) or TRPA1 and AnxA2 (TRPA1+AnxA2). GFP was cotransfected to visualize transfected cells for further analysis. The image shows the cellular response to 10  $\mu$ M MO (MO). One hundred micromolar ATP was applied after MO to control for cellular health;  $\geq 500$  cells analyzed for each MO concentration; n.s.; Student's t-test. Scale bar, 10  $\mu$ m. **F,** Dose dependency of MO-

evoked increase of cellular  $[Ca^{+2}]_i$ . All data are represented as mean  $\pm$  SEM. Electrophysiology recordings were performed by Pratibha Narayanan. From (Avenali et al., 2014).

### **3.1.4 AnxA2 is coexpressed with TRPA1 in nociceptors**

In order to gather more information and investigate deeper the potential influence of AnxA2 association for TRPA1 function, we moved to a physiological cellular setting, i.e., sensory neurons of dorsal root ganglia (DRG). Within DRGs, different subpopulation of primary afferents can be classified, which properties reflect, among others, the range of stimuli transduced and the speed of signal transmitted. Non-myelinated small diameter neurons generally transmit nociceptive signals and can be identified by the expression of the intermediate filament Peripherin. (Patapoutian et al., 2009). Myelinated neurons show instead bigger diameter, mostly signal innocuous stimuli, and express the heavier Neurofilament 200 (NF200). To get insights into AnxA2 localization we characterized its expression pattern in rodent DRGs. First of all we confirmed the specificity of the commercial AnxA2 antibody, as indicated by the absence of signal in tissue from AnxA2 deficient mice (Ling et al., 2004) compared to WT littermates (Fig.7A,B). Then, we measured AnxA2 expression and observed it in  $30.1 \pm 1\%$  of mouse DRG neurons, of which  $66 \pm 1.7\%$  showed coexpression with Peripherin (Fig.7A). This enrichment of AnxA2 in a subpopulation of small non-myelinated neurons is consistent with previous reports (Naciff et al., 1996). Since AnxA2 binds to TRPA1, the two proteins should be coexpressed in sensory neurons. For colocalization studies we had to obviate to the problem that both TRPA1 and AnxA2 antibodies had been raised in the same species. For this reason we shifted to using a mouse AnxA2 antibody in rat tissue. In rat DRGs AnxA2 showed an expression profile very similar to the mouse counterpart, with  $27 \pm 0.7\%$  positive neurons, of which  $68 \pm 1.9\%$  coexpressed Peripherin (Fig.7C). Only a small fraction ( $5 \pm 0.5\%$ ) showed colocalization with NF200, marker for big myelinated neurons (Fig.7D). Importantly, TRPA1 expression was comparable with previous reports using the same antibodies (Schmidt et al., 2009) or different ones (Bautista et al., 2005) and could be detected in  $16.2 \pm 1.5\%$  of rat DRG neurons. In line with our hypothesis, the costaining with AnxA2 revealed an interesting degree of colocalization in rat DRGs, with  $53 \pm 1.4\%$  of TRPA1-positive neurons also expressing AnxA2 (Fig.7E). It is relevant to note that the actual degree of coexpression cannot be unambiguously determined, as these TRPA1 antibodies have been shown to preferentially label neurons with relatively high TRPA1 expression (Huang et al., 2012; Schmidt et al., 2009). These data altogether demonstrate that AnxA2 is expressed in a nociceptive subpopulation of DRG neurons, where it shows relevant colocalization with TRPA1.

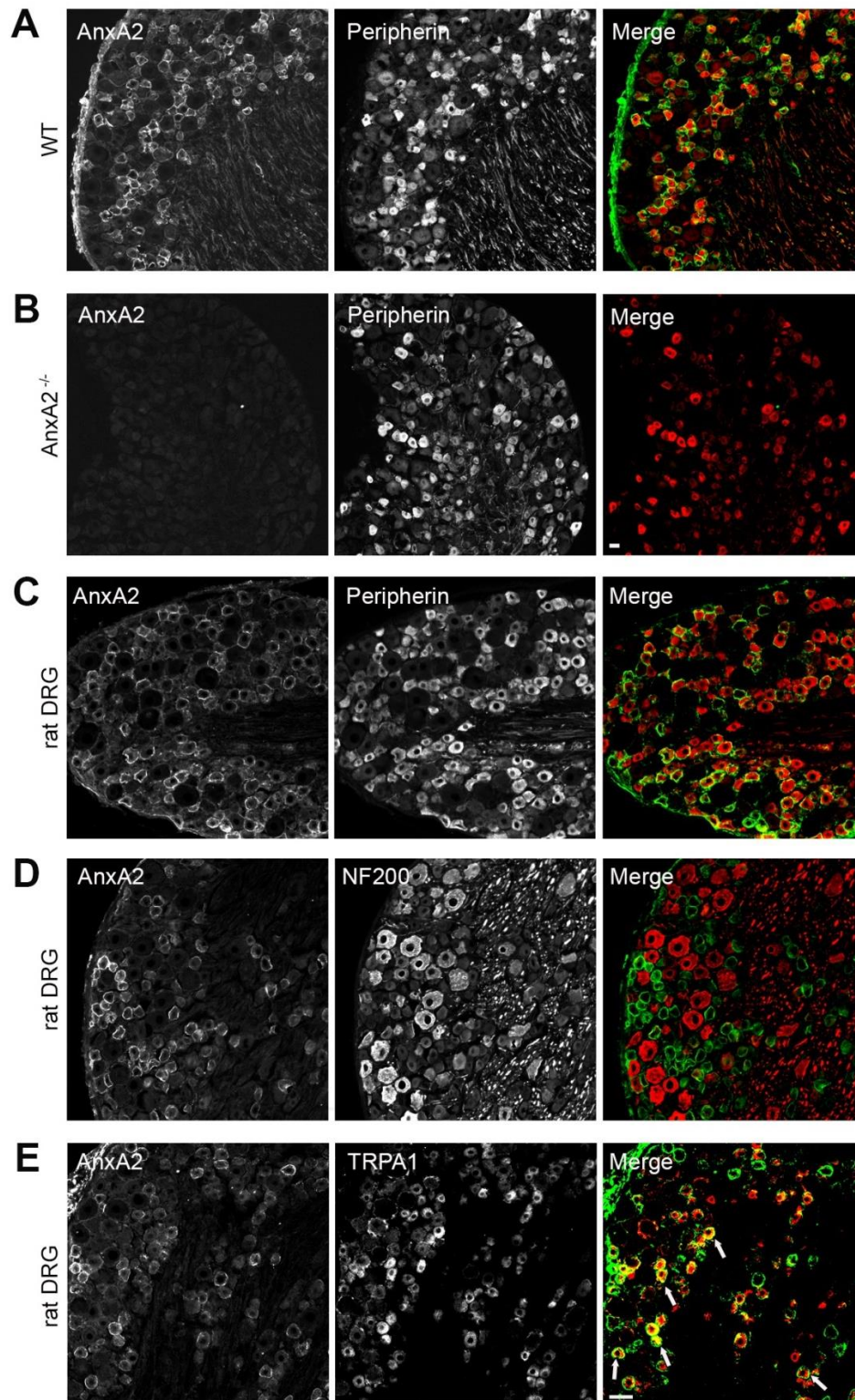


**Figure 7. AnxA2 is coexpressed with TRPA1 in nociceptors.**

**A, B,** Representative images of immunohistochemistry on cryosections of mouse DRG colabeled for AnxA2 and Peripherin in WT mice (**A**) and AnxA2<sup>-/-</sup> (**B**) littermates;  $\geq 3000$  neurons analyzed; Scale bar, 20  $\mu\text{m}$ . **C–E,** Representative images of immunohistochemistry on cryosections of rat DRG colabeled for AnxA2 and Peripherin, NF200, or TRPA1, respectively;  $\geq 5000$  neurons analyzed. White arrows indicate examples of neurons coexpressing AnxA2 and TRPA1. Scale bar, 40  $\mu\text{m}$ . From (Avenali et al., 2014).

### **3.1.5 AnxA2<sup>-/-</sup> mice exhibit increased TRPA1 expression in sensory neurons**

Probably the most commonly used and direct way to get insights into the role and function of a protein is via a loss of function approach and investigating the resulting phenotype. In this line we aimed to determine the consequences of AnxA2 deletion for DRG neurons, therefore, we assessed potential variations in different neuronal subpopulations by measuring the expression of specific markers. Immunohistochemistry in DRG cryosections revealed an interesting increase in the number of TRPA1-positive neurons in AnxA2<sup>-/-</sup> mice compared with WT littermates (WT: 8.1 ± 0.4%; AnxA2<sup>-/-</sup>: 13.6 ± 0.5%; Fig.8). At the same time however, we could not detect any significant change for either neurofilament characterizing myelinated and non-myelinated neurons, namely NF200 and Peripherin (Fig.8). No appreciable difference was measured also in the number of cells immunoreactive for TRPV1, the heat and capsaicin receptor that, as already discussed, is highly coexpressed and in many ways related to TRPA1 (Fig.8). Noteworthy, the values we obtained in terms of TRPA1 expression in DRGs of naïve mice are in line with what reported by other publications using the same antibodies (Huang et al., 2012; Schmidt et al., 2009). In conclusion, these data suggest a specific increase of TRPA1-positive cells in DRG neurons from AnxA2<sup>-/-</sup> mice, without general alteration in the expression of other markers. Additionally, qPCR-based measurement of TRPA1 mRNA levels did not show any difference between genotypes (data not shown), suggesting an alternative mechanism, potentially post-translational, at the base of the difference in TRPA1 label in sensory neurons from AnxA2<sup>-/-</sup> mice.

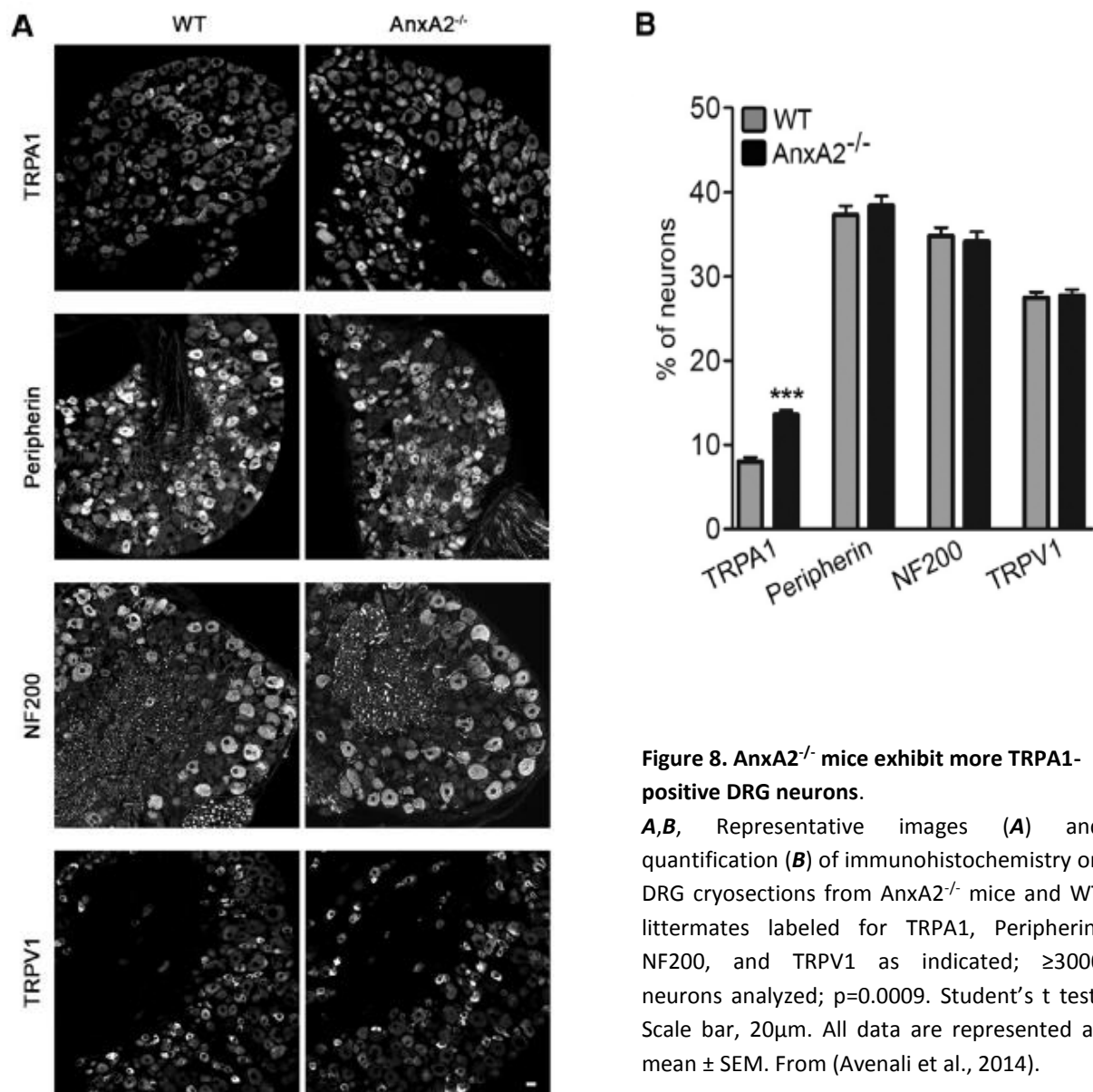


**Figure 8. AnxA2<sup>-/-</sup> mice exhibit more TRPA1-positive DRG neurons.**

**A,B,** Representative images (**A**) and quantification (**B**) of immunohistochemistry on DRG cryosections from AnxA2<sup>-/-</sup> mice and WT littermates labeled for TRPA1, Peripherin, NF200, and TRPV1 as indicated;  $\geq 3000$  neurons analyzed;  $p=0.0009$ . Student's t test. Scale bar, 20 $\mu$ m. All data are represented as mean  $\pm$  SEM. From (Avenali et al., 2014).

### 3.1.6 TRPA1 responses are sensitized in a subset of AnxA2<sup>-/-</sup> sensory neurons

The interpretation of the immunohistochemistry analysis results showing more TRPA1-positive neurons in AnxA2<sup>-/-</sup> mice is open to different interpretations: on the one hand, it could be the result of de novo expression of TRPA1 in additional neurons compared to WT; on the other hand, it could be due to an increase of TRPA1 levels in neurons already expressing the channel. In the latter case in fact, this increase would facilitate the detection by TRPA1 antibodies and result in a higher number of measured immunoreactive cells. In addition, as previously mentioned, our TRPA1 antibodies have already been described to exhibit limited sensitivity and therefore preferentially label neurons with high TRPA1 abundance (Huang et al., 2012; Schmidt et al., 2009). To address this dilemma, we turned to an antibody-independent approach to investigate TRPA1 channels activity: ratiometric calcium imaging in cultured sensory neurons. This technique allows the study of the

dynamics of intracellular calcium levels and in our case can be exploited to monitor the activity of calcium-permeable channels (like TRPA1 and TRPV1) in response to specific stimuli (Bautista et al., 2006; Schmidt et al., 2009). In our case we used mustard oil (MO), a TRPA1 specific agonist (Bautista et al., 2006; Jordt et al., 2004), to compare the consequences of TRPA1 activation between *AnxA2*<sup>-/-</sup> mice and WT littermates. Within DRG neurons, TRPA1 expression varies among cells and spinal levels, and it is quite heterogeneous (Schmidt et al., 2009; Vandewauw et al., 2013), therefore we decided to stimulate the cells with different concentrations of MO: 1) a low or subsaturating concentration (12  $\mu$ M) able to activate only neurons showing high TRPA1 expression; 2) a saturating one (50  $\mu$ M) that will activate all TRPA1-expressing cells, and therefore allow quantitative comparison of the total population between genotypes. As figure 9 shows, we measured a significant increase in the number of neurons responding to the subsaturating MO pulse in *AnxA2*<sup>-/-</sup> cultures respect to WT. At the same time however, the number of responders to the saturating pulse of MO, activating all TRPA1 expressing cells, was not different between genotypes. These data show that in *AnxA2*<sup>-/-</sup> DRGs there is a neuronal subpopulation that is more responsive to MO, while the total population of TRPA1-expressing cells is not changed respect to WT. Moreover, we observed that cellular responses to capsaicin, a TRPV1-specific agonist, are not changed between genotypes. This, together with the facts that the amplitude of responses to the stimuli (Fig.9D) are not affected, and that TRPA1 desensitization mediated by MO (homologous) or capsaicin (heterologous) are unchanged (data not shown), suggest that deletion of *AnxA2* might have a specific effect on TRPA1 in a subpopulation of nociceptive neurons. To further support these findings, and confirm that this effect was specifically dependent on *AnxA2*, we performed a rescue experiment to re-establish *AnxA2* function in deficient neurons. To this end, we transfected *AnxA2*<sup>-/-</sup> DRG cultures with m*AnxA2* or control plasmid (Mock). Strikingly, *AnxA2* re-expression restored the WT phenotype in *AnxA2*<sup>-/-</sup> DRG cultures, meaning the number of responders to the subsaturating pulse of MO was now comparable to WT, and at the same time the responsiveness to the saturating MO concentration or capsaicin (Fig. 9E) and the response amplitudes were similar between conditions (Fig. 9F). Together these results support a role of *AnxA2* in the modulation of TRPA1 channels in a subpopulation of nociceptive neurons, while the total prevalence of TRPA1-expressing cells is not altered.

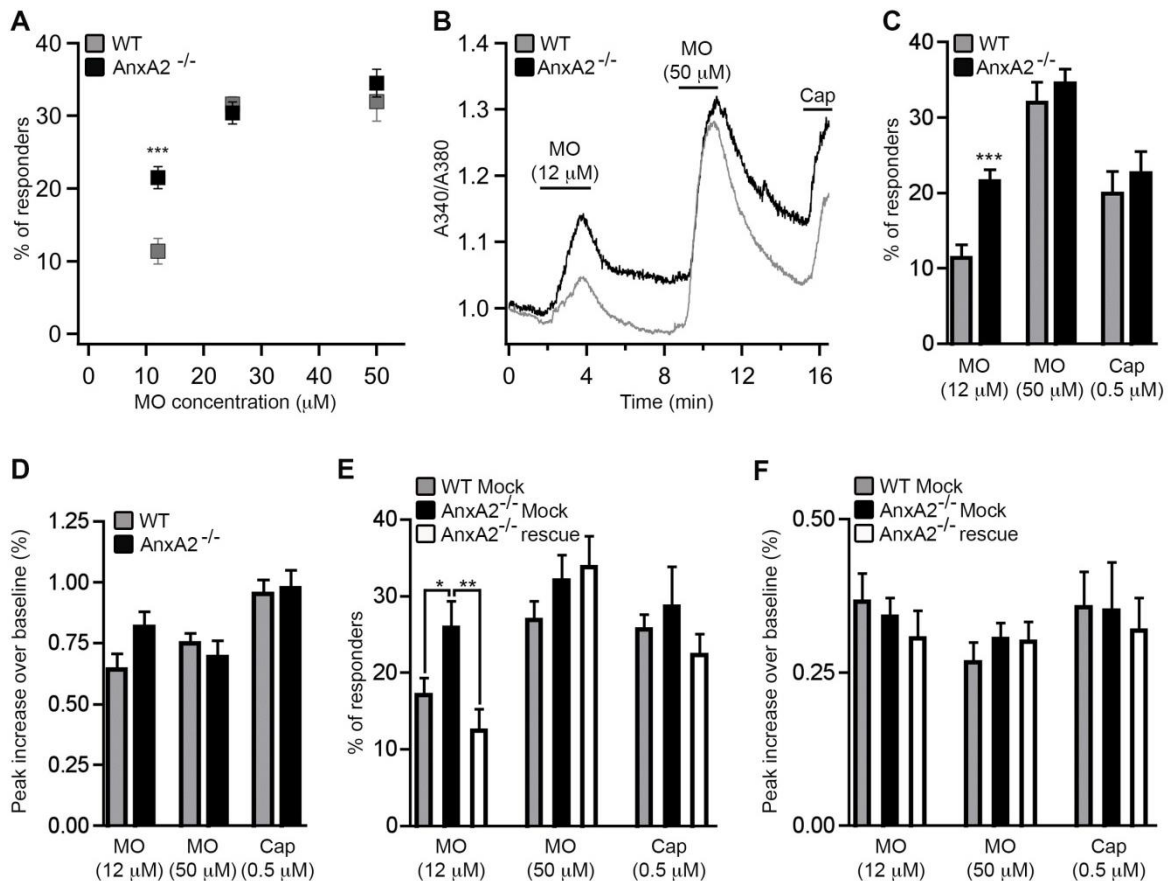


**Figure 9. TRPA1 responses are sensitized in a subset of *AnxA2*<sup>-/-</sup> sensory neurons.**

**A–F**, *AnxA2*<sup>-/-</sup> DRG cultures are more sensitive to low MO concentrations as measured by ratiometric calcium imaging. **A**, The graph depicts the percentage of responders to 12 μM, 25 μM, or 50 μM MO (12 μM, *AnxA2*<sup>-/-</sup>: 21.5 ± 1.5 compared with WT: 11.4 ± 1.7%,  $p=0.0008$ , Student's *t* test;  $n \geq 500$  neurons for each MO concentration from  $N=3$  independent cultures each). **B**, Representative averaged traces from all neurons in one coverslip (including responders and non-responders to applied stimuli) upon application of indicated stimuli. **C**, Quantification of the percentage of neurons responding to each stimulus (MO; 12 μM, see data in **A**; 50 μM, *AnxA2*<sup>-/-</sup>: 34.5 ± 1.9 compared with WT: 32 ± 2.7%, n.s.; Cap 0.5 μM, *AnxA2*<sup>-/-</sup>: 22.6 ± 2.8 compared with WT: 19.9 ± 2.9%, n.s.;  $\geq 500$  neurons per condition,  $N=3$  independent cultures each). **D**, Quantification of response amplitudes to each stimulus (measured as peak increase over baseline). **E**, **F**, Quantification of the percentage of neurons responding to each stimulus (**E**) and the response amplitudes (**F**) in Mock-transfected WT neurons (WT Mock), Mock-transfected *AnxA2*<sup>-/-</sup> neurons (*AnxA2*<sup>-/-</sup> Mock), and *AnxA2*<sup>-/-</sup> neurons transfected with *AnxA2* cDNA (*AnxA2*<sup>-/-</sup> rescue). Twelve micromolar MO (WT Mock: 17.1 ± 2.2, *AnxA2*<sup>-/-</sup> Mock: 25.9 ± 3.4, *AnxA2*<sup>-/-</sup> rescue: 12.4 ± 2.8; \* $p < 0.05$ , \*\* $p < 0.01$ , ANOVA with Newman–Keuls test;  $\geq 250$  neurons per condition;  $N=3$  independent cultures each). Cap, capsaicin. From (Avenali et al., 2014).

### 3.1.7 *AnxA2* limits TRPA1 plasma membrane expression in sensory neurons

In *AnxA2*<sup>-/-</sup> DRG cultures more neurons responded to the low MO pulse respect to WT, but the response to the high MO concentration was unchanged. Considering the heterogeneous expression of TRPA1 in DRG, this outcome could reflect an increase in the number of

channels at the plasma membrane in some neurons, which would explain the enhanced responsiveness to MO. At full-blowing high saturating concentration of MO, all TRPA1-expressing cells would be responding to the stimulation, thereby masking this difference. To test this hypothesis we aimed to identify and quantify selectively TRPA1 channels at the cell surface of sensory neurons by live labeling TRPA1 with specific antibodies targeting extracellular epitopes of the channel. Unfortunately these very same reagents are not suitable to effectively label the low abundant native TRPA1 population in DRG cultures under normal conditions. To overcome this technical problem, we first nucleofected WT and AnxA2<sup>-/-</sup> DRG neuron cultures with recombinant mTRPA1. Live labeling results showed that, in line with our hypothesis, AnxA2<sup>-/-</sup> neurons displayed an increase of signal at the plasma membrane, indicating more TRPA1 channels at the cell surface (Fig.10A). Very nicely, this effect could be rescued by re-expression of AnxA2 in deficient neurons, which restored the membrane signal to a level comparable to WT cultures (Fig.10B). In further support to these data, we performed whole cell patch clamp recordings to measure the entity of TRPA1-mediated currents upon stimulation with the specific agonist MO. Indeed, we measured bigger currents in AnxA2<sup>-/-</sup> DRG neurons compared with WT neurons (again cultures were nucleofected with recombinant mTRPA1 to keep same conditions of live labeling experiments). Time constants of activation and deactivation did not seem to be affected and showed similar values between genotypes (Fig.10C,D). Altogether these data support a model whereby AnxA2 limits TRPA1 expression at the plasma membrane of sensory neurons.

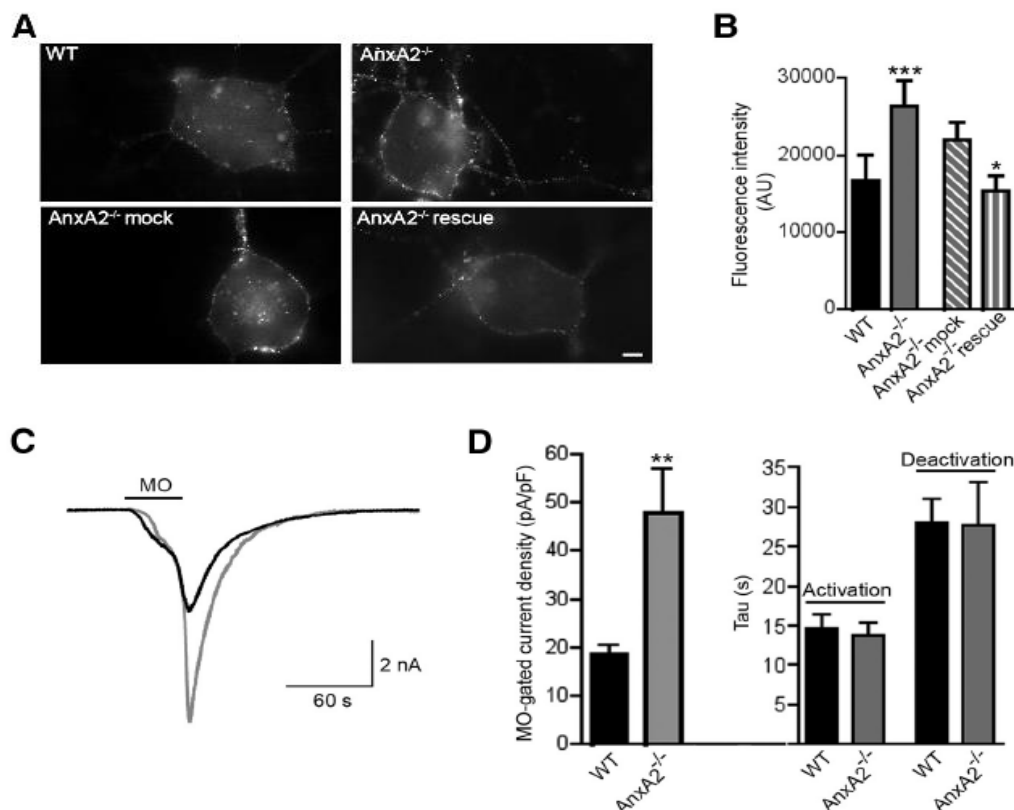


**Figure 10. AnxA2 restricts TRPA1 membrane levels in cultured DRG neurons.**

**A, B,** DRG cultures from AnxA2<sup>-/-</sup> mice and WT littermates were nucleofected with mTRPA1 (top) or conucleofected with AnxA2 cDNA (AnxA2<sup>-/-</sup> rescue; control: AnxA2<sup>-/-</sup> Mock; bottom) and subjected to live

labeling to selectively visualize TRPA1 channels at the plasma membrane. Representative images (**A**) and quantification (**B**) of live labeling (TRPA1 nucleofection:  $p=0.0004$ , Mann–Whitney test;  $n=50$  cells per genotype,  $N=5$  independent cultures each; AnxA2/Mock conucleofection:  $p=0.0115$ , Mann–Whitney test;  $n=40$  cells per genotype,  $N=4$  independent cultures each). Scale bar, 10  $\mu\text{m}$ . All data are represented as mean  $\pm$  SEM. **C**, Representative whole-cell current traces of MO-gated currents at  $-70$  mV in DRG neurons nucleofected with mTRPA1 (black trace: WT; gray trace: AnxA2<sup>-/-</sup>). The upper bar indicates the addition of 5  $\mu\text{M}$  MO to the recording chamber. **D**, Left, Average  $\pm$  SEM of current density after MO application measured at the current peak in each genotype ( $p=0.007$ , Student's *t* test;  $n>12$  neurons;  $N=3$  cultures each). Right, Time constants of MO-induced activation and inactivation measured by a mono-exponential fit to the currents obtained at  $-70$  mV for each genotype (n.s.;  $n>12$  neurons;  $N=3$  cultures each). Electrophysiology recordings were performed by Pratibha Narayanan. From (Avenali et al., 2014).

### 3.1.8 TRPA1-dependent nocifensive behaviors are enhanced in AnxA2<sup>-/-</sup> mice

Previous studies have reported a correlation between TRPA1 expression in sensory neurons and the degree of nocifensive responses in certain animal pain models (Obata et al., 2005; Schmidt et al., 2009; Zhou et al., 2013). Therefore, we asked whether the regulation of TRPA1 membrane level by AnxA2 has functional consequences for nociceptive signaling in vivo. In this line we investigated the result of AnxA2 knock-down for the response of mice to acute mechanical, thermal and chemical stimulation. Mechanical sensitivity was measured using a dynamic plantar aesthesiometer, which applies a ramp of defined force to the mouse hindpaw by means of a blunt probe. The time from application of the stimulus to the reaction of the animal was recorded, and, as shown in figure 11A resulted in no significant difference between WT and AnxA2<sup>-/-</sup> littermates. Thermal sensitivity was assessed in a similar way, but using a Hargreaves plantar test apparatus which uses an infrared source of heat in place of the mechanical probe. Nonetheless this test showed again similar responses in mice of both genotypes (Fig.11A). Next, we tested the mouse response to selective TRPA1 activation, by injecting the animal with a solution of the specific agonist MO into the plantar surface of the left hindpaw, and assessed the resulting nocifensive response. Specifically, this means observing the animal in a certain time window following the injection (10 minutes in this case) and quantifying the time the animal spends licking, flicking or lifting the injected paw as a result of the perceived pain. Very interestingly and in line with the in vitro data, AnxA2<sup>-/-</sup> mice showed to be more sensitive to MO injection, resulting in a significant increase in nocifensive behavior respect to WT littermates (Fig.11B). Notably, this effect was dependent on the concentration of MO injected, with high MO concentrations (60 mM) eliciting equally pronounced nocifensive responses in AnxA2<sup>-/-</sup> and WT mice (Fig.11B). At this high concentration we observed strong and long-lasting nocifensive behavior also in WT mice, which can be related to what we observed in calcium imaging studies, where full activation of all cells expressing TRPA1 would potentially mask the phenotype observed at lower concentrations. In fact, stimulation with saturating MO concentrations would cause all TRPA1-expressing neurons, independently of TRPA1 abundance, to be strongly activated and consequently result in similar neuronal and behavioral responses in WT and AnxA2<sup>-/-</sup> mice, as

indicated by our results. We also probed TRPV1-mediated nociception performing injections of the respective specific agonist capsaicin and, importantly, found no difference in the elicited nocifensive response between genotypes (Fig.11B). Several studies demonstrated a contribution of TRPA1 to specific hypersensitivity states in conditions of inflammatory pain (Bautista et al., 2006; da Costa et al., 2010; del Camino et al., 2010; Obata et al., 2005; Petrus et al., 2007; Zhou et al., 2013). Therefore, we investigated the possible impact of AnxA2 on TRPA1 function during inflammatory pain using the well-established Complete Freund's Adjuvant (CFA) model in mice (da Costa et al., 2010; Obata et al., 2005; Petrus et al., 2007; Zhou et al., 2013). In this model CFA is injected into the plantar surface of one of the mouse hindpaws and leads to long-lasting inflammation and development of hypersensitivity to thermal (to hot and cold temperatures) and mechanical stimuli. At least in the first 48 h following the injection, TRPA1 has been shown to contribute to cold hypersensitivity (da Costa et al., 2010; Obata et al., 2005), while it is dispensable for heat hypersensitivity (Bautista et al., 2006; Petrus et al., 2007) and its role for innocuous mechanical hypersensitivity is still debated (da Costa et al., 2010; Petrus et al., 2007; Zhou et al., 2013). As expected CFA injection reduced the withdrawal latency of the animals on a cold plate, indication of cold allodynia; however, consistent with the view of AnxA2 modulating TRPA1 activity, AnxA2<sup>-/-</sup> mice showed enhanced hypersensitivity to cold respect to WT littermates, indicated by the even lower latency times recorded (Fig.11C). In addition, figure 11D shows how CFA induced allodynia in the mice also in response to heat and mechanical stimulation, but in this case to a similar degree in both genotypes. Contralateral (non-injected) paws were not affected and did not develop hypersensitivity after CFA injection (Fig.11D). These results clearly demonstrate that AnxA2 modulation of TRPA1 extends to the in vivo context, where specifically TRPA1-dependent nocifensive behavior is affected in mice.

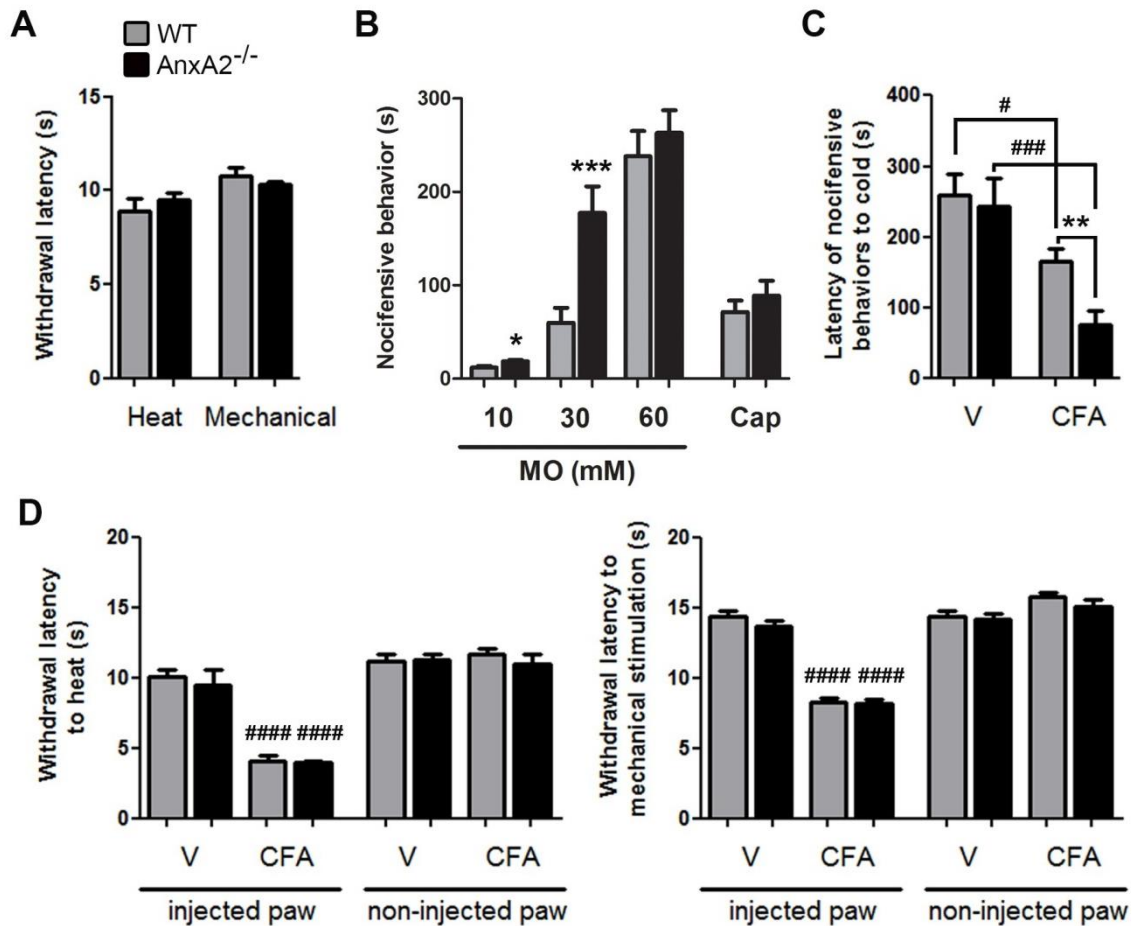


**Figure 11. Enhanced TRPA1-dependent nocifensive behaviors in AnxA2<sup>-/-</sup> mice.**

**A**, Quantification of the latency of withdrawal of both hindpaws when WT mice and AnxA2<sup>-/-</sup> littermates were subjected to radiant heat (Heat) or punctuate mechanical pressure (Heat:  $n=10$  mice each; Mechanical:  $n=9$  mice each; n.s., Student's *t* test). **B**, Quantification of the response duration of acute nocifensive behavior over 10 minutes after injection of different concentrations of MO (10 mM: WT  $11.8 \pm 1.9$  s compared with AnxA2<sup>-/-</sup>  $18.5 \pm 1.6$  s,  $n=10$  mice each;  $p=0.0126$ , Student's *t* test; 30 mM:  $59.9 \pm 15.9$  s,  $n=8$  mice compared with AnxA2<sup>-/-</sup>  $177.4 \pm 28.5$  s,  $n=11$  mice;  $p=0.0009$ , Student's *t* test; 60 mM: WT compared with AnxA2<sup>-/-</sup>,  $n=7$  mice each;  $p=0.5064$ , n.s., Student's *t* test), and after injection of 3  $\mu$ g Cap (WT compared with AnxA2<sup>-/-</sup>;  $n=9$  mice each;  $p=0.4040$ , n.s., Student's *t* test). **C, D**, WT mice and AnxA2<sup>-/-</sup> littermates were unilaterally injected with CFA to elicit inflammatory pain. **C**, Quantification of the latency of nocifensive/escaping behaviors when mice were placed on a cold plate 24 h after vehicle injection (V;  $n=8$  mice each; n.s.) and CFA-injection (WT CFA:  $165.7 \pm 17.1$  s,  $n=15$  mice; AnxA2<sup>-/-</sup> CFA:  $75.2 \pm 19.3$  s,  $n=13$  mice;  $**<p<0.01$  comparing values of CFA of the injected paw between genotypes;  $\#<p<0.05$  and  $###<p<0.001$  comparing values of V and CFA of the injected paw within each genotype, ANOVA with Bonferroni's multiple-comparison test). **D**, Quantification of the latency of withdrawal of the injected hindpaw and non-injected hindpaw when mice were subjected to radiant heat (left) or punctuate mechanical pressure (right) after vehicle injection ( $n=8$  mice each; n.s.) and CFA-injection (Heat:  $n=5$  mice each; n.s. between genotypes; Mechanical:  $n=9$  mice each, n.s. between genotypes;  $####<p<0.0001$  comparing values of V and CFA of the injected paw within each genotype, ANOVA with Bonferroni's multiple-comparison test). Non-injected paws did not develop hypersensitivity after CFA and did not differ between genotypes. All data are represented as mean  $\pm$  SEM. Cap, capsaicin. From (Avenali et al., 2014).

## **3.2 TRPA1 interactome undergoes dramatic changes during inflammatory pain**

### **3.2.1 Identification of TRPA1-protein complexes in different conditions**

The identification and characterization of AnxA2 as a protein interacting with TRPA1 and modulating its activity supports our hypothesis that protein-protein interactions are indeed important determinants of TRPA1 function. In addition, this work paves the way for a more thorough investigation of the potential dynamic changes in TRPA1-associated protein complexes in different pain states. We therefore aimed to identify how different interacting partners and/or quantitative changes within the same complex could contribute to the modulation of TRPA1 channels function in specific pain conditions. This multi-step approach starts with the careful selection of animal pain models, as the basis for performing the interactomics screening. Numerous pain paradigms modeling features of clinically relevant conditions (e.g. inflammatory and neuropathic pain) have been developed for mouse and rat studies. As previously discussed TRPA1 has been reported in several studies to contribute to the modulation of hypersensitivity during inflammatory pain (Bautista et al., 2006; da Costa et al., 2010; del Camino et al., 2010; Obata et al., 2005; Petrus et al., 2007; Zhou et al., 2013); in addition to the results we obtained supporting TRPA1-involvement in CFA-induced allodynia (paragraph 3.1.8), these considerations led us to choose this animal pain model for the interactomics screening (Fig.12A). In this line mice were subjected to CFA injection into the plantar surface of one hindpaw, and the development of inflammation was controlled. The hypersensitivity that accompanies this inflammatory state peaks at 24 h (as measured by dynamic planar aesthesiometer at different time points), at which time the animals were sacrificed for tissue collection. Lumbar DRG containing the cell bodies of neurons innervating the ipsilateral paw (L1 to L5) were dissected and whole cell lysates obtained by detergent solubilization. Native TRPA1-protein complexes were harvested by immuno-affinity purification using TRPA1-specific antibodies, processed as described in detail in the methods section, and submitted to state-of-the-art quantitative mass spectrometry analysis. DRG from mice subjected to vehicle injection (VEH) were used as control. As a further control for potential unspecific binding of some proteins in the immunoprecipitation step, the same procedure was performed using tissue from TRPA1<sup>-/-</sup> mice, where the bait is therefore absent, and which results will be used in the analysis step (described below) to remove false-positive hits. The data-independent acquisition (DIA) proteomics approach we chose for sample analysis has several advantages over the so-called “shotgun mass spectrometry”, namely more depth of acquisition and significantly reduced under-sampling. In addition, we aimed at not only qualitatively investigating our samples, but also identify quantitative changes in TRPA1-protein complexes, which requires the choice of an appropriate quantification method. We chose label-free intensity-based quantification that, in comparison to techniques based on stable isotope labeling, presents major advantages as low sample demand, no costs for labeling reagents, and a high coverage of both, the individual protein sequences and the overall proteome. One factor of utmost importance for

reliable label-free quantification is sample preparation, which has to be accurately performed in order to minimize variability, as the samples are not mixed at any time (in contrast to approaches based on stable isotope labeling). To address this issue, sample preparation was done in parallel for all experimental conditions within each biological replicate. Subsequently, peptide intensity-based quantification was performed according to the so-called Top3 method, where each in-gel digest is spiked with a control digest of known concentration and analyzed by LC-MS in the data-independent acquisition mode. This whole procedure was validated by the consistent identification of endogenous TRPA1 channels in both VEH and CFA samples, whereas the samples from TRPA1<sup>-/-</sup> animals were void of it (Fig.12B). Three separate biological replicates were completed.

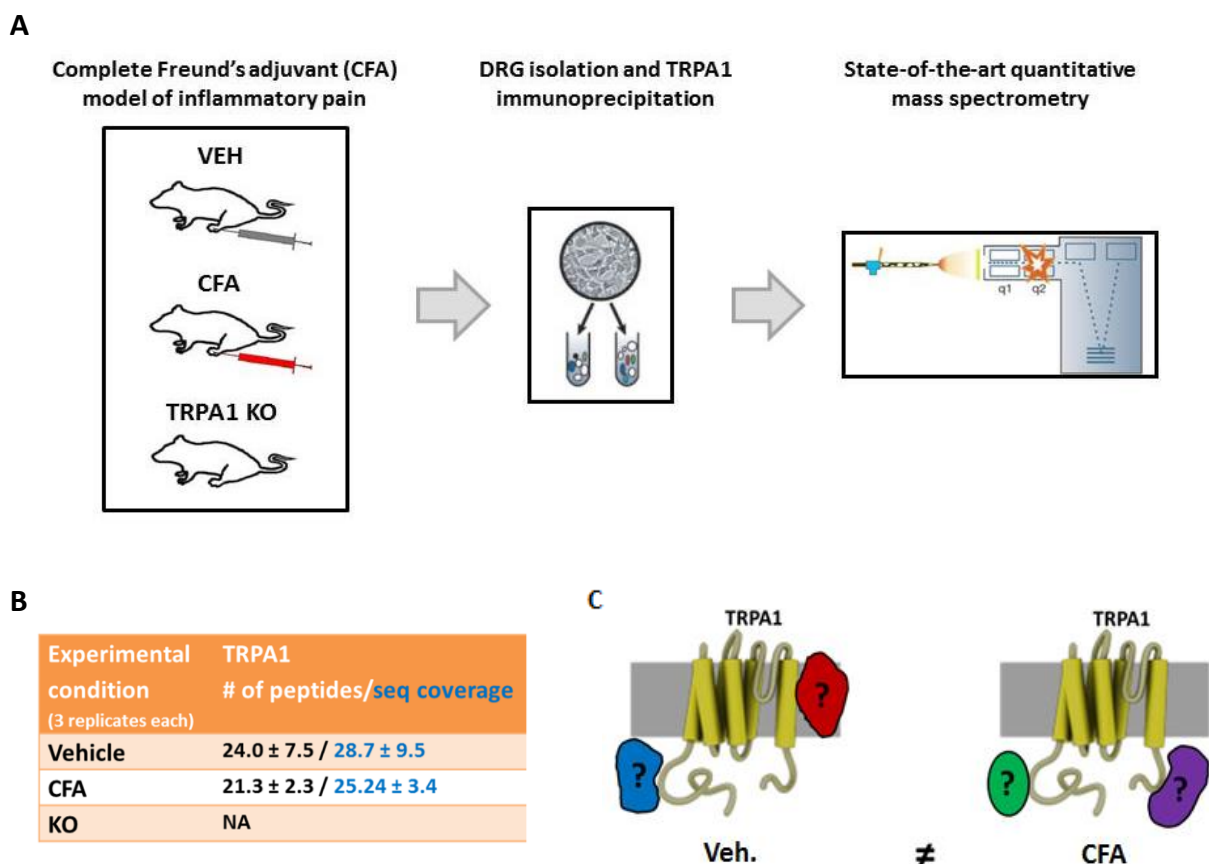


**Figure 12. Identification of TRPA1-protein complexes during inflammatory pain**

**A**, Representation of the experimental workflow followed for the interactomics screening of TRPA1-protein complexes during inflammatory pain. **B**, The table depicts the MS/MS results (identified peptides and sequence coverage) of three independent TRPA1-affinity purifications and corresponding controls. **C**, Cartoon representing an idealized outcome of the study, with TRPA1 associated with different binding partners in the different conditions. Three biological replicates were performed. Mass spectrometry analysis was performed in collaboration with Olaf Jahn (Proteomics Group, Max-Planck Institute of Experimental Medicine, Göttingen). Figures adapted from (Aebersold and Mann, 2003) and [www.siemenslab.de/research\\_TRP.html](http://www.siemenslab.de/research_TRP.html).

### **3.2.2 Mass spectrometry screening reveals significant changes in TRPA1-protein complexes during inflammatory pain**

Mass spectrometry is an extremely powerful tool able to get plentiful information about the composition of a sample and can generate long lists of identified proteins, but proper and accurate analysis is essential for robust reliability of the data. In order to get datasets of proteins with strong evidence of binding to the bait, we decided to set stringent criteria for the analysis of the mass spectrometry results. Only proteins fulfilling both the following criteria were considered as high-confidence TRPA1-interacting partners for further analysis:

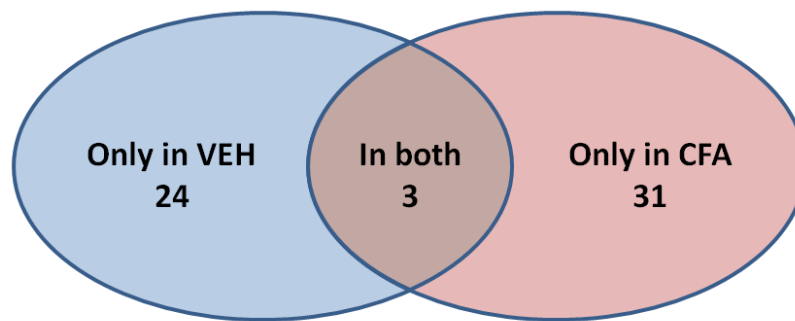
- 1) Detected in each of the three biological replicates;
- 2) In each replicate, identified with amount at least three times greater than what found in the relative TRPA1 KO sample.

We then classified the proteins fulfilling the criteria above as:

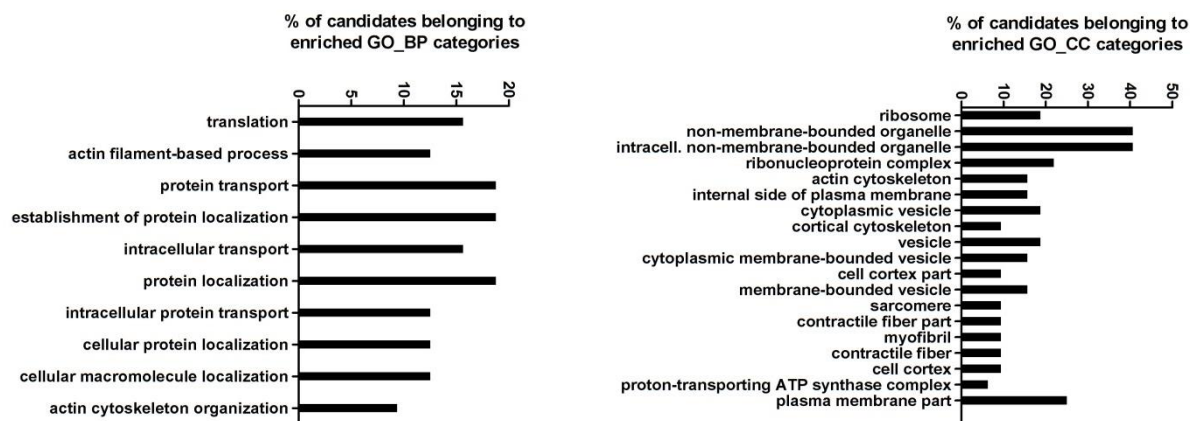
- Only identified in CFA: if fulfilling above criteria in three replicates in CFA samples only;
- Only identified in VEH: if fulfilling above criteria in three replicates in VEH samples only;
- Identified in both: if fulfilling above criteria in three replicates in both VEH and CFA samples.

In this way we obtained a list of selected proteins binding TRPA1 specifically in the context of inflammatory pain (CFA model) that we could differentiate from the control condition. These findings revealed a dramatic alteration of TRPA1 interactome, as shown in figure 13A. The Venn diagram shows very little overlap between the two conditions (VEH and CFA) indicating that TRPA1 interactome critically reshapes, with many binding partners substituted by others that are likely to modulate TRPA1 activity and function in specific ways. A complete list of all selected proteins can be found in Appendix. In order to get a better overview and more information on the obtained data, we performed a gene ontology (GO) analysis using the DAVID functional annotation tool to assign genes with their affiliate GO terms and to order them by enrichment (Huang da et al., 2009a, b). Figure 13B shows protein ontology categories for “biological process (BP)” and “cellular component (CC)” represented by proteins identified in the “Only in CFA” dataset. GO analysis for the “Only in VEH” dataset is not reported as it did not show any significant enrichment.

A



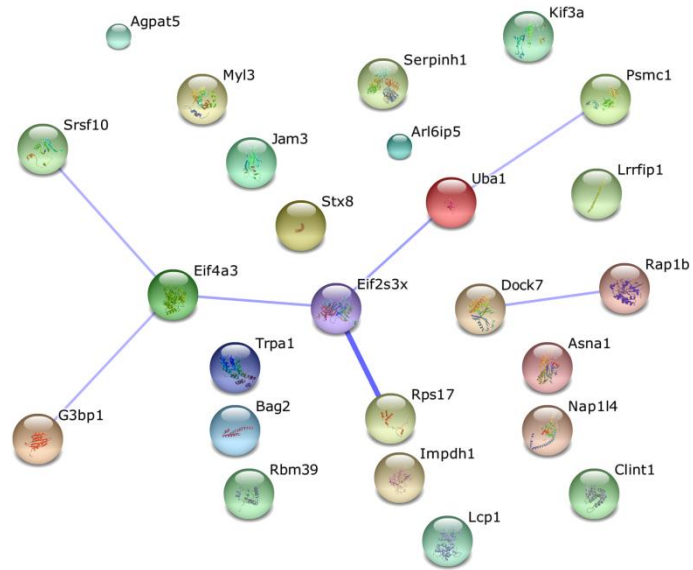
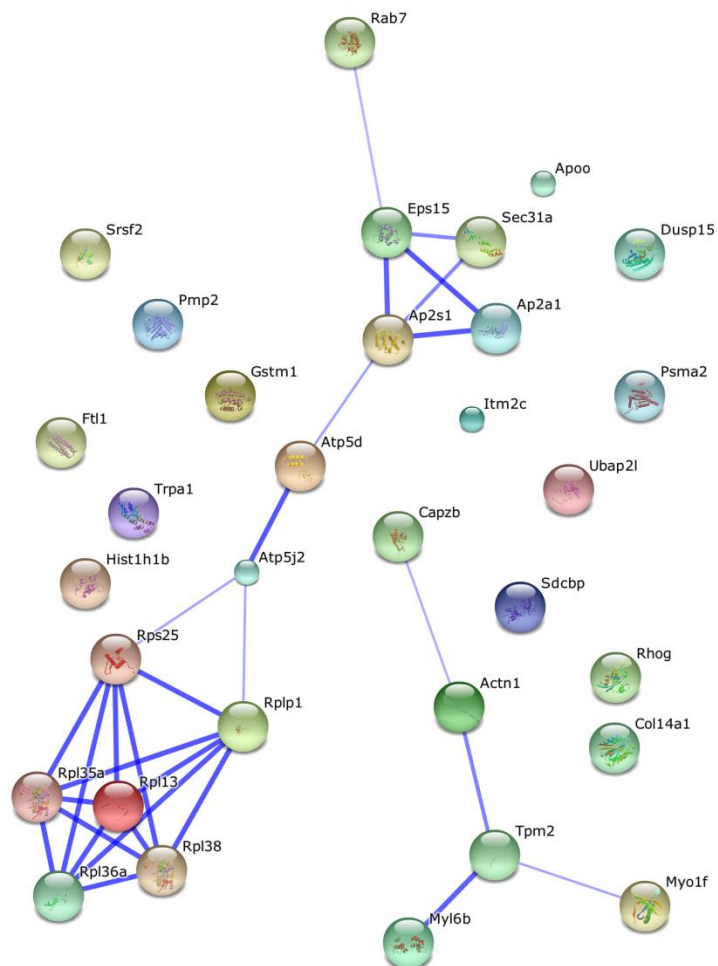
B



**Figure 13. TRPA1 interactome undergoes dramatic changes during inflammatory pain**

**A**, Venn-diagram shows the number of identified candidates in either condition. All considered candidates fulfill the following criteria: >3x enriched compared to KO in all replicates; detected in all 3 replicates in each respective condition. **B**, Gene ontology (GO) analysis using the DAVID functional annotation tool shows significantly enriched ( $p < 0.05$ ) categories for “biological process (BP)” and “cellular component (CC)” represented by proteins identified in the “Only in CFA” dataset.

Identifying known and predicted associations among proteins of the same dataset is a relevant piece of information and can be visually represented by STRING (Jensen et al., 2009) association networks as in figure 14.

**A****B**

**Figure 14. STRING association networks of single datasets**

STRING confidence network views are based on known and predicted functional associations between proteins of the datasets "Only in VEH" (A) and "Only in CFA" (B).

A common way to visualize the large datasets generated by quantitative proteomics experiments is using the so-called volcano plots, which display the distribution of identified proteins according to the p-value ( $-\log_{10}$  transformed) and the fold change ( $\log_2$  transformed). Analyzing volcano plots allows to easily highlight hits that show large fold changes and low p-values, and can therefore be helpful in the selection of high priority candidates for follow-up and validation (Oveland et al., 2015). Therefore, in parallel to our analysis based on the above-mentioned criteria, we found worthwhile to try to visualize our complete dataset in this way, relating the p-value of the comparison of CFA and VEH conditions with the respective fold change. For our specific dataset, the realization of such a kind of plot intrinsically implies that all proteins have been detected in the three biological replicates in both conditions. Since it was not the case for many, we had to obviate to this issue by setting a value of 0.001 (one order of magnitude lower than the limit considered for detection) to all non-identifications. The graph obtained (Fig.15) displays each single protein identified in the three biological replicates as a spot which coordinates are derived from the fold change of CFA respect to vehicle conditions, and the level of significance (p-value). In order to identify the most interesting candidates we defined arbitrary cut-off values as:

- (1) CFA/VEH ratio  $\geq 1.3$  (corresponding to  $\log_2$  CFA/VEH  $\geq 0.38$ ; red vertical line): the protein shows enrichment in CFA.
- (2) CFA/VEH ratio  $\leq 0.7$  (corresponding to  $\log_2$  CFA/VEH  $\leq -0.51$ ; cyan vertical line): the protein shows enrichment in VEH.

We can observe that an important number of protein showed enrichment in either condition, and if we then relate this information to the p-value ( $p < 0.05$ ;  $-\log p\text{-value} > 1.30$ ; horizontal dashed line), it is clear that a fraction reaches statistical significance (39 hits). If we then compared this fraction with the results of our previous analysis, we clearly see that the overlap is very limited. In fact only 4 proteins out of 55 identified in first analysis (ONLY in VEH + ONLY IN CFA, see fig.13A), the ones shown as red spots in figure in figures 15, show a significantly low p-value ( $p < 0.05$ ).

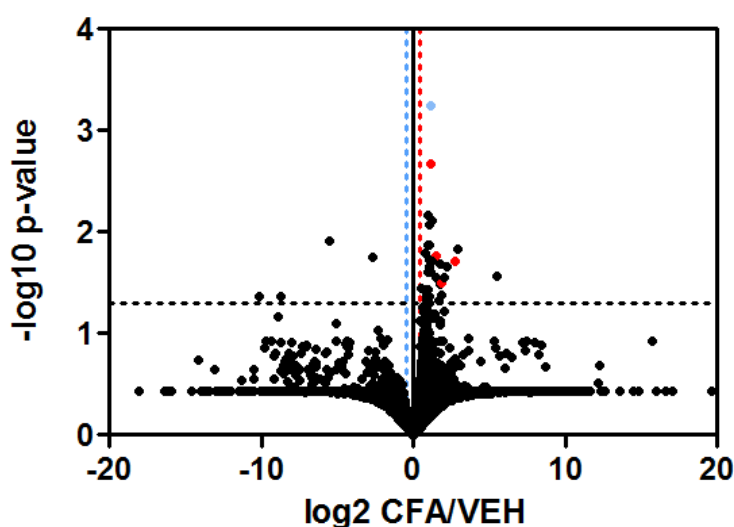


**Figure 15. Volcano plot of quantitative proteomics data**

Each protein identified in the three biological replicates is represented by a single spot. On the Y axis is reported the  $-\log_{10}$  of the comparison between CFA and VEH values from the single replicates. On the X axis is

reported the  $\log_2$  of the ratio between mean CFA and mean VEH, each calculated from the average of the three biological replicates. A value of 0.001 (one order of magnitude lower than the limit considered for detection) was set to all non-identifications. The red vertical line represents a value of 0.38 (corresponding to CFA/VEH ratio 1.3) and the cyan vertical line a value of -0.51 (corresponding to CFA/VEH ratio 0.7). The horizontal dashed line represents a value of 1.3 (corresponding to p-value 0.05). Red spots indicate hits that show significant regulation according to the volcano plot, and also fulfill criteria set in previous analysis (fig.13A). The cyan spot represents a hit that shows significant regulation according to the volcano plot, but does not fulfill criteria set in previous analysis (fig.13A).

This shows the limitations of using such a way of analyzing our dataset. In fact, the p-value can easily become not significant where it happens that data present quite some variability, or a protein fails to be identified in certain conditions. This can indeed be the case for the dataset generated by our experiment, where sample preparation is long and complex, and even involves in vivo behavioral paradigms. Because of this intrinsic variability, a relevant part of the proteins were in fact identified only in some conditions. Theoretically, we could avoid applying the 0,001 value to all non-identifications and measure only the proteins identified in all three biological replicates in both conditions, but in this way we would end up with only a fraction of the hits and not a faithful representation of the data in our hands. This suggests that for the visualization of our dataset the use of a p-value would have only limited benefit. In addition, a visualization of the data in this way results in the loss of a crucial piece of information that was instead included in our previous analysis, which is the TRPA1 KO (KO) condition. This is reflected by the fact that all the other proteins in figure 15 that show p-value lower than 0.05 (35 out of 39), and so look potentially interesting from the volcano plot, do not fulfil the criteria to be selected in our previous analysis. One example is the candidate represented by the cyan spot in figure 15, which indeed shows a significant difference between CFA and VEH conditions, but a suboptimal profile when related to the TRPA1 KO. We could therefore try to incorporate this piece of information for either VEH or CFA conditions, with the ratio CFA/VEH (or the reciprocal) showing enrichment, both reported as  $\log_2$  of fold changes for better visualization (Fig.16).

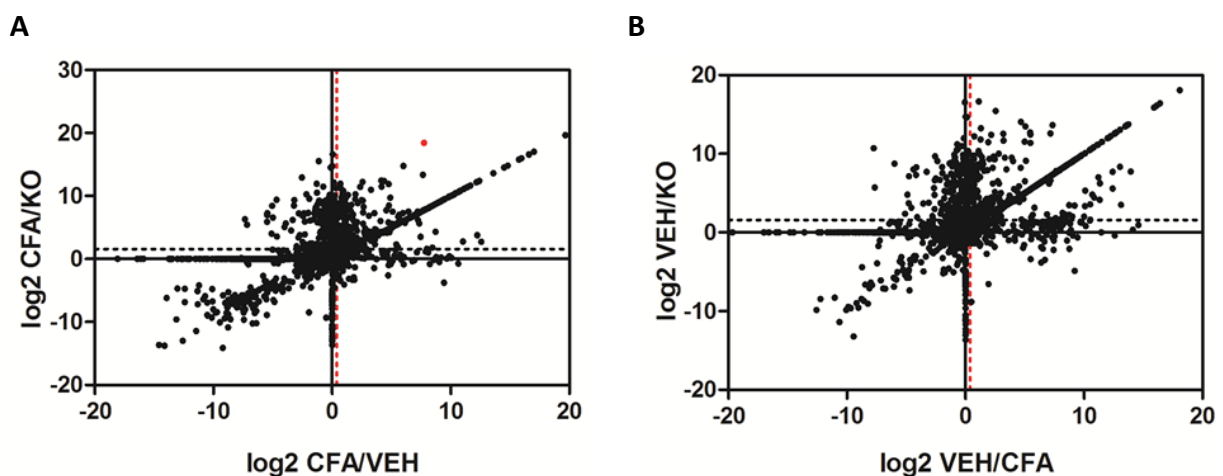


**Figure 16. Alternative scatter plots of quantitative proteomics data**

**A,B,** Each protein identified in the three biological replicates is represented by a single spot. On the Y axis is reported the  $\log_2$  of the ratio between mean CFA and mean KO (A) or mean VEH and KO (B). On the X axis is

reported the log<sub>2</sub> of the ratio between mean CFA and mean VEH (**A**) or the reciprocal (**B**). All ratio values were calculated from the average of the three biological replicates. A value of 0.001 (one order of magnitude lower than the limit considered for detection) was set to all non-identifications. The red vertical line represents a value of 0.38 (corresponding to CFA/VEH or VEH/CFA ratio 1.3). The horizontal dashed line represents a value of 1.58 (corresponding to CFA/KO or VEH/KO ratio 3). The red spot represents a hit that show relevant regulation according to this plot, but does not fulfill criteria set in previous analysis (fig.13A).

To define a protein as identified only in the respective condition (VEH or CFA) but not in KO, an arbitrary cut-off was set:

- (1) CFA/KO ratio  $\geq 3$  corresponding to  $\log_2 \text{CFA/KO} \geq 1.58$ ; horizontal dashed line): only in CFA.
- (2) VEH/KO ratio  $\geq 3$  corresponding to  $\log_2 \text{VEH/KO} \geq 1.58$ ; horizontal dashed line): only in VEH.

These plots show a consistent number of proteins that present enrichment in either condition (ratio CFA/VEH or Veh/CFA  $\geq 1.3$ ; red line) and were significantly identified in the respective condition relative to TRPA1 KO. However, these plots present some issues. In fact the ratio values displayed represent mean values calculated as the average of the amount identified in each of the three biological replicates (again with 0.001 in case of non-detection). In this way a protein like the one represented by the red spot in figure 16A would seem interesting, but instead looking more carefully into raw values we realize that it has been identified only once in CFA (in a relatively high amount) which does not support it as a priority hit in our case. In this way we are in fact not appreciating the information that would come from observing each single replicate, as we did in first analysis. While there is not a perfect way to analyze and display data like these, we can gather information from them all and use it in combination for the best possible selection of high priority candidates for follow-up and validation.

### **3.3 NIPSNAP1 and Nocistatin modulate TRPA1 channels**

Most experiments were performed by Master student Oli Abate Fulas under the author's teaching and supervision and are summarized in Oli's Master thesis (indicated in every figure where applicable).

#### **3.3.1 NIPSNAP1 is abundantly expressed in nociceptors of mouse DRGs**

In a separate set of experiments we focused our attention on a protein called 4-Nitrophenylphosphatase domain and non-neuronal SNAP25-like protein homolog 1 (NIPSNAP1), which function is largely still unknown. In a screening for expression profile of several proteins in mouse DRGs, interestingly NIPSNAP1 antibody detected expression in  $42.2 \pm 1.8\%$  of sensory neurons. What really stood out was the degree of colocalization we measured with a well-known marker of small-diameter non-myelinated nociceptors, namely

the intermediate neurofilament Peripherin. In fact,  $64.4 \pm 1.4\%$  of Peripherin-positive sensory neurons showed NIPSNAP1 expression (Fig.17), which could potentially suggest a still-unknown role of this protein in a subset of mouse nociceptors.

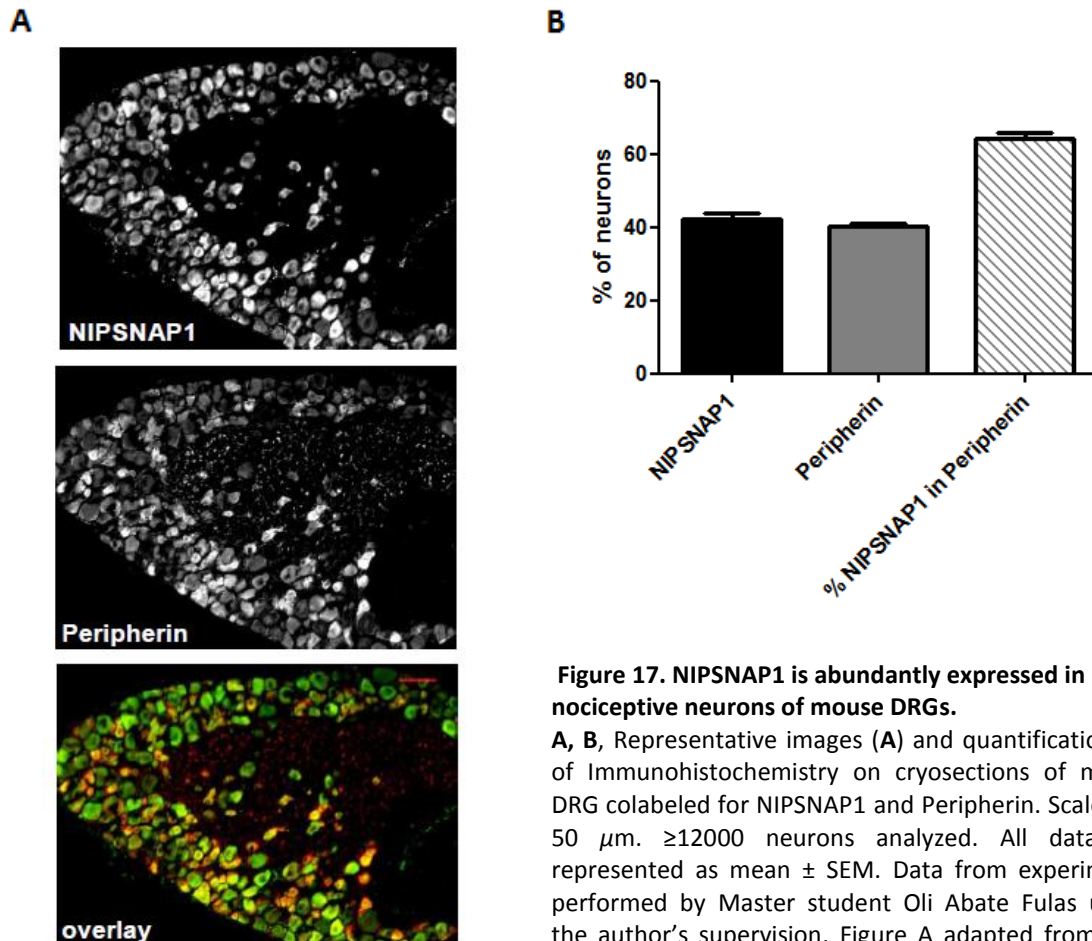


**Figure 17. NIPSNAP1 is abundantly expressed in nociceptive neurons of mouse DRGs.**

**A, B,** Representative images (**A**) and quantification (**B**) of Immunohistochemistry on cryosections of mouse DRG colabeled for NIPSNAP1 and Peripherin. Scale bar, 50  $\mu\text{m}$ .  $\geq 12000$  neurons analyzed. All data are represented as mean  $\pm$  SEM. Data from experiments performed by Master student Oli Abate Fulas under the author's supervision. Figure A adapted from Oli's Master thesis.

To validate the results of the immunohistochemical assays it was of primary importance testing the specificity of the antibody used to detect NIPSNAP1; in this line we transfected HEK293T cells with a vector expressing a myc-tagged construct of NIPSNAP1 and then coimmunostained the cells with antibodies against both NIPSNAP1 and myc. The stainings showed a beautiful colocalization of the signal from the two antibodies, confirming that this NIPSNAP1 antibody specifically recognizes its target protein (Fig.18).

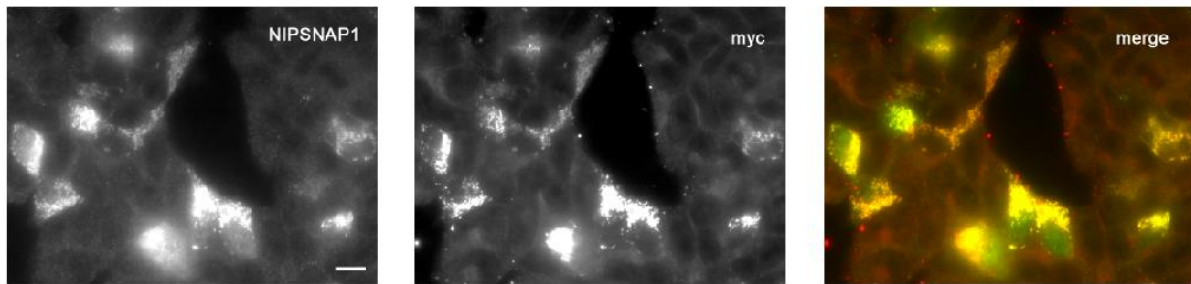


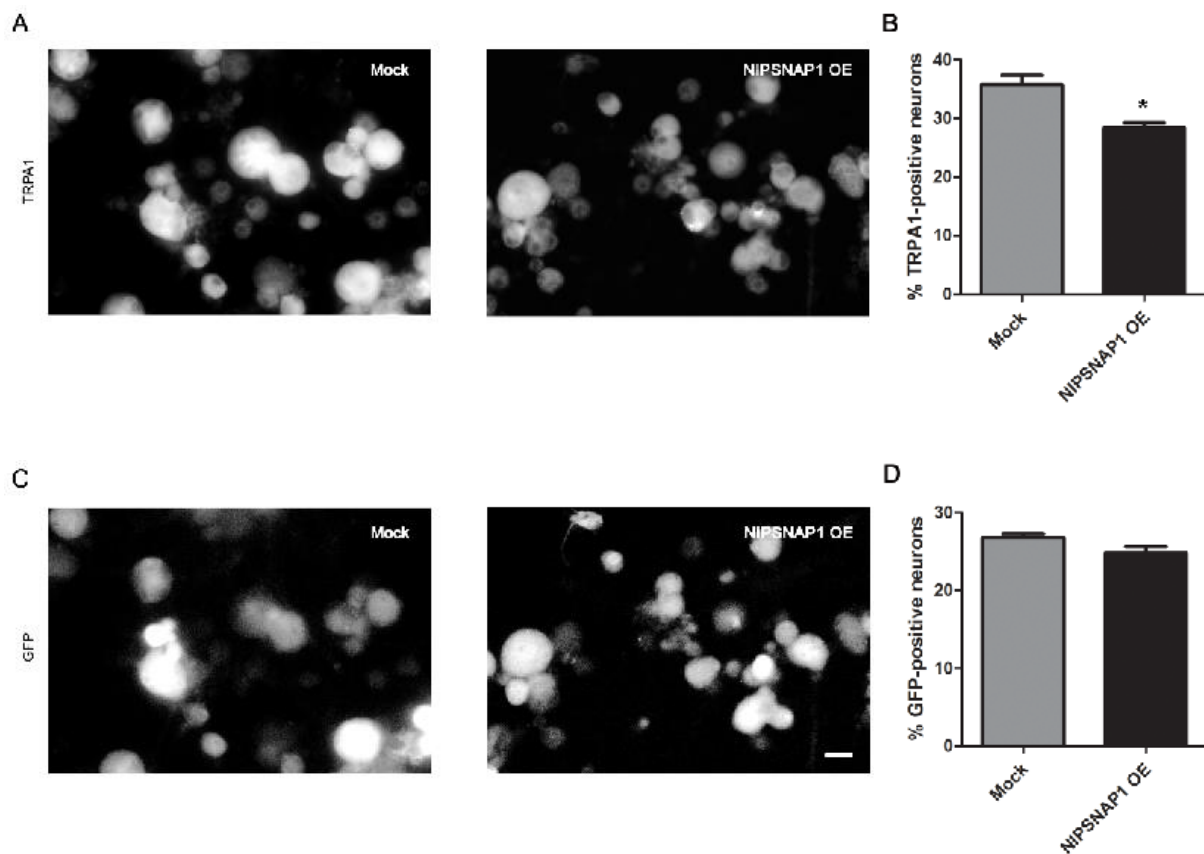
**Figure 18. Validation of NIPSNAP1 antibody specificity**

Immunocytochemistry of NIPSNAP1 in HEK293T cells transfected with a vector expressing a myc-tagged construct of NIPSNAP1. The signals from NIPSNAP1 and myc antibodies overlap perfectly while non-transfected cells do not show any NIPSNAP1 signal. These results validate the specificity of the antibody against NIPSNAP1. Scale bar, 10  $\mu$ m. Experiments were performed by Master student Oli Abate Fulas under the author's supervision.

### **3.3.2 Overexpression of NIPSNAP1 decreases TRPA1 expression in sensory neurons**

The role of NIPSNAP1 in a nociceptive subset of mouse DRG neurons can be manifold. Despite the handful of studies on NIPSNAP proteins and their potential roles, there is recent evidence indicating that NIPSNAP1 associates with TRPV6 channels in mouse liver cells, which results in a dramatic inhibition of the channel function, with currents virtually abolished (Schoeber et al., 2008). NIPSNAP2, another member of the NIPSNAP family has instead been shown to modulate L-type Ca(2+) channels, and downstream CREB signaling, in a neuronal cell line (Brittain et al., 2012). These studies potentially suggest a role for the proteins of the NIPSNAP family in the regulation of ion channels. As already discussed, TRPA1 channels play an essential role as primary detectors of noxious stimuli in primary afferent nociceptors, where they are highly enriched (Patapoutian et al., 2009; Story et al., 2003). Therefore it was interesting to note that the enriched expression of NIPSNAP1 in a subpopulation of small non-myelinated nociceptive neurons is likely to match, at least to a certain extent, the subset which expresses TRPA1. Unfortunately direct colocalization studies of the two proteins were not possible as both NIPSNAP1 and TRPA1 antibodies were raised in the same species. Hence we first aimed at investigating the consequences of NIPSNAP1 protein modulation for TRPA1 expression. The most common way to test the function of a protein is via a loss of function approach and knocking down its expression. However, different members of the NIPSNAP family are expressed in the nervous system (Buechler et al., 2004; Nautiyal et al., 2010; Schoeber et al., 2008; Tummala et al., 2010), one example being NIPSNAP2, which shares 75% homology with NIPSNAP1 (Nautiyal et al., 2010) and which, as mentioned, has already been reported to modulate ion channels (Brittain et al., 2012). This concerned us about the possibility that, following NIPSNAP1 knock-down, compensatory mechanisms by other family members could mask a potential phenotype. For this reason we preferred to use a gain of function approach and tested the effect of

NIPSNAP1 overexpression for TRPA1 protein expression in sensory neurons via immunocytochemistry. Currently available TRPA1 antibodies are not suitable to effectively label the low-abundant native TRPA1 population in DRG cultures under normal conditions, therefore we nucleofected cultures of both genotypes with recombinant mTRPA1 and either NIPSNAP1 or empty vector. Very interestingly we measured a significant decrease in the number of TRPA1-immunoreactive cells in cultures overexpressing NIPSNAP1 (Mock:  $35.7 \pm 1.6\%$ ; NIPSNAP1 OE:  $28.4 \pm 0.8\%$ ) as shown in figure 19. Importantly, this effect was not just an artifact due to saturation of the cell's translational machinery upon NIPSNAP1 overexpression, as the expression level of a cotransfected GFP marker was not affected. These data suggest a potential intriguing role of NIPSNAP1 in modulating TRPA1 expression in sensory neurons.

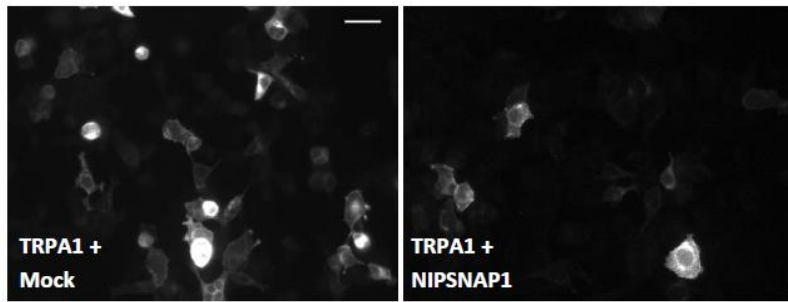
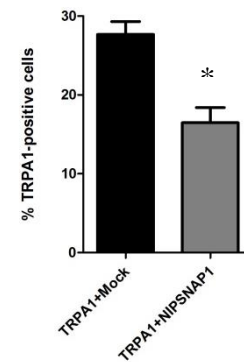
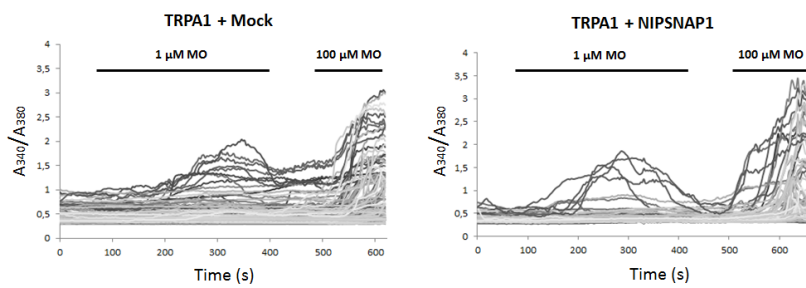
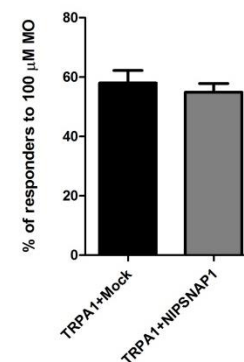
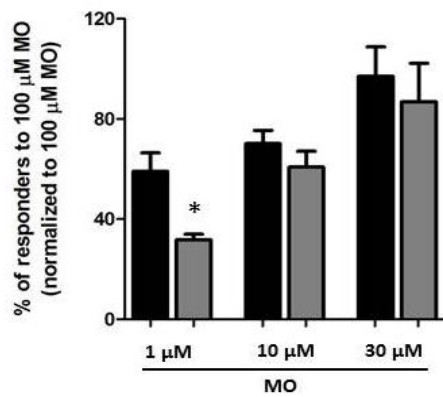
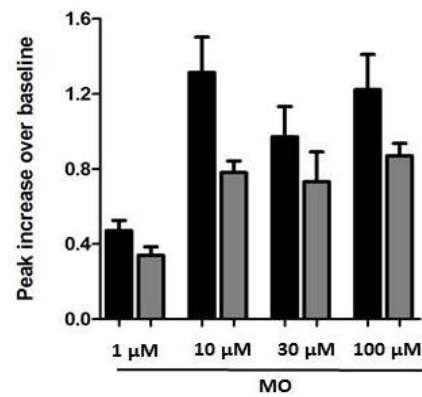


**Figure 19. DRG neuron cultures show less TRPA1-positive cells upon NIPSNAP1 overexpression**

**A,B**, Representative images (**A**) and quantification (**B**) of immunocytochemistry of mouse DRG neurons cultured for 24 h after transfection with TRPA1+Mock (Mock) or TRPA1+NIPSNAP1 (NIPSNAP1 OE) and stained with TRPA1 specific antibody;  $p=0.0158$ ; Student's *t* test;  $\geq 2000$  neurons analyzed per condition from  $N=3$  independent cultures. **C,D**, Representative images (**C**) and quantification (**D**) of GFP-positive cells. Scale bar, 20 $\mu$ m. All data are represented as mean  $\pm$  SEM. OE, overexpression.

### **3.3.3 NIPSNAP1 decreases TRPA1 expression and activity in a heterologous expression system**

Motivated by these results, we speculated that this decrease in TRPA1-positive cells would be reflected by cellular calcium responses upon TRPA1 activation by the specific agonist MO. If the effect of NIPSNAP1 on TRPA1 activity is modest, it would be hard to reveal it by testing TRPA1 responses from the highly heterogeneous population of sensory neurons in DRG cultures. Therefore, in order to better study the contribution of NIPSNAP1 to TRPA1 activity and avoid the complications coming from DRG cultures that already express NIPSNAP1 and potentially other family members (Buechler et al., 2004; Nautiyal et al., 2010; Schoeber et al., 2008; Tummala et al., 2010), we aimed to employ a system where we could more selectively manipulate and study NIPSNAP1. HEK293T cells is a heterologous expression system that is widely used in the field, well established for overexpression studies of TRPA1 and, as shown by the immunocytochemistry results in figure 18, does not show any detectable NIPSNAP1 expression. These features made of it a preferable candidate system for us to study the effect of NIPSNAP1 overexpression on TRPA1 activity. In this line we first of all wanted to confirm the same phenotype observed in sensory neurons, so we overexpressed mTRPA1 and either NIPSNAP1 or empty vector and, indeed, obtained comparable results, meaning a decrease of TRPA1-positive cells upon NIPSNAP1 overexpression. While TRPA1 + Mock cotransfected HEK293T cells showed  $27.7 \pm 1.6\%$  TRPA1-positive cells, this amount was reduced to just  $16.2 \pm 4.7\%$  upon NIPSNAP1 overexpression (Fig.20A,B). Next, we questioned whether this phenotype resulted in changes in TRPA1-mediated calcium responses by ratiometric calcium imaging. In order to test this, we used a protocol consisting of a first stimulation with a low concentration of MO (1, 10 or 30  $\mu\text{M}$ ), followed by a saturating pulse (100  $\mu\text{M}$ ) that would activate all TRPA1-expressing cells. The results of these experiments showed that the response to the 1  $\mu\text{M}$  MO application (normalized to the response to 100  $\mu\text{M}$  MO) was significantly lower for NIPSNAP1-cotransfected cells ( $31.8 \pm 2.4\%$ ) compared to mock-transfected ones ( $59.1 \pm 7.8\%$ ). On the contrary, the response elicited by higher concentrations of MO (10, 30, 100  $\mu\text{M}$ ) remained similar between conditions (Fig.20C-F). These calcium imaging results indicate that overexpression of NIPSNAP1 does not induce changes in the number of cells that express TRPA1, but rather decreases cellular response to TRPA1 agonist, which is potentially due to changes in expression and/or activity of the channel. Together these findings suggest that TRPA1 plasma membrane expression and/or TRPA1 activation are affected by NIPSNAP1 overexpression.

**A****B****C****D****E****F**

**Figure 20. NIPSNAP1 decreases TRPA1 expression and activity in HEK293T cells**

**A,B**, Representative images (**A**) and quantification (**B**) of immunocytochemistry of TRPA1 in HEK293T cells cotransfected with TRPA1 and either NIPSNAP1 (TRPA1+NIPSNAP1) or empty vector (TRPA1+Mock);  $p=0.047$ ; Student's *t*-test; Scale bar, 20  $\mu\text{m}$ . **C-F**, Ratiometric calcium imaging shows that HEK293T cells coexpressing TRPA1 and NIPSNAP1 are less sensitive to low MO concentration. Representative traces (**C**) showing response to 1  $\mu\text{M}$  MO; quantification of the percentage of neurons responding to each MO concentration (**E**) normalized to the total number of responders to 100  $\mu\text{M}$  MO (**D**); 1  $\mu\text{M}$  MO ( $p=0.012$ ); 10  $\mu\text{M}$  MO ( $p=0.315$ ); 30  $\mu\text{M}$  MO ( $p=0.848$ ); 100  $\mu\text{M}$  ( $p=0.631$ ). **F**, Comparison of mean amplitudes of calcium response to each MO concentration in HEK293T cells transfected with TRPA1 and either NIPSNAP1 or mock; Student's *t* test;  $\geq 370$  cells analyzed from  $N \geq 3$  independent cultures; All data are represented as mean  $\pm$  SEM. Data from experiments performed by Master student Oli Abate Fulas under the author's supervision. Figure A adapted from Oli's Master thesis.

### 3.3.4 Nocistatin specifically sensitizes TRPA1 responses in sensory neurons

A compelling recent study uncovered the physical association between NIPSNAP1 and Nocistatin, a neuropeptide already known to be involved in pain transmission (Okuda-Ashitaka et al., 2012), even though its precise molecular function and mechanisms remain still unclear. In light of our current findings on the potential modulation of TRPA1 by NIPSNAP1, we decided to investigate whether Nocistatin is involved as well in TRPA1 regulation. In this line we used ratiometric calcium imaging to measure the effect of Nocistatin on TRPA1-mediated cellular responses in DRG neuron cultures. Ten micromolar Nocistatin (Ahmadi et al., 2001; Ahmadi et al., 2003; Zeilhofer et al., 2000) was pre-applied and coadministered with two different concentrations of MO in order to investigate cellular response to both subsaturating and saturating stimuli. Interestingly, we measured a significant increase in the number of responders to 25  $\mu$ M MO in the Nocistatin-treated group ( $24.4 \pm 2.2\%$ ) compared to vehicle-treated controls ( $11.5 \pm 2.2\%$ ), as shown in figure 21A,B. In contrast, we could not observe any effect of Nocistatin treatment on the response elicited by different concentrations of capsaicin (0.1  $\mu$ M and 1  $\mu$ M), which probes TRPV1-dependent calcium influx (Fig.21C,D). These findings reveal an enhancement of TRPA1-mediated calcium response upon Nocistatin application and, together with the facts that response to capsaicin and response amplitudes were not changed, suggest a certain degree of specificity for the action of Nocistatin on TRPA1-mediated nociceptive signaling.

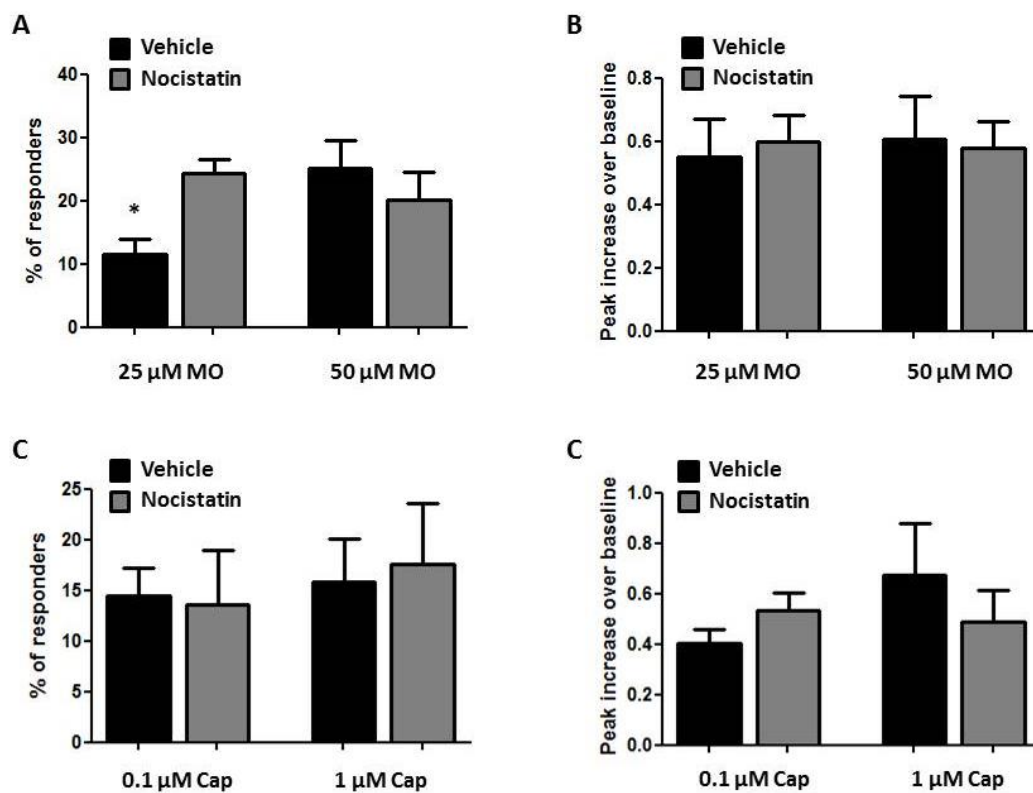


**Figure 21. Nocistatin specifically modulates TRPA1-mediated calcium response in DRG neurons.**

**A,B,** Quantification of the percentage of neurons responding (A) and mean amplitude of neuronal calcium response (B), after stimulation with 25 $\mu$ M MO or 50  $\mu$ M MO along with 10  $\mu$ M Nocistatin or vehicle.  $p=0.017$ ;

Student's *t*-test;  $\geq 700$  neurons analyzed from  $N=3$  independent cultures. **C,D**, Nocistatin does not affect the percentage of responders (**C**) and mean amplitude response (**D**) to 0.1  $\mu\text{M}$  and 1  $\mu\text{M}$  capsaicin in DRG neuron cultures. All data are represented as mean  $\pm$  SEM. Data from experiments performed by Master student Oli Abate Fulas under the author's supervision.

### 3.3.5 Nocistatin does not alter TRPA1 cell surface expression

The increase we measured in TRPA1-mediated response upon Nocistatin treatment could be explained in different ways: (1) Nocistatin might directly sensitize TRPA1 or (2) Nocistatin could affect TRPA1 trafficking to the plasma membrane, where the channel is active and able to mediate calcium influx in response to activation. In this line, Nocistatin effect could be explained by an increase in TRPA1 plasma membrane expression, possibly due to enhanced trafficking to the membrane (this hypothesis implies that these new channels that reach the cell surface are functional), or decreasing internalization of the channels. To explore this possibility we aimed at live labeling selectively cell surface TRPA1 channels, an established procedure to study TRPA1 membrane levels in DRG neuron cultures (Schmidt et al., 2009). As already discussed in a previous chapter currently available TRPA1 antibodies are not suitable to effectively label the low-abundant native TRPA1 population in DRG cultures under normal conditions, therefore we first nucleofected cultures of both genotypes with recombinant mTRPA1, and then live labeled TRPA1 channels at the cell surface following Nocistatin treatment. Incubation with 10  $\mu\text{M}$  Nocistatin in a way that recapitulates calcium imaging conditions, did not significantly alter TRPA1 label (Fig.22), indicating that TRPA1 cell surface expression is not changed and suggesting another mechanism through which Nocistatin enhances TRPA1-mediated calcium influx in sensory neurons.

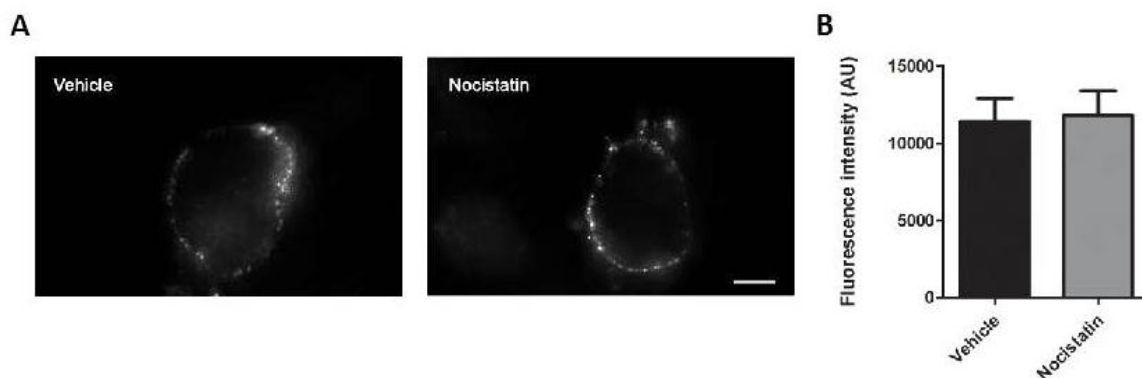


**Figure 22. Nocistatin does not alter TRPA1 cell surface expression in cultured DRG neurons**

**A, B**, DRG neurons were nucleofected with mTRPA1, cultured for 24 h and treated with either 10  $\mu\text{M}$  Nocistatin or vehicle, followed by live labeling to selectively visualize TRPA1 channels at the plasma membrane. Representative images (**A**) and quantification (**B**) of live labeling signal, similar between conditions;  $\geq 30$  cells analyzed. All data are represented as mean  $\pm$  SEM.

### 3.3.6 Nocistatin's effect on TRPA1 does not require NIPSNAP1

As Nocistatin has been reported to interact with NIPSNAP1 (Okuda-Ashitaka et al., 2012), and with our results suggesting that both have potential modulatory activity on TRPA1-mediated responses, we considered the possibility that the two binding partners act together in the regulation of TRPA1. Hypothetically, NIPSNAP1 might represent an intermediate element necessary for the increase in TRPA1-mediated responses induced by Nocistatin. In order to test this, we studied the consequences of NIPSNAP1 knock-down for Nocistatin-induced enhancement of MO responses via calcium imaging in DRG cultures. First and foremost, the efficacy of siRNA-mediated NIPSNAP1 knock-down was assessed at both mRNA (by qPCR) and protein level (by immunocytochemistry). From the qPCR studies we could evince that the relative expression of NIPSNAP1 mRNA declined by  $75.7 \pm 5\%$  in cultures treated with NIPSNAP1 siRNA (Fig.23B). Accordingly, immunostainings showed that  $65.8 \pm 2.7\%$  of all neurons express NIPSNAP1 under control conditions, compared to  $37.6 \pm 3.4\%$  upon NIPSNAP1 knock-down (Fig.23A,C). These results, in addition to further affirm the specificity of the NIPSNAP1 antibody, prove the effectiveness of this protocol for NIPSNAP1 protein knock-down.

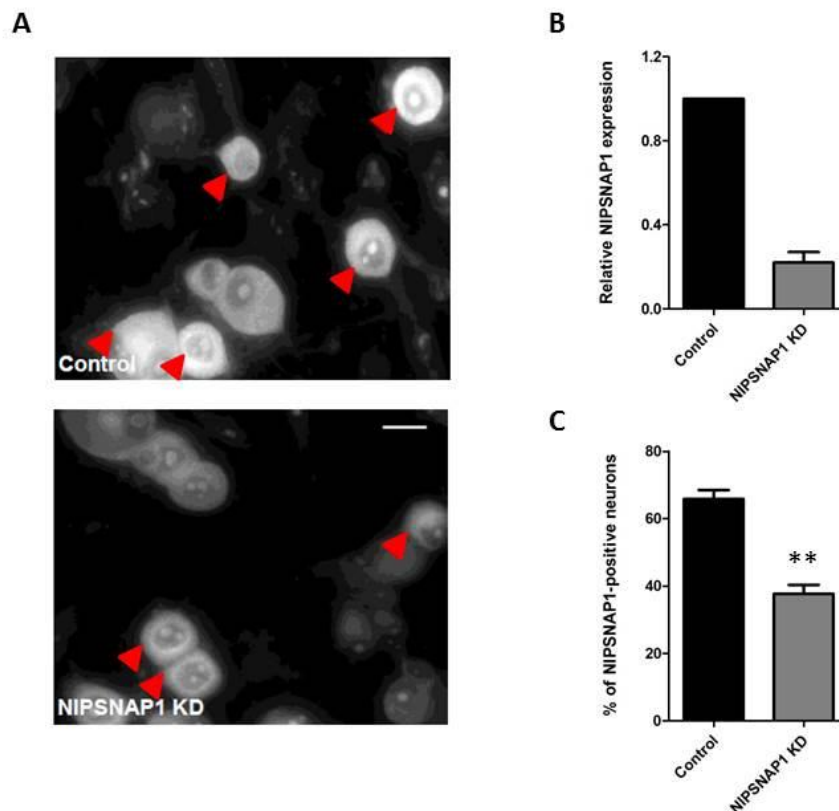


**Figure 23. NIPSNAP1 siRNA effectively knocks down the expression of NIPSNAP1 in DRG neuron cultures.**

**A**, Representative images of immunocytochemistry for NIPSNAP1 on DRG neuron cultures 3 days after transfection with NIPSNAP1 siRNA (NIPSNAP1 KD) or scramble control siRNA (Control). The extent of NIPSNAP1 knock-down after treatment with NIPSNAP1 siRNA was measured by qPCR (relative to housekeeping gene GAPDH) (**B**) and immunocytochemistry (**C**) (red arrowheads show examples of NIPSNAP1-positive neurons).  $\geq 700$  neurons analyzed from N=3 independent cultures. Scale bar, 10  $\mu\text{m}$ .  $p=0.002$ ; Student's t test. All data are

represented as mean  $\pm$  SEM. Data from experiments performed by Master student Oli Abate Fulas under the author's supervision. Figure A adapted from Oli's Master thesis.

We could then examine TRPA1-mediated calcium response with and without coapplication of Nocistatin upon knock-down of NIPSNAP1. The knock-down of NIPSNAP1 did not seem to affect the Nocistatin-induced enhancement of responses to 25  $\mu$ M MO, which was still visible in both siRNA- and mock-transfected DRG cultures (Fig.24). Specifically, the number of responders showed a trend that reflect what observed in WT cultures treated with Nocistatin, although, because of the poor health of the cultures, it did not reach statistical significance in this set of experiments. In contrast, responses to 50  $\mu$ M MO were similar between conditions, as well as response amplitudes. These results suggest that NIPSNAP1 is not necessary for the enhancement of TRPA1-mediated responses induced by its binding partner Nocistatin and additional rounds of the experiment will be performed to confirm this piece of data.

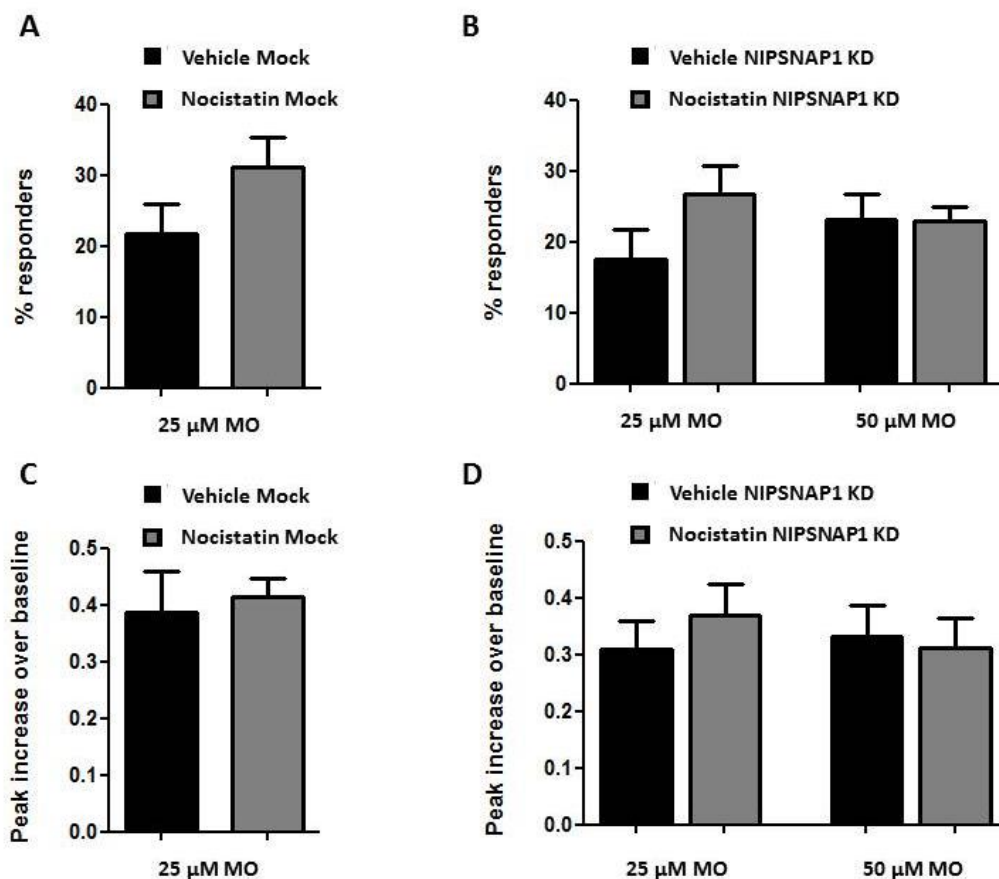


**Figure 24. NIPSNAP1 knock-down does not seem to affect Nocistatin's enhancement of TRPA1-mediated calcium response in DRG neuron cultures.**

**A**, Control siRNA-treated (Mock) DRG neurons show enhanced ( $p=0.134$ ) calcium response to 25  $\mu$ M MO upon coadministration of Nocistatin. **B**, The percentage of responders to 25  $\mu$ M MO in NIPSNAP1-siRNA-transfected neurons (NIPSNAP1 KD) still shows an increase ( $p=0.124$ ) upon Nocistatin treatment. **C,D**, Mean amplitude of response to either MO concentration is not altered in Mock-transfected (**C**) or NIPSNAP1 siRNA treated (**D**) cultures;  $\geq 350$  neurons analyzed per condition; Student's t test. All data are represented as mean  $\pm$  SEM. Data from experiments performed by Master student Oli Abate Fulas under the author's supervision.

## 4. DISCUSSION

The transient receptor potential A1 (TRPA1) channel is an essential component of the molecular mechanisms that originate and modulate pain signaling in vertebrates. In nociceptive neurons where it is highly enriched, TRPA1 plays a fundamental role as a primary detector of noxious stimuli, by sensing a wide variety of exogenous and endogenous molecules with pro-inflammatory and pro-algesic properties. (Andrade et al., 2012; Bautista et al., 2013). TRPA1 has been implicated in the development and maintenance of hypersensitivity in a number of animal pain models, and is critically involved in different pain states (Nassini et al., 2014; Nilius et al., 2012). Regulation of TRPA1 activity is indeed one of the factors that translate in the reduced threshold and enhanced responsiveness of sensory neurons that contribute to the pathophysiology of clinically-relevant chronic pain syndromes (Schmidt et al., 2009). Even though TRPA1 activation modalities have been studied extensively, comprehensive knowledge on the mechanisms of TRPA1 regulation is still missing. This is especially true for the whole network of protein interacting with TRPA1 (the so-called TRPA1 interactome), which might constitute a potentially relevant contributor to channel activity and function. Considering the crucial role of TRPA1 in pain signaling, it is mandatory to shed light on the elusive molecular machinery regulating TRPA1 channels in sensory neurons. The principal aim of this study was therefore to contribute to our understanding of the mechanisms of TRPA1 regulation by identifying and characterizing TRPA1-protein complexes and study their role for nociceptive signaling.

### 4.1 Annexin A2 (AnxA2) regulates TRPA1-dependent nociception

The gross part of the text relative to this section is based on (Avenali et al., 2014).

A mass spectrometry-based proteomics approach led to the identification of the physical interaction of Annexin A2 (AnxA2) with native TRPA1 in mouse sensory neurons. We then used a combination of *in vitro* assays and *in vivo* mouse behavioral studies to demonstrate that AnxA2 is an endogenous modulator of TRPA1 membrane availability in sensory neurons, which in turn influences TRPA1-dependent animal pain response. Annexin A2 (or AnxA2) belongs to the Annexin superfamily of calcium-effector proteins, which encompasses several members with distinct architecture and broad range of functions. The biochemical hallmarks of the Annexins are the unique  $\text{Ca}^{2+}$  and lipid binding properties that endow them with the ability to associate with negatively charged phospholipids in a  $\text{Ca}^{2+}$ -dependent and reversible manner. As a consequence, the functions of most Annexins are linked to their ability to interact with cellular membranes in a regulated fashion (Gerke et al., 2005). Like many other family members, AnxA2 is involved in a wide range of membrane trafficking processes and also contributes to the biogenesis of multivesicular bodies (Banks et al., 2011; Gerke et al.,

2005; Luo and Hajjar, 2013). Many reports have highlighted the involvement of AnxA2 in delivering and retrieving various transmembrane proteins to and from the plasma membrane. For instance, AnxA2 is required for cAMP-induced aquaporin-2 (AQP2) translocation to the apical membrane in renal cells (Tamma et al., 2008), and its interaction with the Na(+)-K(+)-2Cl(-) cotransporter (NKCC2) mediates lipid-raft-dependent trafficking and therefore surface expression of the protein (Dathe et al., 2014). AnxA2 has also been reported to regulate  $\beta$ 1 integrin internalization and degradation, suggesting an important role in modulating the cell-matrix adhesive properties of epithelial cells (Rankin et al., 2013). AnxA2 exerts its manifold functions in monomeric form or in heteromultimeric complexes with its best-known binding partner p11 (also designated S100A10), a member of the EF-hand superfamily of calcium-binding proteins. The AnxA2-p11 complex plays a critical role in hemostasis: in endothelial cells it has been shown to bind tissue plasminogen activator accelerating the catalytic generation of plasmin. Plasmin in turn hydrolyzes insoluble fibrin, thus maintaining blood vessel patency. If this mechanism is impaired, fibrin accumulates and predisposition to blood clotting significantly increases (Kim and Hajjar, 2002). The AnxA2-p11 complex also participates in  $Ca^{2+}$ -evoked exocytotic events in adrenal chromaffin granules (Ali et al., 1989) and Weibel–Palade bodies of endothelial cells (Gerke et al., 2005). Interestingly, the complex has also been reported to bind and modulate the function of proteins and ion channels involved in nociception, such as TRPV4 (Ning et al., 2012) and Nav1.8 (Okuse et al., 2002). Our study identified AnxA2 as a direct interacting protein of TRPA1, as revealed by mass spectrometry-based screening and also from overexpression studies in a well-established heterologous expression system. HEK293T cells studies showed that p11 does not bind TRPA1 and that the AnxA2-TRPA1 interaction does not require a neuronal cell-specific mediator. These data, together with the fact that we did not detect p11 in proteomics results, suggest that AnxA2 might be interacting with TRPA1 in its homomeric form (without p11). This hypothesis is further supported by our identification of the AnxA2 domain involved in the interaction with TRPA1 in the first 15 residues of the AnxA2 protein; this region has indeed been demonstrated in previous studies to constitute the binding site of p11 (Kube et al., 1992) and suggests that TRPA1 and p11 could potentially even compete for binding AnxA2. Recently, a TRPA1 splice variant baptized TRPA1b has been described to interact and increase TRPA1 levels at the plasma membrane of sensory neurons (Zhou et al., 2013). Even though our data show that AnxA2 and TRPA1 physically interact independently of TRPA1b in a heterologous expression system, we cannot exclude the possibility that AnxA2 binds TRPA1b as well and regulates its function in sensory neurons. Currently available TRPA1 antibodies are in fact not suitable to differentiate among TRPA1 isoforms and cannot help to address this question. This study identified and characterized a role of AnxA2 as an endogenous modulator of TRPA1 activity in nociceptive neurons *in vitro* and *in vivo*. The mechanisms underlying this regulation can be manifold. Our findings suggest that in sensory neurons the absence of AnxA2 translates in an increase of TRPA1 plasma membrane expression and function in a subpopulation of nociceptive neurons, as indicated by immunohistochemistry, live labeling, electrophysiology and calcium imaging studies. Specifically, in AnxA2<sup>-/-</sup> neurons we observe enhancement of TRPA1-dependent

neuronal calcium responses and MO-gated currents, which correlate with an increase of TRPA1 channels at the surface of sensory neurons. As a confirmation that the observed phenotypes are due to the lack of AnxA2, its re-expression was able to counteract the increase in TRPA1 surface levels and neuronal sensitivity to the TRPA1 agonist MO measured in AnxA2<sup>-/-</sup> neurons. Previous studies demonstrated that the expression, activity and function of TRPA1 channels can be regulated by different signaling pathways involving inflammatory signals (Dai et al., 2007; Schmidt et al., 2009; Wang et al., 2008a), growth factors (Diogenes et al., 2007), microRNA (Park et al., 2014) and interaction with TRPV1 and the splice variant TRPA1b (Akopian et al., 2007; Staruschenko et al., 2010; Zhou et al., 2013). While mechanistically we demonstrated a clear role of AnxA2 in regulating TRPA1 plasma membrane expression, the potential contribution of AnxA2 to each of these processes remains to be investigated. Our in vivo studies showed that the enhanced TRPA1 plasma membrane expression in AnxA2<sup>-/-</sup> sensory neurons nicely correlates with enhanced TRPA1-dependent pain behaviors in AnxA2<sup>-/-</sup> mice. These findings highlight the importance that controlling TRPA1 membrane availability might have for in vivo nociceptive signaling and are in accordance with previous studies (Obata et al., 2005; Schmidt et al., 2009; Zhou et al., 2013). The results of our immunohistochemical experiments confirm early reports (Naciff et al., 1996), showing that AnxA2 is expressed in both TRPA1-positive and TRPA1-negative subpopulations of DRG neurons. Therefore it might modulate other proteins and signaling pathways in addition to TRPA1. In sensory neurons, TRPA1 is also usually coexpressed with the capsaicin receptor TRPV1, in small diameter peptidergic afferent fibers (Kobayashi et al., 2005; Story et al., 2003). In fact, ablation of TRPV1 neurons with resiniferatoxin (a superpotent TRPV1 agonist) has been shown to induce loss of response to both capsaicin and mustard oil (Pecze et al., 2009), suggesting a high degree of colocalization of the two channels. This and other characteristics that make the two channels close relatives, led us to investigate the potential effect of AnxA2 on TRPV1 both in vitro and in vivo. Specifically we observed that: (1) from biochemical data in HEK293T cells AnxA2 does not physically bind to TRPV1; (2) cellular calcium responses to capsaicin were not altered in DRG cultures from AnxA2<sup>-/-</sup> mice compared to WT littermates; (3) in DRG cryosections the number of sensory neurons immunoreactive to TRPV1 was not changed; (4) mouse response to heat and nocifensive behaviors following intraplantar capsaicin injection were not different between genotypes. These results support a certain degree of specificity for the role of AnxA2 in regulating TRPA1-dependent nociception. Noteworthy, relevant evidence that nociceptive signaling is not generally perturbed in the absence of AnxA2 derives from the fact that baseline thermal and mechanical responses are not altered in AnxA2<sup>-/-</sup> mice. Moreover, the pain paradigms where we performed intraplantar injection of the specific agonist (MO or capsaicin) followed by assessment of nocifensive response require transmission via primary afferent nociceptors followed by supraspinal processing of the stimulus (Wang et al., 2013). Hence, the selective alteration of TRPA1-mediated behaviors argues against gross changes in supraspinal nociceptive signaling in AnxA2<sup>-/-</sup> mice. This is further supported by the fact that upon CFA-induced inflammatory pain, in these animals only specific hypersensitivity states (cold but not heat and mechanical allodynia) are affected. In conclusion, this study on the

characterization of AnxA2 as a novel TRPA1-interacting partner contributed to decipher the elusive composition of TRPA1-associated protein complexes. We demonstrated a role for AnxA2 as an endogenous modulator of TRPA1 activity *in vitro* and *in vivo*, and defined a mechanism capable of regulating TRPA1-mediated nociception in vertebrates. Furthermore, these results highlight the impact of protein-protein interactions in the modulation of TRPA1 activity and nociceptive signaling. A crucial question that follows these conclusions relates to the possibility of dynamic changes of TRPA1 interactome in different conditions. In the next chapter we tried to contribute to addressing this question.

## **4.2 TRPA1 interactome undergoes dramatic changes during inflammatory pain**

The study on the identification and characterization of AnxA2 as a novel modulator of TRPA1 function paved the way for a more thorough investigation of the dynamic changes of TRPA1-associated protein complexes. Considering the established contribution of TRPA1 to the modulation of inflammatory pain states (Bautista et al., 2006; da Costa et al., 2010; del Camino et al., 2010; Obata et al., 2005; Petrus et al., 2007; Zhou et al., 2013), and our results supporting TRPA1-involvement in CFA-induced allodynia (paragraph 3.1.8), we performed an interactomics screening of TRPA1-protein complexes in mice subjected to the CFA-model of inflammatory pain. In our hypothesis, TRPA1 interactome could undergo substantial changes between a physiological and a pathophysiological context, and also among different pain states. This would potentially translate in dramatic alterations of TRPA1 activity and sensitization, which, as already discussed, is known to contribute to nociceptor excitability and ultimately to hypersensitivity and altered pain perception (Basbaum et al., 2009; Patapoutian et al., 2009). A qualitative comparison of specifically identified proteins would give insights into pain-related channel protein complexes, and might even uncover novel targets for pain treatment. Furthermore, a relevant part of the changes associated to a targeted alteration of a biological system can be appreciated only with access to quantitative information. Here is where quantitative proteomics comes into play, dramatically raising the quality and depth of the obtained data. Until just about a decade ago, quantitative studies were limited to investigation of changes in gene expression mainly using oligonucleotide chips, in so-called transcriptomics studies (Ong and Mann, 2005). However, in this way only changes at the mRNA level can be assessed, and parallel analyses even using advanced technology have generally reported that, globally, transcriptome and proteome exhibit poor correlation (Bonaldi et al., 2008; Kumar and Mann, 2009).

In fact, proteins form the executive machinery that carry out most cellular functions, usually via stable or transient association into protein complexes. To date many proteomics studies have been performed to elucidate the components of multiprotein complexes (the

interactome) for several ion channels and receptors. Relevant studies contributed to the identification of cornichons proteins as auxiliary subunits of AMPA-type glutamate receptors, which have been shown to affect channel gating and expression in the rat brain (Schwenk et al., 2009); another study characterized the composition of NMDAR multiprotein complexes in the mouse brain, and their role in synaptic plasticity and learning (Husi et al., 2000). In a very recent and relevant study, Hanack and colleagues used a proteomics approach to identify components of TRPV1-associated protein complexes and thus uncovered a new role for the GABA<sub>B1</sub> receptor subunit in the modulation of TRPV1 sensitization. They generated transgenic mice expressing an affinity-tagged version of TRPV1, and then used sensory neurons from these animals for coimmunoprecipitation and mass spectrometry analysis (Hanack et al., 2015). While this strategy proved successful in the identification of the GABA<sub>B1</sub> receptor subunit as a novel binding partner and modulator of TRPV1 activity, this represents a major difference respect to the approach we adopted. We decided to use sensory neurons from naïve animals as the biological basis for the interactomics screening in order to selectively target native TRPA1 channel; while this necessarily demands more tissue, in this way we were more likely to detect real and biologically relevant interactions, respect to a system where the bait is overexpressed and, therefore, very likely not in physiological amounts. This factor might have a significant impact in the incidence of false positive identifications, which is likely to be less with our approach. Moreover, the absence of any exogenous affinity tag would further support this hypothesis. Several proteomics profiling studies advocate that gene expression and protein composition can undergo fundamental reorganization from physiological to pathological conditions (Huang et al., 2008; Melemedjian et al., 2013; Vacca et al., 2014; Zou et al., 2012). Nevertheless, to date only very few studies compared ion channel-multiprotein complexes between physiological and pathological conditions (Tu et al., 2010; Van den Oever et al., 2008). Our mass spectrometry-based proteomics approach revealed the interactome of TRPA1 channels in the context of inflammatory pain induced by CFA. The large datasets generated by quantitative proteomics can be difficult to interpret and we performed extensive data analysis in order to get relevant information. Upon application of selective criteria and analysis of the raw data coming from each single biological replicate, we determined high-confidence TRPA1-binding partners specific for either condition (VEH and CFA), and measured very limited overlap between them (Fig.13A). We realized volcano plots and tested different variations thereof to visualize the results, finding positive as well as negative characteristics in the way the data were represented. While there is not a perfect way to analyze and display data like these, we can gather information from them all and use it in combination for the best possible selection of high priority candidates for follow-up and validation. For example, we could prioritize candidates already selected according to our criteria in first analysis, and which on top show a significant p-value, as the ones identified by red spots in the volcano plot (Fig.15). Very importantly, the changes we observed by mass-spectrometry are now in the process of being validated with different orthogonal methods, among which are western blotting, immunostainings and proximity ligation assays (PLA). The gene ontology (GO) analysis indicate that an important fraction of the proteins interacting

with TRPA specifically during inflammatory pain is involved in protein transport and localization (Fig.13B). This is in line with a potential role in the trafficking of TRPA1 channels that can in turn determine its turnover, plasma membrane expression and function. Interestingly, we and others (Schmidt et al., 2009; Zhou et al., 2013) have already demonstrated a correlation between TRPA1 expression at the cell surface with nociceptor response and TRPA1-mediated nocifensive behavior in vivo (see chapter 3.1). The STRING association networks analysis allows the visualization of known and predicted interactions among proteins of the same database. On the one hand this information can help identifying potential pathways and cellular processes that are affected or modulated in the specific conditions. On the other hand it could also reflect an indirect association of some of these candidates to the bait. In fact, some proteins could interact and form complexes where only one member displays association to TRPA1, but upon coimmunoprecipitation they would be pulled-down together. While this indirect interaction could still be relevant and regulate TRPA1 function, it is unlikely that it could be reproduced for instance in a heterologous expression system where the intermediate link would be missing. These considerations, together with those described above and extensive literature search will drive orthogonal validation and the selection of the most interesting candidates for follow-up and investigation of the biological relevance of the interaction for nociceptive transmission. While this interactomics screening was performed at the peak of CFA-induced hypersensitivity for the mice (as measured by dynamic plantar aesthesiometer), we can speculate that the network of TRPA1-protein interactions might undergo significant changes over the course of the paradigm, especially once pain and hypersensitivity subside. The analysis of such dynamics might contribute to reveal mechanisms involved in the desensitization of TRPA1 and would be focus of further investigation. One more point that needs to be underlined is the fact that our study is based on the use of sole male mice for the pain paradigm. This choice was justified by the widely held notion that the reproductive cycle renders females intrinsically more variable than males, and that employing same gender animals would avoid undesired additional variability. However, several reports are raising awareness about the need of considering both sexes in animal studies, which is relevant also in the pain field. For example, a recent study showed that mechanical pain hypersensitivity is mediated by different immune cells in male and female mice (Sorge et al., 2015), and even proteomics studies reported sex-related differences during neuropathic pain (Vacca et al., 2014). While studies of both sexes necessarily result in additional expenses and workload, this issue had to be pointed out and will be considered for future studies. Nevertheless, our work significantly contributes to our understanding of TRPA1-associated protein complexes and future studies will reveal the contribution of selected candidates for TRPA1-mediated nociceptive signaling.

#### **4.2.1 Potential relevance of these findings**

Numerous reports have established that the activity and function of receptors and ion channels are crucially modulated by their association into protein complexes. Our study contributed to show that protein complexes can be dynamic and occur specifically under certain conditions. The identification and characterization of such protein complexes characterizing the specific (patho-)physiological state can provide relevant information about channel function, and moreover contribute to the development of novel therapeutic strategies. As already discussed, direct targeting of primary noxious stimuli detectors seemed to provide only limited benefits, due to related side-effects. One example is direct TRPV1 antagonism, which correlated to hyperthermia and impaired noxious pain sensation, which critically increases the susceptibility to injury (Brederson et al., 2013). Targeting specific channel-protein interactions holds therefore the possibility for a better-targeted intervention.

In a strategy ultimately aimed at quelling pain, the modulation of protein complexes to alter ion channel activity can be approached in different ways, which relates to the nature of the interaction. Some proteins have in fact been reported to enhance the activity of a pro-nociceptive ion channel. In such a case, either the removal of the binding partner or the “uncoupling” of the interaction are desirable, which would lead to decreased pain behavior. On the other hand, protein complexes might contribute to limit channel activity, as we showed to be the case for AnxA2. In this case, the strategy would be to ameliorate the interaction, increasing the affinity or the number of binding partners (Rouwette et al., 2015). The identification of pain state-specific channel-protein complexes will give valuable insights into the molecular mechanisms of these conditions; furthermore, such knowledge could be exploited to selectively interfere with altered ion channel activity during pathological pain states, while preserving the physiological protective ability to detect noxious stimuli. This study and future ones regarding dynamic changes of TRPA1-associated proteins in different pain states could therefore open the possibility to develop targeted therapeutics for TRPA1-related pain disorders.

#### **4.3 NIPSNAP1 and Nocistatin modulate TRPA1 channels**

In a parallel line of research we focused our attention on a protein called 4-Nitrophenylphosphatase domain and non-neuronal SNAP25-like protein homolog 1 (NIPSNAP1), which showed an interesting expression profile in mouse DRG neurons. In this line we performed a series of in vitro experiments aimed to investigate a potential role of NIPSNAP1 in TRPA1 regulation. Our results suggest that NIPSNAP1 is a protein expressed in nociceptors of DRGs where it possibly regulates the membrane expression and/or activity of TRPA1. In an attempt to further characterize this functional association, we investigated also the role of Nocistatin, a recently uncovered NIPSNAP1-binding partner and well known pain-

modulator (Okuda-Ashitaka et al., 2012), for TRPA1-mediated nociception. This work revealed that both proteins have the potential to affect TRPA1 activity, while the characterization of the specific underlying mechanisms will be focus of further investigation. NIPSNAP1 belongs to the largely uncharacterized NIPSNAP family of proteins which comprises three additional members: NIPSNAP2, NIPSNAP3 and NIPSNAP4 (Okuda-Ashitaka et al., 2012). The peculiar nomenclature derives from the fact that some portions of the proteins structure resemble a 4-nitrophenylphosphatase domain and non-neuronal SNAP25-like protein (Seroussi et al., 1998). The physiological functions of the NIPSNAP family remain elusive, even though the distinct genetic location of NIPSNAP1 sequence suggests a potential involvement in vesicular transport (Seroussi et al., 1998). NIPSNAP1 showed predominant expression in the brain, spinal cord, liver, and kidney (Okuda-Ashitaka et al., 2012). In the brain, it is especially enriched in synaptic membranes, cell surface and mitochondria of neuronal cells, but not glia. (Nautiyal et al., 2010). Over the past few years, NIPSNAP1 has been associated to a number of metabolic and nervous system pathologies. For instance, it has been reported to bind the amyloid precursor protein that is implicated in Alzheimer disease (Tummala et al., 2010), and NIPSNAP1 levels are increased during generalized seizures induced by kainate (Satoh et al., 2002). Despite the handful of studies on NIPSNAP proteins and their potential roles, there is recent evidence indicating that NIPSNAP1 associates with TRPV6 channels in mouse liver cells, which results in a dramatic inhibition of the channel function, with currents virtually abolished (Schoeber et al., 2008). NIPSNAP2, another member of the NIPSNAP family has instead been shown to modulate L-type Ca<sup>2+</sup> channels, and downstream CREB (cAMP response element-binding protein) signaling, in a neuronal cell line (Brittain et al., 2012). These studies potentially suggest a role for the proteins of the NIPSNAP family in the regulation of ion channels. Although NIPSNAP1 expression has already been described in different brain regions (Nautiyal et al., 2010), no report had previously reported of its distribution in the peripheral nervous system. Our immunohistochemical studies established that NIPSNAP1 is abundantly expressed in sensory neurons of mouse DRGs and furthermore demonstrate enrichment in a nociceptive subpopulation coexpressing the marker Peripherin. This expression pattern potentially suggests a still-unknown role of NIPSNAP1 in a subset of mouse nociceptors which is likely to match, at least to a certain extent, the subset which expresses TRPA1. We therefore aimed at investigating a potential role of NIPSNAP1 in TRPA1 regulation, by testing the outcomes of NIPSNAP1 modulation in vitro in sensory neuron cultures. Concerned by potential compensatory mechanisms that would possibly mask a phenotype following selective NIPSNAP1 knock-down, we aimed at overexpressing the protein in DRG cultures. Interestingly, immunostainings revealed a decrease in the number of TRPA1-immunoreactive neurons upon NIPSNAP1 overexpression, suggesting a potential intriguing role of NIPSNAP1 in modulating TRPA1 expression in sensory neurons. We then proposed that these changes could be reflected by TRPA1-mediated cellular calcium responses, which directly reflect the number and activity of TRPA1 channels expressed at the plasma membrane. If the modulation of TRPA1 by NIPSNAP1 is modest, the high heterogeneity of sensory neuron populations in DRG cultures would complicate the identification of a possible phenotype.

Therefore we translated these findings to a heterologous expression system (HEK293T cells) where we could maintain better control over the cellular environment and more easily manipulate NIPSNAP1 expression. In agreement with DRG data, we measured lower number of TRPA1-positive cells upon NIPSNAP1 overexpression. We then correlated the decreased TRPA1-immunoreactivity measured upon NIPSNAP1 overexpression with a reduction of neuronal response to specific TRPA activation. Noteworthy, the total number of TRPA1-expressing cells did not show any difference between conditions. As already mentioned, the TRPA1 antibody used has been reported to preferentially label cells with relatively high expression of TRPA1 (Schmidt et al., 2009); this therefore suggests that the observed difference is related to this subpopulation of TRPA1-expressing cells. This phenotype could be explained by an action of NIPSNAP1 at different levels, ultimately affecting TRPA1 expression and function. Hypothetically, NIPSNAP1 could directly interact with TRPA1, targeting the channel for degradation. This process may in turn require one or more accessory proteins, acting as an intermediate link. Alternatively, NIPSNAP1 could be affecting other cellular pathways, possibly even at pre-translational level, which would ultimately result in a decreased TRPA1 expression. In an attempt to address some of these questions and evaluate a potential direct interaction between NIPSNAP1 and TRPA1, we performed coimmunoprecipitation experiments in HEK293T cells transfected with both proteins. Unfortunately, preliminary results from these efforts (data not shown, experiments performed by Oli Abate Fulas and Julia Sondermann) are inconclusive and do not allow us clear statements about the molecular relation between the two proteins. At the same time, NIPSNAP1 could also be directly inhibiting TRPA1 activity, mechanism that has already been suggested for its modulating action on TRPV6 channels (Schoeber et al., 2008).

An intriguing recent study has shed some lights on a novel potential role of NIPSNAP1 in pain transmission by uncovering its interaction with Nocistatin, a neuropeptide that is produced from the same precursor protein as Nociceptin/orphanin FQ (N/OFQ) (Okuda-Ashitaka et al., 2012). Nocistatin is well known to be involved in nociceptive signaling: *in vivo* it counteracts N/OFQ-induced allodynia and hyperalgesia, and directly modulates inflammatory pain responses in a dose-dependent manner (Nakano et al., 2000; Okuda-Ashitaka et al., 1998; Okuda-Ashitaka et al., 2012; Zeilhofer et al., 2000). The study from Okuda-Ashitaka and colleagues reported the interaction between Nocistatin and NIPSNAP1 and described that the inhibition of Nociceptin-induced allodynia by Nocistatin measured in WT mice was completely lacking in NIPSNAP1-deficient animals (Okuda-Ashitaka et al., 2012). In the light of these findings, we attempted to further investigate the functional association between NIPSNAP1 and TRPA1 by examining Nocistatin. Interestingly, calcium imaging experiments revealed that stimulation with Nocistatin significantly enhances TRPA1-mediated calcium responses in sensory neuron cultures. These results are in line with previous reports showing a pro-nociceptive effect of Nocistatin, which facilitates nociceptive flexor reflexes (Xu et al., 1999) and enhances nocifensive behavior in the rat formalin test (Zeilhofer et al., 2000). A study from Inoue and colleagues suggested that part of these effects is mediated by neurotransmitter release from a population of capsaicin-sensitive (and therefore TRPV1-

expressing) neurons (Inoue et al., 2003). Interestingly, a subset of these neurons is also bound to express TRPA1 as the two channels are known to be largely coexpressed (Pecze et al., 2009; Story et al., 2003). Despite almost a decade has passed and extensive literature accumulated about Nocistatin and its role in pain, the specific molecular mechanisms and target(s) of its action are still elusive (Okuda-Ashitaka and Ito, 2015). These considerations, together with the fact that cellular responses to TRPV1 activation by capsaicin were not affected, led us to hypothesize a potential involvement of TRPA1 as one of the target receptors through which Nocistatin modulates pain transmission. Our data showed that MO-gated neuronal calcium responses are enhanced by Nocistatin. Mechanistically, this effect did not seem to be mediated by alteration of the plasma membrane expression of the channel, as showed by live labeling of surface TRPA1. While we cannot exclude a different phenotype at higher concentrations, Nocistatin did not induce cellular calcium influx on its own (data not shown), and therefore it is likely not gating TRPA1 directly. It is possible that Nocistatin's effect is mediated by an enhancement of TRPA1 activity at the cell surface: this could be the result of either direct action on the channel (as an allosteric modulator) or in turn mediated by alteration of other intracellular signaling pathways that regulate TRPA1 activity (Lapointe and Altier, 2011). Whether biophysical properties of the channel are modulated by treatment with Nocistatin will be focus of further investigation. In this context we also hypothesized that Nocistatin-induced enhancement of cellular responses to MO might require NIPSNAP1, as this is known to be the case for the inhibition of Nociceptin-induced allodynia exerted by Nocistatin (Okuda-Ashitaka et al., 2012). However, calcium imaging studies upon NIPSNAP1 knock-down showed a trend that reflects what observed in WT cultures treated with Nocistatin, suggesting that NIPSNAP1 is dispensable for the observed phenotype.

In conclusion we uncovered a potential role for both NIPSNAP1 and Nocistatin as endogenous modulators of TRPA1 activity in vitro in sensory neurons. While our studies suggest that NIPSNAP1 and Nocistatin act independently to affect TRPA1 activity, future studies will contribute to characterize the underlying mechanisms and also the potential relevance for TRPA1-mediated nociception in vivo.

## 5. SUMMARY

The transient receptor potential A1 (TRPA1) channel is essential for vertebrate pain. TRPA1 plays a fundamental role as a primary detector of noxious stimuli of physical and chemical nature, and is critically involved in different pain states. Even though TRPA1 activation modalities have been studied extensively, the network of protein interactions regulating TRPA1 (the so-called TRPA1 interactome) is only poorly understood. Considering the crucial role of TRPA1 in pain signaling, it is mandatory to shed light on the elusive molecular machinery regulating TRPA1 channels in sensory neurons. This project was therefore aimed at getting insights into the mechanisms of TRPA1 regulation by identifying TRPA1-protein complexes and characterizing their biological meaning in the context of nociception.

A mass spectrometry-based proteomics approach led to the discovery of the physical association of Annexin A2 (AnxA2) with native TRPA1 in mouse sensory neurons. AnxA2 is enriched in a subpopulation of sensory neurons and coexpressed with TRPA1. Furthermore, we observed an increase of TRPA1 membrane levels in cultured sensory neurons from AnxA2-deficient mice. Functional studies suggest that AnxA2 limits the availability and consequently the activity of TRPA1 channels at the plasma membrane of sensory neurons. Moreover, our *in vitro* observations were reflected in enhanced nocifensive responses of AnxA2 knock-out mice specifically upon TRPA1 activation *in vivo*. TRPA1 channels have been shown to contribute to hypersensitivity to cold stimuli during inflammation. We therefore investigated the possible impact of AnxA2 on TRPA1 function also in this context employing the well-established complete Freund's adjuvant (CFA) model of persistent inflammation in mice. AnxA2-deficient mice showed enhanced hypersensitivity on a cold plate upon CFA injection, whereas the hypersensitivity to heat and mechanical stimulation were not affected. In conclusion, we characterized AnxA2 as a novel TRPA1-associated protein which specifically regulates TRPA1 channels *in vitro* and *in vivo*.

These findings pave the way for a more thorough investigation of the dynamic changes in TRPA1-associated protein complexes in different conditions. In this context we submitted mice to the established Complete Freund's Adjuvant (CFA)-model of inflammatory pain and isolated TRPA1-protein complexes from sensory neurons. Samples were submitted to state-of-the-art quantitative mass spectrometry analysis to compare complexes between CFA and control mice and therefore identify dynamic changes in TRPA1 interactome. This work revealed a dramatic alteration of TRPA1-associated protein complexes in the context of inflammatory pain, and the functional characterization of selected candidates that will follow this study might uncover new players in the development and maintenance of inflammatory pain.

In a separate set of experiments we focused our attention on a protein called 4-Nitrophenylphosphatase domain and non-neuronal SNAP25-like protein homolog 1

(NIPSNAP1), which function is largely still unknown. NIPSNAP1 showed to be expressed in nociceptive neurons of mouse dorsal root ganglia and functional studies suggested that it can modulate TRPA1 expression and/or function upon overexpression. A role of NIPSNAP1 in nociceptive transmission has been recently uncovered by the identification of its physical association with Nocistatin, a neuropeptide involved in pain signaling. In this context we investigated Nocistatin and found that it enhances TRPA1-mediated cellular calcium responses in DRG neurons. Mechanistically, this effect does not seem to be mediated by a modulation of TRPA1 plasma membrane expression, and NIPSNAP1 knock-down did not affect it. Future studies will contribute to characterize the underlying mechanisms and also the potential relevance for TRPA1-mediated nociception in vivo.

## 6. REFERENCES

- Aebersold, R., and Mann, M. (2003). Mass spectrometry-based proteomics. *Nature* 422, 198-207.
- Ahmadi, S., Kotalla, C., Guhring, H., Takeshima, H., Pahl, A., and Zeilhofer, H.U. (2001). Modulation of synaptic transmission by nociceptin/orphanin FQ and nocistatin in the spinal cord dorsal horn of mutant mice lacking the nociceptin/orphanin FQ receptor. *Molecular pharmacology* 59, 612-618.
- Ahmadi, S., Muth-Selbach, U., Lauterbach, A., Lipfert, P., Neuhuber, W.L., and Zeilhofer, H.U. (2003). Facilitation of spinal NMDA receptor currents by spillover of synaptically released glycine. *Science (New York, NY)* 300, 2094-2097.
- Akopian, A.N., Ruparel, N.B., Jeske, N.A., and Hargreaves, K.M. (2007). Transient receptor potential TRPA1 channel desensitization in sensory neurons is agonist dependent and regulated by TRPV1-directed internalization. *The Journal of physiology* 583, 175-193.
- Alessandri-Haber, N., Dina, O.A., Chen, X., and Levine, J.D. (2009). TRPC1 and TRPC6 channels cooperate with TRPV4 to mediate mechanical hyperalgesia and nociceptor sensitization. *The Journal of neuroscience : the official journal of the Society for Neuroscience* 29, 6217-6228.
- Alessandri-Haber, N., Yeh, J.J., Boyd, A.E., Parada, C.A., Chen, X., Reichling, D.B., and Levine, J.D. (2003). Hypotonicity induces TRPV4-mediated nociception in rat. *Neuron* 39, 497-511.
- Ali, S.M., Geisow, M.J., and Burgoyne, R.D. (1989). A role for calpactin in calcium-dependent exocytosis in adrenal chromaffin cells. *Nature* 340, 313-315.
- Almaraz, L., Manenschijn, J.A., de la Pena, E., and Viana, F. (2014). TRPM8. *Handbook of experimental pharmacology* 222, 547-579.
- Almeida, T.F., Roizenblatt, S., and Tufik, S. (2004). Afferent pain pathways: a neuroanatomical review. *Brain research* 1000, 40-56.
- Andrade, E.L., Meotti, F.C., and Calixto, J.B. (2012). TRPA1 antagonists as potential analgesic drugs. *Pharmacology & therapeutics* 133, 189-204.
- Anggono, V., and Huganir, R.L. (2012). Regulation of AMPA receptor trafficking and synaptic plasticity. *Current opinion in neurobiology* 22, 461-469.
- Apkarian, A.V., Bushnell, M.C., Treede, R.D., and Zubieta, J.K. (2005). Human brain mechanisms of pain perception and regulation in health and disease. *European journal of pain (London, England)* 9, 463-484.

Avenali, L., Narayanan, P., Rouwette, T., Cervellini, I., Sereda, M., Gomez-Varela, D., and Schmidt, M. (2014). Annexin A2 regulates TRPA1-dependent nociception. *The Journal of neuroscience : the official journal of the Society for Neuroscience* 34, 14506-14516.

Bandell, M., Macpherson, L.J., and Patapoutian, A. (2007). From chills to chilis: mechanisms for thermosensation and chemesthesis via thermoTRPs. *Current opinion in neurobiology* 17, 490-497.

Bandell, M., Story, G.M., Hwang, S.W., Viswanath, V., Eid, S.R., Petrus, M.J., Earley, T.J., and Patapoutian, A. (2004). Noxious cold ion channel TRPA1 is activated by pungent compounds and bradykinin. *Neuron* 41, 849-857.

Banks, G.T., Haas, M.A., Line, S., Shepherd, H.L., Alqatari, M., Stewart, S., Rishal, I., Philpott, A., Kalmar, B., Kuta, A., *et al.* (2011). Behavioral and other phenotypes in a cytoplasmic Dynein light intermediate chain 1 mutant mouse. *The Journal of neuroscience : the official journal of the Society for Neuroscience* 31, 5483-5494.

Basbaum, A.I., Bautista, D.M., Scherrer, G., and Julius, D. (2009). Cellular and molecular mechanisms of pain. *Cell* 139, 267-284.

Basbaum A, Jessell T. The perception of pain. In: Kandel ER, Schwartz JH, Jessell TM, editors. *Principles of Neural Science*. 4th ed. New York: McGraw-Hill, Health Professions Division; 2000

Bautista, D.M., Jordt, S.E., Nikai, T., Tsuruda, P.R., Read, A.J., Poblete, J., Yamoah, E.N., Basbaum, A.I., and Julius, D. (2006). TRPA1 mediates the inflammatory actions of environmental irritants and proalgesic agents. *Cell* 124, 1269-1282.

Bautista, D.M., Movahed, P., Hinman, A., Axelsson, H.E., Sterner, O., Hogestatt, E.D., Julius, D., Jordt, S.E., and Zygmunt, P.M. (2005). Pungent products from garlic activate the sensory ion channel TRPA1. *Proceedings of the National Academy of Sciences of the United States of America* 102, 12248-12252.

Bautista, D.M., Pellegrino, M., and Tsunozaki, M. (2013). TRPA1: A gatekeeper for inflammation. *Annual review of physiology* 75, 181-200.

Bautista, D.M., Siemens, J., Glazer, J.M., Tsuruda, P.R., Basbaum, A.I., Stucky, C.L., Jordt, S.E., and Julius, D. (2007). The menthol receptor TRPM8 is the principal detector of environmental cold. *Nature* 448, 204-208.

Benemei, S., Patacchini, R., Trevisani, M., and Geppetti, P. (2015). TRP channels. *Current opinion in pharmacology* 22, 18-23.

Bonaldi, T., Straub, T., Cox, J., Kumar, C., Becker, P.B., and Mann, M. (2008). Combined use of RNAi and quantitative proteomics to study gene function in *Drosophila*. *Molecular cell* 31, 762-772.

- Boulay, G., Zhu, X., Peyton, M., Jiang, M., Hurst, R., Stefani, E., and Birnbaumer, L. (1997). Cloning and expression of a novel mammalian homolog of *Drosophila* transient receptor potential (Trp) involved in calcium entry secondary to activation of receptors coupled by the Gq class of G protein. *The Journal of biological chemistry* 272, 29672-29680.
- Bourinet, E., Altier, C., Hildebrand, M.E., Trang, T., Salter, M.W., and Zamponi, G.W. (2014). Calcium-permeable ion channels in pain signaling. *Physiological reviews* 94, 81-140.
- Brederson, J.D., Kym, P.R., and Szallasi, A. (2013). Targeting TRP channels for pain relief. *European journal of pharmacology* 716, 61-76.
- Breivik, H., Collett, B., Ventafridda, V., Cohen, R., and Gallacher, D. (2006). Survey of chronic pain in Europe: prevalence, impact on daily life, and treatment. *European journal of pain (London, England)* 10, 287-333.
- Brittain, J.M., Wang, Y., Wilson, S.M., and Khanna, R. (2012). Regulation of CREB signaling through L-type Ca<sup>2+</sup> channels by Nipsnap-2. *Channels (Austin, Tex)* 6, 94-102.
- Buechler, C., Bodzioch, M., Bared, S.M., Sigrüener, A., Boettcher, A., Lapicka-Bodzioch, K., Aslanidis, C., Duong, C.Q., Grandl, M., Langmann, T., *et al.* (2004). Expression pattern and raft association of NIPSNAP3 and NIPSNAP4, highly homologous proteins encoded by genes in close proximity to the ATP-binding cassette transporter A1. *Genomics* 83, 1116-1124.
- Calvo, R.R., Meegalla, S.K., Parks, D.J., Parsons, W.H., Ballentine, S.K., Lubin, M.L., Schneider, C., Colburn, R.W., Flores, C.M., and Player, M.R. (2012). Discovery of vinylcycloalkyl-substituted benzimidazole TRPM8 antagonists effective in the treatment of cold allodynia. *Bioorganic & medicinal chemistry letters* 22, 1903-1907.
- Caspani, O., and Heppenstall, P.A. (2009). TRPA1 and Cold Transduction: An Unresolved Issue? *The Journal of General Physiology* 133, 245-249.
- Caterina, M.J., Leffler, A., Malmberg, A.B., Martin, W.J., Trafton, J., Petersen-Zeitz, K.R., Koltzenburg, M., Basbaum, A.I., and Julius, D. (2000). Impaired nociception and pain sensation in mice lacking the capsaicin receptor. *Science (New York, NY)* 288, 306-313.
- Caterina, M.J., Rosen, T.A., Tominaga, M., Brake, A.J., and Julius, D. (1999). A capsaicin-receptor homologue with a high threshold for noxious heat. *Nature* 398, 436-441.
- Caterina, M.J., Schumacher, M.A., Tominaga, M., Rosen, T.A., Levine, J.D., and Julius, D. (1997). The capsaicin receptor: a heat-activated ion channel in the pain pathway. *Nature* 389, 816-824.
- Chen, Y., Yang, C., and Wang, Z.J. (2011). Proteinase-activated receptor 2 sensitizes transient receptor potential vanilloid 1, transient receptor potential vanilloid 4, and transient receptor potential ankyrin 1 in paclitaxel-induced neuropathic pain. *Neuroscience* 193, 440-451.
- Chu, K.L., Chandran, P., Joshi, S.K., Jarvis, M.F., Kym, P.R., and McGaraughty, S. (2011). TRPV1-related modulation of spinal neuronal activity and behavior in a rat model of osteoarthritic pain. *Brain research* 1369, 158-166.

Chuang, H.H., Prescott, E.D., Kong, H., Shields, S., Jordt, S.E., Basbaum, A.I., Chao, M.V., and Julius, D. (2001). Bradykinin and nerve growth factor release the capsaicin receptor from PtdIns(4,5)P2-mediated inhibition. *Nature* 411, 957-962.

Clapham, D.E. (2003). TRP channels as cellular sensors. *Nature* 426, 517-524.

Clapham, D.E. (2015). Structural biology: Pain-sensing TRPA1 channel resolved. *Nature* 520, 439-441.

Colburn, R.W., Lubin, M.L., Stone, D.J., Jr., Wang, Y., Lawrence, D., D'Andrea, M.R., Brandt, M.R., Liu, Y., Flores, C.M., and Qin, N. (2007). Attenuated cold sensitivity in TRPM8 null mice. *Neuron* 54, 379-386.

Coste, B., Mathur, J., Schmidt, M., Earley, T.J., Ranade, S., Petrus, M.J., Dubin, A.E., and Patapoutian, A. (2010). Piezo1 and Piezo2 are essential components of distinct mechanically activated cation channels. *Science (New York, NY)* 330, 55-60.

Costigan, M., Scholz, J., and Woolf, C.J. (2009). Neuropathic pain: a maladaptive response of the nervous system to damage. *Annual review of neuroscience* 32, 1-32.

Cox, J.J., Reimann, F., Nicholas, A.K., Thornton, G., Roberts, E., Springell, K., Karbani, G., Jafri, H., Mannan, J., Raashid, Y., *et al.* (2006). An SCN9A channelopathy causes congenital inability to experience pain. *Nature* 444, 894-898.

Cruz-Orengo, L., Dhaka, A., Heuermann, R.J., Young, T.J., Montana, M.C., Cavanaugh, E.J., Kim, D., and Story, G.M. (2008). Cutaneous nociception evoked by 15-delta PGJ2 via activation of ion channel TRPA1. *Molecular pain* 4, 30.

Cvetkov, T.L., Huynh, K.W., Cohen, M.R., and Moiseenkova-Bell, V.Y. (2011). Molecular architecture and subunit organization of TRPA1 ion channel revealed by electron microscopy. *The Journal of biological chemistry* 286, 38168-38176.

da Costa, D.S., Meotti, F.C., Andrade, E.L., Leal, P.C., Motta, E.M., and Calixto, J.B. (2010). The involvement of the transient receptor potential A1 (TRPA1) in the maintenance of mechanical and cold hyperalgesia in persistent inflammation. *Pain* 148, 431-437.

Dai, Y., Wang, S., Tominaga, M., Yamamoto, S., Fukuoka, T., Higashi, T., Kobayashi, K., Obata, K., Yamanaka, H., and Noguchi, K. (2007). Sensitization of TRPA1 by PAR2 contributes to the sensation of inflammatory pain. *The Journal of clinical investigation* 117, 1979-1987.

Dathe, C., Daigeler, A.L., Seifert, W., Jankowski, V., Mrowka, R., Kalis, R., Wanker, E., Mutig, K., Bachmann, S., and Paliege, A. (2014). Annexin A2 mediates apical trafficking of renal Na(+)-K(+)-2Cl(-) cotransporter. *The Journal of biological chemistry* 289, 9983-9997.

Davis, J.B., Gray, J., Gunthorpe, M.J., Hatcher, J.P., Davey, P.T., Overend, P., Harries, M.H., Latcham, J., Clapham, C., Atkinson, K., *et al.* (2000). Vanilloid receptor-1 is essential for inflammatory thermal hyperalgesia. *Nature* 405, 183-187.

de Bono, M., Tobin, D.M., Davis, M.W., Avery, L., and Bargmann, C.I. (2002). Social feeding in *Caenorhabditis elegans* is induced by neurons that detect aversive stimuli. *Nature* 419, 899-903.

del Camino, D., Murphy, S., Heiry, M., Barrett, L.B., Earley, T.J., Cook, C.A., Petrus, M.J., Zhao, M., D'Amours, M., Deering, N., *et al.* (2010). TRPA1 contributes to cold hypersensitivity. *The Journal of neuroscience : the official journal of the Society for Neuroscience* 30, 15165-15174.

Derry, S., Sven-Rice, A., Cole, P., Tan, T., and Moore, R.A. (2013). Topical capsaicin (high concentration) for chronic neuropathic pain in adults. *The Cochrane database of systematic reviews* 2, Cd007393.

Dhaka, A., Viswanath, V., and Patapoutian, A. (2006). Trp ion channels and temperature sensation. *Annual review of neuroscience* 29, 135-161.

Diogenes, A., Akopian, A.N., and Hargreaves, K.M. (2007). NGF up-regulates TRPA1: implications for orofacial pain. *Journal of dental research* 86, 550-555.

Distler, U., Kuharev, J., Navarro, P., Levin, Y., Schild, H., and Tenzer, S. (2014). Drift time-specific collision energies enable deep-coverage data-independent acquisition proteomics. *Journal of proteome research* 13, 167-170.

Djoughri, L., and Lawson, S.N. (2004). Abeta-fiber nociceptive primary afferent neurons: a review of incidence and properties in relation to other afferent A-fiber neurons in mammals. *Brain research Brain research reviews* 46, 131-145.

Doerner, J.F., Gisselmann, G., Hatt, H., and Wetzel, C.H. (2007). Transient receptor potential channel A1 is directly gated by calcium ions. *The Journal of biological chemistry* 282, 1155-1161.

Donier, E., Rugiero, F., Okuse, K., and Wood, J.N. (2005). Annexin II light chain p11 promotes functional expression of acid-sensing ion channel ASIC1a. *The Journal of biological chemistry* 280, 38666-38672.

Dubin, A.E., and Patapoutian, A. (2010). Nociceptors: the sensors of the pain pathway. *The Journal of clinical investigation* 120, 3760-3772.

Edelmayer, R.M., Le, L.N., Yan, J., Wei, X., Nassini, R., Materazzi, S., Preti, D., Appendino, G., Geppetti, P., Dodick, D.W., *et al.* (2012). Activation of TRPA1 on dural afferents: a potential mechanism of headache pain. *Pain* 153, 1949-1958.

Eid, S.R., Crown, E.D., Moore, E.L., Liang, H.A., Choong, K.C., Dima, S., Henze, D.A., Kane, S.A., and Urban, M.O. (2008). HC-030031, a TRPA1 selective antagonist, attenuates inflammatory- and neuropathy-induced mechanical hypersensitivity. *Molecular pain* 4, 48.

Fernandes, E.S., Russell, F.A., Spina, D., McDougall, J.J., Graepel, R., Gentry, C., Staniland, A.A., Mountford, D.M., Keeble, J.E., Malcangio, M., *et al.* (2011). A distinct role for transient receptor potential ankyrin 1, in addition to transient receptor potential vanilloid 1, in tumor

necrosis factor alpha-induced inflammatory hyperalgesia and Freund's complete adjuvant-induced monoarthritis. *Arthritis and rheumatism* 63, 819-829.

Ferrandiz-Huertas, C., Mathivanan, S., Wolf, C.J., Devesa, I., and Ferrer-Montiel, A. (2014). Trafficking of ThermoTRP Channels. *Membranes* 4, 525-564.

Fischer, M.J., Balasuriya, D., Jeggle, P., Goetze, T.A., McNaughton, P.A., Reeh, P.W., and Edwardson, J.M. (2014). Direct evidence for functional TRPV1/TRPA1 heteromers. *Pflugers Archiv : European journal of physiology* 466, 2229-2241.

Fischer, M.J., Btsh, J., and McNaughton, P.A. (2013). Disrupting sensitization of transient receptor potential vanilloid subtype 1 inhibits inflammatory hyperalgesia. *The Journal of neuroscience : the official journal of the Society for Neuroscience* 33, 7407-7414.

Gavva, N.R., Treanor, J.J., Garami, A., Fang, L., Surapaneni, S., Akrami, A., Alvarez, F., Bak, A., Darling, M., Gore, A., *et al.* (2008). Pharmacological blockade of the vanilloid receptor TRPV1 elicits marked hyperthermia in humans. *Pain* 136, 202-210.

Gerke, V., Creutz, C.E., and Moss, S.E. (2005). Annexins: linking Ca<sup>2+</sup> signalling to membrane dynamics. *Nature reviews Molecular cell biology* 6, 449-461.

Geromanos, S.J., Hughes, C., Ciavarini, S., Vissers, J.P., and Langridge, J.I. (2012). Using ion purity scores for enhancing quantitative accuracy and precision in complex proteomics samples. *Analytical and bioanalytical chemistry* 404, 1127-1139.

Gold MS. Ion channels: recent advances and clinical applications. In: Flor H, Kaslo E, Dostrovsky JO, eds. *Proceedings of the 11th World Congress on Pain.*; Seattle, WA: IASP Press; 2006; pp. 73-92.

Gomez-Varela, D., Schmidt, M., Schoellerman, J., Peters, E.C., and Berg, D.K. (2012). PMCA2 via PSD-95 controls calcium signaling by alpha7-containing nicotinic acetylcholine receptors on aspiny interneurons. *The Journal of neuroscience : the official journal of the Society for Neuroscience* 32, 6894-6905.

Hanack, C., Moroni, M., Lima, W.C., Wende, H., Kirchner, M., Adelfinger, L., Schrenk-Siemens, K., Tappe-Theodor, A., Wetzels, C., Kuich, P.H., *et al.* (2015). GABA blocks pathological but not acute TRPV1 pain signals. *Cell* 160, 759-770.

Haraguchi, K., Kawamoto, A., Isami, K., Maeda, S., Kusano, A., Asakura, K., Shirakawa, H., Mori, Y., Nakagawa, T., and Kaneko, S. (2012). TRPM2 contributes to inflammatory and neuropathic pain through the aggravation of pronociceptive inflammatory responses in mice. *The Journal of neuroscience : the official journal of the Society for Neuroscience* 32, 3931-3941.

Haus, B.M., Hsu, A.R., Yim, E.S., Meter, J.J., and Rinsky, L.A. (2010). Long-term follow-up of the surgical management of neuropathic arthropathy of the spine. *The spine journal : official journal of the North American Spine Society* 10, e6-e16.

Huang, D., Li, S., Dhaka, A., Story, G.M., and Cao, Y.Q. (2012). Expression of the transient receptor potential channels TRPV1, TRPA1 and TRPM8 in mouse trigeminal primary afferent neurons innervating the dura. *Molecular pain* 8, 66.

Huang da, W., Sherman, B.T., and Lempicki, R.A. (2009a). Bioinformatics enrichment tools: paths toward the comprehensive functional analysis of large gene lists. *Nucleic acids research* 37, 1-13.

Huang da, W., Sherman, B.T., and Lempicki, R.A. (2009b). Systematic and integrative analysis of large gene lists using DAVID bioinformatics resources. *Nature protocols* 4, 44-57.

Huang, H.L., Cendan, C.M., Roza, C., Okuse, K., Cramer, R., Timms, J.F., and Wood, J.N. (2008). Proteomic profiling of neuromas reveals alterations in protein composition and local protein synthesis in hyper-excitabile nerves. *Molecular pain* 4, 33.

Hucho, T., and Levine, J.D. (2007). Signaling pathways in sensitization: toward a nociceptor cell biology. *Neuron* 55, 365-376.

Husi, H., Ward, M.A., Choudhary, J.S., Blackstock, W.P., and Grant, S.G. (2000). Proteomic analysis of NMDA receptor-adhesion protein signaling complexes. *Nature neuroscience* 3, 661-669.

Indo, Y., Tsuruta, M., Hayashida, Y., Karim, M.A., Ohta, K., Kawano, T., Mitsubuchi, H., Tonoki, H., Awaya, Y., and Matsuda, I. (1996). Mutations in the TRKA/NGF receptor gene in patients with congenital insensitivity to pain with anhidrosis. *Nature genetics* 13, 485-488.

Inoue, M., Kawashima, T., Allen, R.G., and Ueda, H. (2003). Nocistatin and prepro-nociceptin/orphanin FQ 160-187 cause nociception through activation of Gi/o in capsaicin-sensitive and of Gs in capsaicin-insensitive nociceptors, respectively. *The Journal of pharmacology and experimental therapeutics* 306, 141-146.

Jaquemar, D., Schenker, T., and Trueb, B. (1999). An ankyrin-like protein with transmembrane domains is specifically lost after oncogenic transformation of human fibroblasts. *The Journal of biological chemistry* 274, 7325-7333.

Jensen, L.J., Kuhn, M., Stark, M., Chaffron, S., Creevey, C., Muller, J., Doerks, T., Julien, P., Roth, A., Simonovic, M., *et al.* (2009). STRING 8--a global view on proteins and their functional interactions in 630 organisms. *Nucleic acids research* 37, D412-416.

Ji, R.R., Kohno, T., Moore, K.A., and Woolf, C.J. (2003). Central sensitization and LTP: do pain and memory share similar mechanisms? *Trends in neurosciences* 26, 696-705.

Jordt, S.E., Bautista, D.M., Chuang, H.H., McKemy, D.D., Zygmunt, P.M., Hogestatt, E.D., Meng, I.D., and Julius, D. (2004). Mustard oils and cannabinoids excite sensory nerve fibres through the TRP channel ANKTM1. *Nature* 427, 260-265.

Julius, D. (2013). TRP channels and pain. *Annual review of cell and developmental biology* 29, 355-384.

Karashima, Y., Talavera, K., Everaerts, W., Janssens, A., Kwan, K.Y., Vennekens, R., Nilius, B., and Voets, T. (2009). TRPA1 acts as a cold sensor in vitro and in vivo. *Proceedings of the National Academy of Sciences of the United States of America* 106, 1273-1278.

Keller, A., Nesvizhskii, A.I., Kolker, E., and Aebersold, R. (2002). Empirical statistical model to estimate the accuracy of peptide identifications made by MS/MS and database search. *Analytical chemistry* 74, 5383-5392.

Kidd, B.L., and Urban, L.A. (2001). Mechanisms of inflammatory pain. *British journal of anaesthesia* 87, 3-11.

Kim, A.Y., Tang, Z., Liu, Q., Patel, K.N., Maag, D., Geng, Y., and Dong, X. (2008). Pirt, a phosphoinositide-binding protein, functions as a regulatory subunit of TRPV1. *Cell* 133, 475-485.

Kim, J., and Hajjar, K.A. (2002). Annexin II: a plasminogen-plasminogen activator co-receptor. *Frontiers in bioscience : a journal and virtual library* 7, d341-348.

Knowlton, W.M., Bifulco-Fisher, A., Bautista, D.M., and McKemy, D.D. (2010). TRPM8, but not TRPA1, is required for neural and behavioral responses to acute noxious cold temperatures and cold-mimetics in vivo. *Pain* 150, 340-350.

Kobayashi, K., Fukuoka, T., Obata, K., Yamanaka, H., Dai, Y., Tokunaga, A., and Noguchi, K. (2005). Distinct expression of TRPM8, TRPA1, and TRPV1 mRNAs in rat primary afferent neurons with delta/c-fibers and colocalization with trk receptors. *The Journal of comparative neurology* 493, 596-606.

Koivisto, A., Hukkanen, M., Saarnilehto, M., Chapman, H., Kuokkanen, K., Wei, H., Viisanen, H., Akerman, K.E., Lindstedt, K., and Pertovaara, A. (2012). Inhibiting TRPA1 ion channel reduces loss of cutaneous nerve fiber function in diabetic animals: sustained activation of the TRPA1 channel contributes to the pathogenesis of peripheral diabetic neuropathy. *Pharmacological research* 65, 149-158.

Kollarik, M., Ru, F., and Brozmanova, M. (2010). Vagal afferent nerves with the properties of nociceptors. *Autonomic neuroscience : basic & clinical* 153, 12.

Kremeyer, B., Lopera, F., Cox, J.J., Momin, A., Rugiero, F., Marsh, S., Woods, C.G., Jones, N.G., Paterson, K.J., Fricker, F.R., *et al.* (2010). A gain-of-function mutation in TRPA1 causes familial episodic pain syndrome. *Neuron* 66, 671-680.

Kube, E., Becker, T., Weber, K., and Gerke, V. (1992). Protein-protein interaction studied by site-directed mutagenesis. Characterization of the annexin II-binding site on p11, a member of the S100 protein family. *The Journal of biological chemistry* 267, 14175-14182.

Kudoh, J., Nagamine, K., Asakawa, S., Abe, I., Kawasaki, K., Maeda, H., Tsujimoto, S., Minoshima, S., Ito, F., and Shimizu, N. (1997). Localization of 16 exons to a 450-kb region involved in the autoimmune polyglandular disease type I (APECED) on human chromosome

21q22.3. DNA research : an international journal for rapid publication of reports on genes and genomes 4, 45-52.

Kuharev, J., Navarro, P., Distler, U., Jahn, O., and Tenzer, S. (2015). In-depth evaluation of software tools for data-independent acquisition based label-free quantification. *Proteomics* 15, 3140-3151.

Kumar, C., and Mann, M. (2009). Bioinformatics analysis of mass spectrometry-based proteomics data sets. *FEBS letters* 583, 1703-1712.

Kwan, K.Y., Allchorne, A.J., Vollrath, M.A., Christensen, A.P., Zhang, D.S., Woolf, C.J., and Corey, D.P. (2006). TRPA1 contributes to cold, mechanical, and chemical nociception but is not essential for hair-cell transduction. *Neuron* 50, 277-289.

Laing, R.J., and Dhaka, A. (2015). ThermoTRPs and Pain. *The Neuroscientist : a review journal bringing neurobiology, neurology and psychiatry*.

Lapointe, T.K., and Altier, C. (2011). The role of TRPA1 in visceral inflammation and pain. *Channels (Austin, Tex)* 5, 525-529.

Lee, N., Chen, J., Sun, L., Wu, S., Gray, K.R., Rich, A., Huang, M., Lin, J.H., Feder, J.N., Janovitz, E.B., *et al.* (2003). Expression and characterization of human transient receptor potential melastatin 3 (hTRPM3). *The Journal of biological chemistry* 278, 20890-20897.

Leffler, A., Lattrell, A., Kronewald, S., Niedermirtl, F., and Nau, C. (2011). Activation of TRPA1 by membrane permeable local anesthetics. *Molecular pain* 7, 62.

Leipold, E., Liebmann, L., Korenke, G.C., Heinrich, T., Giesselmann, S., Baets, J., Ebbinghaus, M., Goral, R.O., Stodberg, T., Hennings, J.C., *et al.* (2013). A de novo gain-of-function mutation in SCN11A causes loss of pain perception. *Nature genetics* 45, 1399-1404.

Li, G.Z., Vissers, J.P., Silva, J.C., Golick, D., Gorenstein, M.V., and Geromanos, S.J. (2009). Database searching and accounting of multiplexed precursor and product ion spectra from the data independent analysis of simple and complex peptide mixtures. *Proteomics* 9, 1696-1719.

Liedtke, W., Choe, Y., Marti-Renom, M.A., Bell, A.M., Denis, C.S., Sali, A., Hudspeth, A.J., Friedman, J.M., and Heller, S. (2000). Vanilloid receptor-related osmotically activated channel (VR-OAC), a candidate vertebrate osmoreceptor. *Cell* 103, 525-535.

Ling, Q., Jacovina, A.T., Deora, A., Febbraio, M., Simantov, R., Silverstein, R.L., Hempstead, B., Mark, W.H., and Hajjar, K.A. (2004). Annexin II regulates fibrin homeostasis and neoangiogenesis in vivo. *The Journal of clinical investigation* 113, 38-48.

Liu, X.J., Gingrich, J.R., Vargas-Caballero, M., Dong, Y.N., Sengar, A., Beggs, S., Wang, S.H., Ding, H.K., Frankland, P.W., and Salter, M.W. (2008). Treatment of inflammatory and neuropathic pain by uncoupling Src from the NMDA receptor complex. *Nature medicine* 14, 1325-1332.

Lumpkin, E.A., and Caterina, M.J. (2007). Mechanisms of sensory transduction in the skin. *Nature* 445, 858-865.

Luo, M., and Hajjar, K.A. (2013). Annexin A2 system in human biology: cell surface and beyond. *Seminars in thrombosis and hemostasis* 39, 338-346.

Mabilleau, G., and Edmonds, M.E. (2010). Role of neuropathy on fracture healing in Charcot neuro-osteoarthropathy. *Journal of musculoskeletal & neuronal interactions* 10, 84-91.

Macpherson, L.J., Dubin, A.E., Evans, M.J., Marr, F., Schultz, P.G., Cravatt, B.F., and Patapoutian, A. (2007). Noxious compounds activate TRPA1 ion channels through covalent modification of cysteines. *Nature* 445, 541-545.

Materazzi, S., Fusi, C., Benemei, S., Pedretti, P., Patacchini, R., Nilius, B., Prenen, J., Creminon, C., Geppetti, P., and Nassini, R. (2012). TRPA1 and TRPV4 mediate paclitaxel-induced peripheral neuropathy in mice via a glutathione-sensitive mechanism. *Pflugers Archiv : European journal of physiology* 463, 561-569.

Matta, J.A., Cornett, P.M., Miyares, R.L., Abe, K., Sahibzada, N., and Ahern, G.P. (2008). General anesthetics activate a nociceptive ion channel to enhance pain and inflammation. *Proceedings of the National Academy of Sciences of the United States of America* 105, 8784-8789.

McCoy, D.D., Knowlton, W.M., and McKemy, D.D. (2011). Scraping through the ice: uncovering the role of TRPM8 in cold transduction. *American journal of physiology Regulatory, integrative and comparative physiology* 300, R1278-1287.

McGaraughty, S., Chu, K.L., Perner, R.J., Didomenico, S., Kort, M.E., and Kym, P.R. (2010). TRPA1 modulation of spontaneous and mechanically evoked firing of spinal neurons in uninjured, osteoarthritic, and inflamed rats. *Molecular pain* 6, 14.

McNamara, C.R., Mandel-Brehm, J., Bautista, D.M., Siemens, J., Deranian, K.L., Zhao, M., Hayward, N.J., Chong, J.A., Julius, D., Moran, M.M., and Fanger, C.M. (2007). TRPA1 mediates formalin-induced pain. *Proceedings of the National Academy of Sciences of the United States of America* 104, 13525-13530.

Melemedjian, O.K., Yassine, H.N., Shy, A., and Price, T.J. (2013). Proteomic and functional annotation analysis of injured peripheral nerves reveals ApoE as a protein upregulated by injury that is modulated by metformin treatment. *Molecular pain* 9, 14.

Merskey H, Bogduk N. Classification of Chronic Pain: descriptions of chronic pain syndromes and definitions of pain terms. IASP press, Seattle, 1994, p.210.

Meseguer, V., Alpizar, Y.A., Luis, E., Tajada, S., Denlinger, B., Fajardo, O., Manenschijn, J.A., Fernandez-Pena, C., Talavera, A., Kichko, T., *et al.* (2014). TRPA1 channels mediate acute neurogenic inflammation and pain produced by bacterial endotoxins. *Nature communications* 5, 3125.

Minett, M.S., Quick, K., and Wood, J.N. (2011). Behavioral Measures of Pain Thresholds. *Current protocols in mouse biology* 1, 383-412.

Moiseenkova-Bell, V., and Wensel, T.G. (2011). Functional and structural studies of TRP channels heterologously expressed in budding yeast. *Advances in experimental medicine and biology* 704, 25-40.

Montell, C. (2001). Physiology, phylogeny, and functions of the TRP superfamily of cation channels. *Science's STKE : signal transduction knowledge environment* 2001, re1.

Montell, C., and Rubin, G.M. (1989). Molecular characterization of the *Drosophila trp* locus: a putative integral membrane protein required for phototransduction. *Neuron* 2, 1313-1323.

Moparthi, L., Survery, S., Kreir, M., Simonsen, C., Kjellbom, P., Hogestatt, E.D., Johanson, U., and Zygmunt, P.M. (2014). Human TRPA1 is intrinsically cold- and chemosensitive with and without its N-terminal ankyrin repeat domain. *Proceedings of the National Academy of Sciences of the United States of America* 111, 16901-16906.

Naciff, J.M., Kaetzel, M.A., Behbehani, M.M., and Dedman, J.R. (1996). Differential expression of annexins I-VI in the rat dorsal root ganglia and spinal cord. *The Journal of comparative neurology* 368, 356-370.

Nagata, K., Duggan, A., Kumar, G., and Garcia-Anoveros, J. (2005). Nociceptor and hair cell transducer properties of TRPA1, a channel for pain and hearing. *The Journal of neuroscience : the official journal of the Society for Neuroscience* 25, 4052-4061.

Nagy, I., and Rang, H. (1999). Noxious heat activates all capsaicin-sensitive and also a sub-population of capsaicin-insensitive dorsal root ganglion neurons. *Neuroscience* 88, 995-997.

Nakano, H., Minami, T., Abe, K., Arai, T., Tokumura, M., Ibi, N., Okuda-Ashitaka, E., Mori, H., and Ito, S. (2000). Effect of intrathecal nocistatin on the formalin-induced pain in mice versus that of nociceptin/orphanin FQ. *The Journal of pharmacology and experimental therapeutics* 292, 331-336.

Nassini, R., Gees, M., Harrison, S., De Siena, G., Materazzi, S., Moretto, N., Failli, P., Preti, D., Marchetti, N., Cavazzini, A., *et al.* (2011). Oxaliplatin elicits mechanical and cold allodynia in rodents via TRPA1 receptor stimulation. *Pain* 152, 1621-1631.

Nassini, R., Materazzi, S., Benemei, S., and Geppetti, P. (2014). The TRPA1 channel in inflammatory and neuropathic pain and migraine. *Reviews of physiology, biochemistry and pharmacology* 167, 1-43.

Nautiyal, M., Sweatt, A.J., MacKenzie, J.A., Mark Payne, R., Szucs, S., Matalon, R., Wallin, R., and Hutson, S.M. (2010). Neuronal localization of the mitochondrial protein NIPSNAP1 in rat nervous system. *The European journal of neuroscience* 32, 560-569.

Nilius, B., Appendino, G., and Owsianik, G. (2012). The transient receptor potential channel TRPA1: from gene to pathophysiology. *Pflugers Archiv : European journal of physiology* 464, 425-458.

Nilius, B., and Flockerzi, V. (2014). Mammalian transient receptor potential (TRP) cation channels. Preface. *Handbook of experimental pharmacology* 223, v - vi.

Nilius, B., Owsianik, G., Voets, T., and Peters, J.A. (2007). Transient receptor potential cation channels in disease. *Physiological reviews* 87, 165-217.

Nilius, B., Prenen, J., and Owsianik, G. (2011). Irritating channels: the case of TRPA1. *The Journal of physiology* 589, 1543-1549.

Ning, L., Wang, C., Ding, X., Zhang, Y., Wang, X., and Yue, S. (2012). Functional interaction of TRPV4 channel protein with annexin A2 in DRG. *Neurological research* 34, 685-693.

Obata, K., Katsura, H., Mizushima, T., Yamanaka, H., Kobayashi, K., Dai, Y., Fukuoka, T., Tokunaga, A., Tominaga, M., and Noguchi, K. (2005). TRPA1 induced in sensory neurons contributes to cold hyperalgesia after inflammation and nerve injury. *The Journal of clinical investigation* 115, 2393-2401.

Okuda-Ashitaka, E., and Ito, S. (2015). Nocistatin: milestone of one decade of research. *Current pharmaceutical design* 21, 868-884.

Okuda-Ashitaka, E., Minami, T., Tachibana, S., Yoshihara, Y., Nishiuchi, Y., Kimura, T., and Ito, S. (1998). Nocistatin, a peptide that blocks nociceptin action in pain transmission. *Nature* 392, 286-289.

Okuda-Ashitaka, E., Minami, T., Tsubouchi, S., Kiyonari, H., Iwamatsu, A., Noda, T., Handa, H., and Ito, S. (2012). Identification of NIPSNAP1 as a nocistatin-interacting protein involving pain transmission. *The Journal of biological chemistry* 287, 10403-10413.

Okuse, K., Malik-Hall, M., Baker, M.D., Poon, W.Y., Kong, H., Chao, M.V., and Wood, J.N. (2002). Annexin II light chain regulates sensory neuron-specific sodium channel expression. *Nature* 417, 653-656.

Ong, S.E., and Mann, M. (2005). Mass spectrometry-based proteomics turns quantitative. *Nature chemical biology* 1, 252-262.

Oveland, E., Muth, T., Rapp, E., Martens, L., Berven, F.S., and Barsnes, H. (2015). Viewing the proteome: how to visualize proteomics data? *Proteomics* 15, 1341-1355.

Park, C.K., Xu, Z.Z., Berta, T., Han, Q., Chen, G., Liu, X.J., and Ji, R.R. (2014). Extracellular microRNAs activate nociceptor neurons to elicit pain via TLR7 and TRPA1. *Neuron* 82, 47-54.

Parks, D.J., Parsons, W.H., Colburn, R.W., Meegalla, S.K., Ballentine, S.K., Illig, C.R., Qin, N., Liu, Y., Hutchinson, T.L., Lubin, M.L., *et al.* (2011). Design and optimization of benzimidazole-

containing transient receptor potential melastatin 8 (TRPM8) antagonists. *Journal of medicinal chemistry* 54, 233-247.

Patapoutian, A., Peier, A.M., Story, G.M., and Viswanath, V. (2003). ThermoTRP channels and beyond: mechanisms of temperature sensation. *Nature reviews Neuroscience* 4, 529-539.

Patapoutian, A., Tate, S., and Woolf, C.J. (2009). Transient receptor potential channels: targeting pain at the source. *Nature reviews Drug discovery* 8, 55-68.

Paulsen, C.E., Armache, J.P., Gao, Y., Cheng, Y., and Julius, D. (2015). Structure of the TRPA1 ion channel suggests regulatory mechanisms. *Nature* 525, 552.

Pecze, L., Pelsoczi, P., Kecskes, M., Winter, Z., Papp, A., Kaszas, K., Letoha, T., Vizler, C., and Olah, Z. (2009). Resiniferatoxin mediated ablation of TRPV1+ neurons removes TRPA1 as well. *The Canadian journal of neurological sciences Le journal canadien des sciences neurologiques* 36, 234-241.

Peier, A.M., Moqrich, A., Hergarden, A.C., Reeve, A.J., Andersson, D.A., Story, G.M., Earley, T.J., Dragoni, I., McIntyre, P., Bevan, S., and Patapoutian, A. (2002a). A TRP channel that senses cold stimuli and menthol. *Cell* 108, 705-715.

Peier, A.M., Reeve, A.J., Andersson, D.A., Moqrich, A., Earley, T.J., Hergarden, A.C., Story, G.M., Colley, S., Hogenesch, J.B., McIntyre, P., *et al.* (2002b). A heat-sensitive TRP channel expressed in keratinocytes. *Science (New York, NY)* 296, 2046-2049.

Petrus, M., Peier, A.M., Bandell, M., Hwang, S.W., Huynh, T., Olney, N., Jegla, T., and Patapoutian, A. (2007). A role of TRPA1 in mechanical hyperalgesia is revealed by pharmacological inhibition. *Molecular pain* 3, 40.

Pingle, S.C., Matta, J.A., and Ahern, G.P. (2007). Capsaicin receptor: TRPV1 a promiscuous TRP channel. *Handbook of experimental pharmacology*, 155-171.

Ramsey, I.S., Delling, M., and Clapham, D.E. (2006). An introduction to TRP channels. *Annual review of physiology* 68, 619-647.

Rankin, C.R., Hilgarth, R.S., Leoni, G., Kwon, M., Den Beste, K.A., Parkos, C.A., and Nusrat, A. (2013). Annexin A2 regulates beta1 integrin internalization and intestinal epithelial cell migration. *The Journal of biological chemistry* 288, 15229-15239.

Rescher, U., and Gerke, V. (2004). Annexins--unique membrane binding proteins with diverse functions. *Journal of cell science* 117, 2631-2639.

Rouvette, T., Avenali, L., Sondermann, J., Narayanan, P., Gomez-Varela, D., and Schmidt, M. (2015). Modulation of nociceptive ion channels and receptors via protein-protein interactions: implications for pain relief. *Channels (Austin, Tex)* 9, 175-185.

Ruparel, N.B., Patwardhan, A.M., Akopian, A.N., and Hargreaves, K.M. (2008). Homologous and heterologous desensitization of capsaicin and mustard oil responses utilize different cellular pathways in nociceptors. *Pain* 135, 271-279.

Salas, M.M., Hargreaves, K.M., and Akopian, A.N. (2009). TRPA1-mediated responses in trigeminal sensory neurons: interaction between TRPA1 and TRPV1. *The European journal of neuroscience* 29, 1568-1578.

Samad, A. (2011). The C-terminal basic residues contribute to the chemical- and. 433, 197-204.

Satoh, K., Takeuchi, M., Oda, Y., Deguchi-Tawarada, M., Sakamoto, Y., Matsubara, K., Nagasu, T., and Takai, Y. (2002). Identification of activity-regulated proteins in the postsynaptic density fraction. *Genes to cells : devoted to molecular & cellular mechanisms* 7, 187-197.

Schmidt, C., Hesse, D., Raabe, M., Urlaub, H., and Jahn, O. (2013). An automated in-gel digestion/iTRAQ-labeling workflow for robust quantification of gel-separated proteins. *Proteomics* 13, 1417-1422.

Schmidt, M., Dubin, A.E., Petrus, M.J., Earley, T.J., and Patapoutian, A. (2009). Nociceptive signals induce trafficking of TRPA1 to the plasma membrane. *Neuron* 64, 498-509.

Schoeber, J.P., Topala, C.N., Lee, K.P., Lambers, T.T., Ricard, G., van der Kemp, A.W., Huynen, M.A., Hoenderop, J.G., and Bindels, R.J. (2008). Identification of Nipsnap1 as a novel auxiliary protein inhibiting TRPV6 activity. *Pflugers Archiv : European journal of physiology* 457, 91-101.

Schwenk, J., Harmel, N., Brechet, A., Zolles, G., Berkefeld, H., Muller, C.S., Bildl, W., Baehrens, D., Huber, B., Kulik, A., *et al.* (2012). High-resolution proteomics unravel architecture and molecular diversity of native AMPA receptor complexes. *Neuron* 74, 621-633.

Schwenk, J., Harmel, N., Zolles, G., Bildl, W., Kulik, A., Heimrich, B., Chisaka, O., Jonas, P., Schulte, U., Fakler, B., and Klocker, N. (2009). Functional proteomics identify cornichon proteins as auxiliary subunits of AMPA receptors. *Science (New York, NY)* 323, 1313-1319.

Seroussi, E., Pan, H.Q., Kedra, D., Roe, B.A., and Dumanski, J.P. (1998). Characterization of the human NIPSNAP1 gene from 22q12: a member of a novel gene family. *Gene* 212, 13-20.

Sherrington, C.S. (1903). Qualitative difference of spinal reflex corresponding with qualitative difference of cutaneous stimulus. *The Journal of physiology* 30, 39-46.

Sherrington C. *The Integrative Action of the Nervous System*. Oxford: Oxford University Press; 1906.

Silva, J.C., Denny, R., Dorschel, C.A., Gorenstein, M., Kass, I.J., Li, G.Z., McKenna, T., Nold, M.J., Richardson, K., Young, P., and Geromanos, S. (2005). Quantitative proteomic analysis by accurate mass retention time pairs. *Analytical chemistry* 77, 2187-2200.

Silva, J.C., Gorenstein, M.V., Li, G.Z., Vissers, J.P., and Geromanos, S.J. (2006). Absolute quantification of proteins by LCMSE: a virtue of parallel MS acquisition. *Molecular & cellular proteomics* : MCP 5, 144-156.

Smani, T., Shapovalov, G., Skryma, R., Prevarskaya, N., and Rosado, J.A. (2015). Functional and physiopathological implications of TRP channels. *Biochimica et biophysica acta* 1853, 1772-1782.

Smith, G.D., Gunthorpe, M.J., Kelsell, R.E., Hayes, P.D., Reilly, P., Facer, P., Wright, J.E., Jerman, J.C., Walhin, J.P., Ooi, L., *et al.* (2002). TRPV3 is a temperature-sensitive vanilloid receptor-like protein. *Nature* 418, 186-190.

Snider, W.D., and McMahon, S.B. (1998). Tackling pain at the source: new ideas about nociceptors. *Neuron* 20, 629-632.

Sorge, R.E., Mapplebeck, J.C.S., Rosen, S., Beggs, S., Taves, S., Alexander, J.K., Martin, L.J., Austin, J.-S., Sotocinal, S.G., Chen, D., *et al.* (2015). Different immune cells mediate mechanical pain hypersensitivity in male and female mice. *Nature neuroscience* 18, 1081-1083.

Sousa-Valente, J., Andreou, A.P., Urban, L., and Nagy, I. (2014). Transient receptor potential ion channels in primary sensory neurons as targets for novel analgesics. *British journal of pharmacology* 171, 2508-2527.

Statuschenko, A., Jeske, N.A., and Akopian, A.N. (2010). Contribution of TRPV1-TRPA1 interaction to the single channel properties of the TRPA1 channel. *The Journal of biological chemistry* 285, 15167-15177.

Stokes, A., Wakano, C., Koblan-Huberson, M., Adra, C.N., Fleig, A., and Turner, H. (2006). TRPA1 is a substrate for de-ubiquitination by the tumor suppressor CYLD. *Cellular signalling* 18, 1584-1594.

Story, G.M., Peier, A.M., Reeve, A.J., Eid, S.R., Mosbacher, J., Hricik, T.R., Earley, T.J., Hergarden, A.C., Andersson, D.A., Hwang, S.W., *et al.* (2003). ANKTM1, a TRP-like channel expressed in nociceptive neurons, is activated by cold temperatures. *Cell* 112, 819-829.

Svenningsson, P., Chergui, K., Rachleff, I., Flajolet, M., Zhang, X., El Yacoubi, M., Vaugeois, J.M., Nomikos, G.G., and Greengard, P. (2006). Alterations in 5-HT<sub>1B</sub> receptor function by p11 in depression-like states. *Science (New York, NY)* 311, 77-80.

Szabo, A., Helyes, Z., Sandor, K., Bite, A., Pinter, E., Nemeth, J., Banvolgyi, A., Bolcskei, K., Elekes, K., and Szolcsanyi, J. (2005). Role of transient receptor potential vanilloid 1 receptors in adjuvant-induced chronic arthritis: in vivo study using gene-deficient mice. *The Journal of pharmacology and experimental therapeutics* 314, 111-119.

Tamma, G., Procino, G., Mola, M.G., Svelto, M., and Valenti, G. (2008). Functional involvement of Annexin-2 in cAMP induced AQP2 trafficking. *Pflugers Archiv : European journal of physiology* 456, 729-736.

Tappe-Theodor, A., Agarwal, N., Katona, I., Rubino, T., Martini, L., Swiercz, J., Mackie, K., Monyer, H., Parolaro, D., Whistler, J., *et al.* (2007). A molecular basis of analgesic tolerance to cannabinoids. *The Journal of neuroscience : the official journal of the Society for Neuroscience* 27, 4165-4177.

Tappe, A., Klugmann, M., Luo, C., Hirlinger, D., Agarwal, N., Benrath, J., Ehrenguber, M.U., Doring, M.J., and Kuner, R. (2006). Synaptic scaffolding protein Homer1a protects against chronic inflammatory pain. *Nature medicine* 12, 677-681.

Taylor-Clark, T.E., McAlexander, M.A., Nassenstein, C., Sheardown, S.A., Wilson, S., Thornton, J., Carr, M.J., and Undem, B.J. (2008a). Relative contributions of TRPA1 and TRPV1 channels in the activation of vagal bronchopulmonary C-fibres by the endogenous autacoid 4-oxononanal. *The Journal of physiology* 586, 3447-3459.

Taylor-Clark, T.E., Undem, B.J., Macglashan, D.W., Jr., Ghatta, S., Carr, M.J., and McAlexander, M.A. (2008b). Prostaglandin-induced activation of nociceptive neurons via direct interaction with transient receptor potential A1 (TRPA1). *Molecular pharmacology* 73, 274-281.

Trevisani, M., Siemens, J., Materazzi, S., Bautista, D.M., Nassini, R., Campi, B., Imamachi, N., Andre, E., Patacchini, R., Cottrell, G.S., *et al.* (2007). 4-Hydroxynonanal, an endogenous aldehyde, causes pain and neurogenic inflammation through activation of the irritant receptor TRPA1. *Proceedings of the National Academy of Sciences of the United States of America* 104, 13519-13524.

Tu, W., Xu, X., Peng, L., Zhong, X., Zhang, W., Soundarapandian, M.M., Balel, C., Wang, M., Jia, N., Zhang, W., *et al.* (2010). DAPK1 interaction with NMDA receptor NR2B subunits mediates brain damage in stroke. *Cell* 140, 222-234.

Tummala, H., Li, X., and Homayouni, R. (2010). Interaction of a novel mitochondrial protein, 4-nitrophenylphosphatase domain and non-neuronal SNAP25-like protein homolog 1 (NIPSNAP1), with the amyloid precursor protein family. *The European journal of neuroscience* 31, 1926-1934.

Ueda, H., and Ueda, M. (2009). Mechanisms underlying morphine analgesic tolerance and dependence. *Front Biosci (Landmark Ed)* 14, 5260-5272.

Vacca, V., Marinelli, S., Pieroni, L., Urbani, A., Luvisetto, S., and Pavone, F. (2014). Higher pain perception and lack of recovery from neuropathic pain in females: a behavioural, immunohistochemical, and proteomic investigation on sex-related differences in mice. *Pain* 155, 388-402.

van de Graaf, S.F., Hoenderop, J.G., Gkika, D., Lamers, D., Prenen, J., Rescher, U., Gerke, V., Staub, O., Nilius, B., and Bindels, R.J. (2003). Functional expression of the epithelial Ca(2+)

channels (TRPV5 and TRPV6) requires association of the S100A10-annexin 2 complex. The EMBO journal 22, 1478-1487.

Van den Oever, M.C., Goriounova, N.A., Li, K.W., Van der Schors, R.C., Binnekade, R., Schoffelmeer, A.N., Mansvelder, H.D., Smit, A.B., Spijker, S., and De Vries, T.J. (2008). Prefrontal cortex AMPA receptor plasticity is crucial for cue-induced relapse to heroin-seeking. Nature neuroscience 11, 1053-1058.

Vandewauw, I., Owsianik, G., and Voets, T. (2013). Systematic and quantitative mRNA expression analysis of TRP channel genes at the single trigeminal and dorsal root ganglion level in mouse. BMC neuroscience 14, 21.

Vriens, J., Owsianik, G., Hofmann, T., Philipp, S.E., Stab, J., Chen, X., Benoit, M., Xue, F., Janssens, A., Kerselaers, S., *et al.* (2011). TRPM3 is a nociceptor channel involved in the detection of noxious heat. Neuron 70, 482-494.

Wan, X., Lu, Y., Chen, X., Xiong, J., Zhou, Y., Li, P., Xia, B., Li, M., Zhu, M.X., and Gao, Z. (2014). Bimodal voltage dependence of TRPA1: mutations of a key pore helix residue reveal strong intrinsic voltage-dependent inactivation. Pflugers Archiv : European journal of physiology 466, 1273-1287.

Wang, S., Dai, Y., Fukuoka, T., Yamanaka, H., Kobayashi, K., Obata, K., Cui, X., Tominaga, M., and Noguchi, K. (2008a). Phospholipase C and protein kinase A mediate bradykinin sensitization of TRPA1: a molecular mechanism of inflammatory pain. Brain : a journal of neurology 131, 1241-1251.

Wang, X., Miyares, R.L., and Ahern, G.P. (2005). Oleoylethanolamide excites vagal sensory neurones, induces visceral pain and reduces short-term food intake in mice via capsaicin receptor TRPV1. The Journal of physiology 564, 541-547.

Wang, X., Zhang, J., Eberhart, D., Urban, R., Meda, K., Solorzano, C., Yamanaka, H., Rice, D., and Basbaum, A.I. (2013). Excitatory superficial dorsal horn interneurons are functionally heterogeneous and required for the full behavioral expression of pain and itch. Neuron 78, 312-324.

Wang, Y.Y., Chang, R.B., Waters, H.N., McKemy, D.D., and Liman, E.R. (2008b). The nociceptor ion channel TRPA1 is potentiated and inactivated by permeating calcium ions. The Journal of biological chemistry 283, 32691-32703.

Weng, H.J., Patel, K.N., Jeske, N.A., Bierbower, S.M., Zou, W., Tiwari, V., Zheng, Q., Tang, Z., Mo, G.C., Wang, Y., *et al.* (2015). Tmem100 Is a Regulator of TRPA1-TRPV1 Complex and Contributes to Persistent Pain. Neuron.

Wood, J.N., Abrahamsen, B., Baker, M.D., Boorman, J.D., Donier, E., Drew, L.J., Nassar, M.A., Okuse, K., Seereeram, A., Stirling, C.L., and Zhao, J. (2004). Ion channel activities implicated in pathological pain. Novartis Foundation symposium 261, 32-40; discussion 40-54.

Woolf, C.J. (2010). What is this thing called pain? *The Journal of clinical investigation* 120, 3742-3744.

Woolf, C.J., and Ma, Q. (2007). Nociceptors--noxious stimulus detectors. *Neuron* 55, 353-364.

Xu, I.S., Hashemi, M., Calo, G., Regoli, D., Wiesenfeld-Hallin, Z., and Xu, X.J. (1999). Effects of intrathecal nocistatin on the flexor reflex and its interaction with orphanin FQ nociceptin. *Neuroreport* 10, 3681-3684.

Zeilhofer, H.U., Selbach, U.M., Guhring, H., Erb, K., and Ahmadi, S. (2000). Selective suppression of inhibitory synaptic transmission by nocistatin in the rat spinal cord dorsal horn. *The Journal of neuroscience : the official journal of the Society for Neuroscience* 20, 4922-4929.

Zhang, X., Li, L., and McNaughton, P.A. (2008). Proinflammatory mediators modulate the heat-activated ion channel TRPV1 via the scaffolding protein AKAP79/150. *Neuron* 59, 450-461.

Zheng, J. (2013). Molecular mechanism of TRP channels. *Comprehensive Physiology* 3, 221-242.

Zhou, X.L., Batiza, A.F., Loukin, S.H., Palmer, C.P., Kung, C., and Saimi, Y. (2003). The transient receptor potential channel on the yeast vacuole is mechanosensitive. *Proceedings of the National Academy of Sciences of the United States of America* 100, 7105-7110.

Zhou, Y., Suzuki, Y., Uchida, K., and Tominaga, M. (2013). Identification of a splice variant of mouse TRPA1 that regulates TRPA1 activity. *Nature communications* 4, 2399.

Zitt, C., Zobel, A., Obukhov, A.G., Harteneck, C., Kalkbrenner, F., Luckhoff, A., and Schultz, G. (1996). Cloning and functional expression of a human Ca<sup>2+</sup>-permeable cation channel activated by calcium store depletion. *Neuron* 16, 1189-1196.

Zou, W., Zhan, X., Li, M., Song, Z., Liu, C., Peng, F., and Guo, Q. (2012). Identification of differentially expressed proteins in the spinal cord of neuropathic pain models with PKC $\gamma$  silence by proteomic analysis. *Brain research* 1440, 34-46.

Zurborg, S., Yurgionas, B., Jira, J.A., Caspani, O., and Heppenstall, P.A. (2007). Direct activation of the ion channel TRPA1 by Ca<sup>2+</sup>. *Nature neuroscience* 10, 277-279.

## Acknowledgments

I would like to express my deepest gratitude to my supervisor Dr. Manuela Schmidt for the opportunity to study in her lab, for the constant support and for the guidance during these challenging years of my PhD. Thank you so much Manuela.

I am sincerely grateful also to Dr. David Gomez-Varela for his help whenever it was needed, his guidance and all the interesting scientific as well as non-scientific discussions. Thank you so much David.

Thank you Manuela and David for all you have taught me during this PhD and for your support at any time, especially the most difficult ones.

I would also like to extend my deep appreciation to Prof. Dr. Martin C. Göpfert and Prof. Dr. Klaus-Armin Nave for the fruitful discussions and helpful suggestions as members of my PhD thesis committee.

I am grateful to Prof. Dr. Michael W. Sereda, Prof. Dr. Luis A. Pardo and Prof. Dr. Ralf Heinrich for their willingness to take part to my examination board.

I wish to acknowledge all collaborators for their essential contribution: Dr. Olaf Jahn, Prof. Dr. Michael W. Sereda, Dr. Susanne Quintes and Dr. Ilaria Cervellini.

Special thanks go to Julia, Pratibha, Sergej, Tom, Oli and Madlen for their contribution to all this, their help, fruitful discussions and the pleasant time spent together.

I had the opportunity to be a member of the GGNB Sensory and Motor Neuroscience program. I would like to thank the whole GGNB team for accepting me in this excellent graduate program, for the travel grant and especially for their kind assistance during these years of my PhD.

As I promised, I would like to deeply thank Dr. med. Johannes Meller, Dr. med. Carsten-Oliver Sahlmann, all the members of the division of Nuclear Medicine of the UMG and especially Dr. med. Marianne Lückerrath for their special role in making all this possible.

Tutto questo non sarebbe stato possibile senza l'aiuto della mia famiglia. Prima di tutto i miei amori grandi Leonardo e Cristina che mi sono stati sempre vicino, e poi babbo mamma e mio fratello che anche da lontano ci hanno fatto sentire sempre a casa. Grazie nonni Urbano, Patrizia, Luciano, Luisa per tutti i viaggi e l'aiuto in questi anni. Grazie a tutti!

**Appendix. List of proteins identified in the interactomics screening for TRPA1-protein complexes in inflammatory pain according to the Venn diagram and the criteria shown in figure 13A.**

**A) Proteins belonging to the dataset “Only in CFA”**

<b>Description</b>	<b>Gene name</b>	<b>Uniprot accession</b>
Ras-related protein Rab-7a OS=Mus musculus GN=Rab7a PE=1 SV=2	Rab7a	P51150
AP-2 complex subunit alpha-1 OS=Mus musculus GN=Ap2a1 PE=1 SV=1	Ap2a1	P17426
Protein transport protein Sec31A OS=Mus musculus GN=Sec31a PE=1 SV=2	Sec31a	Q3UPL0
Dual specificity protein phosphatase 15 OS=Mus musculus GN=Dusp15 PE=2 SV=3	Dusp15	Q8R4V2
ATP synthase subunit f, mitochondrial OS=Mus musculus GN=Atp5j2 PE=1 SV=3	Atp5j2	P56135
Serine/arginine-rich splicing factor 2 OS=Mus musculus GN=Srsf2 PE=1 SV=4	Srsf2	Q62093
Myelin P2 protein OS=Mus musculus GN=Pmp2 PE=2 SV=2	Pmp2	P24526
Rho-related GTP-binding protein RhoG OS=Mus musculus GN=Rhog PE=2 SV=1	Rhog	P84096
AP-2 complex subunit sigma OS=Mus musculus GN=Ap2s1 PE=1 SV=1	Ap2s1	P62743
F-actin-capping protein subunit beta OS=Mus musculus GN=Capzb PE=1 SV=3	Capzb	P47757
Alpha-actinin-1 OS=Mus musculus GN=Actn1 PE=1 SV=1	Actn1	Q7TPR4
40S ribosomal protein S25 OS=Mus musculus GN=Rps25 PE=1 SV=1	Rps25	P62852
60S acidic ribosomal protein P1 OS=Mus musculus GN=Rplp1 PE=2 SV=1	Rplp1	P47955
Tropomyosin beta chain OS=Mus musculus GN=Tpm2 PE=1 SV=1	Tpm2	P58774
Unconventional myosin-I <sub>f</sub> OS=Mus musculus GN=Myo1f PE=1 SV=1	Myo1f	P70248
Histone H1.5 OS=Mus musculus GN=Hist1h1b PE=1 SV=2	Hist1h1b	P43276
60S ribosomal protein L36a OS=Mus musculus GN=Rpl36a PE=1 SV=2	Rpl36a	P83882
Myosin light chain 6B OS=Mus musculus GN=Myl6b PE=2 SV=1	Myl6b	Q8CI43
Proteasome subunit alpha type-2 OS=Mus musculus GN=Psm2 PE=1 SV=3	Psm2	P49722

ATP synthase subunit delta, mitochondrial OS=Mus musculus GN=Atp5d PE=1 SV=1	Atp5d	Q9D3D9
60S ribosomal protein L38 OS=Mus musculus GN=Rpl38 PE=2 SV=3	Rpl38	Q9JJI8
Ferritin light chain 1 OS=Mus musculus GN=Ftl1 PE=1 SV=2	Ftl1	P29391
Ubiquitin-associated protein 2-like OS=Mus musculus GN=Uba2l1 PE=1 SV=1	Uba2l1	Q80X50
60S ribosomal protein L35a OS=Mus musculus GN=Rpl35a PE=1 SV=2	Rpl35a	O55142
Syntenin-1 OS=Mus musculus GN=Sdcbp PE=1 SV=1	Sdcbp	O08992
60S ribosomal protein L13 OS=Mus musculus GN=Rpl13 PE=2 SV=3	Rpl13	P47963
Epidermal growth factor receptor substrate 15 OS=Mus musculus GN=Eps15 PE=1 SV=1	Eps15	P42567
Collagen alpha-1(XIV) chain OS=Mus musculus GN=Col14a1 PE=2 SV=2	Col14a1	Q80X19
Glutathione S-transferase Mu 1 OS=Mus musculus GN=Gstm1 PE=1 SV=2	Gstm1	P10649
Apolipoprotein O OS=Mus musculus GN=Apoo PE=2 SV=1	Apoo	Q9DCZ4
Integral membrane protein 2C OS=Mus musculus GN=Itm2c PE=2 SV=2	Itm2c	Q91VK4

## B) Proteins belonging to the dataset “Only in VEH”

Description	Gene name	Uniprot accession
Inosine-5'-monophosphate dehydrogenase 1 OS=Mus musculus GN=Impdh1 PE=2 SV=2	Impdh1	P50096
Kinesin-like protein KIF3A OS=Mus musculus GN=Kif3a PE=1 SV=2	Kif3a	P28741
Ubiquitin-like modifier-activating enzyme 1 OS=Mus musculus GN=Uba1 PE=1 SV=1	Uba1	Q02053
Leucine-rich repeat flightless-interacting protein 1 OS=Mus musculus GN=Lrrfip1 PE=1 SV=2	Lrrfip1	Q3UZ39
1-acyl-sn-glycerol-3-phosphate acyltransferase epsilon OS=Mus musculus GN=Agpat5 PE=2 SV=2	Agpat5	Q9D1E8
PRA1 family protein 3 OS=Mus musculus GN=Arl6ip5 PE=1 SV=2	Arl6ip5	Q8R5J9
Nucleosome assembly protein 1-like 4 OS=Mus musculus GN=Nap1l4 PE=1 SV=1	Nap1l4	Q78ZA7
Serine/arginine-rich splicing factor 10 OS=Mus musculus	Srsf10	Q9R0U0

GN=Srsf10 PE=1 SV=2		
Serpin H1 OS=Mus musculus GN=Serpinh1 PE=1 SV=3	Serpinh1	P19324
Eukaryotic initiation factor 4A-III OS=Mus musculus GN=Eif4a3 PE=2 SV=3	Eif4a3	Q91VC3
Eukaryotic translation initiation factor 2 subunit 3, X-linked OS=Mus musculus GN=Eif2s3x PE=1 SV=2	Eif2s3x	Q9Z0N1
RNA-binding protein 39 OS=Mus musculus GN=Rbm39 PE=1 SV=2	Rbm39	Q8VH51
ATPase Asna1 OS=Mus musculus GN=Asna1 PE=1 SV=2	Asna1	O54984
Ras GTPase-activating protein-binding protein 1 OS=Mus musculus GN=G3bp1 PE=1 SV=1	G3bp1	P97855
Junctional adhesion molecule C OS=Mus musculus GN=Jam3 PE=1 SV=2	Jam3	Q9D8B7
Plastin-2 OS=Mus musculus GN=Lcp1 PE=1 SV=4	Lcp1	Q61233
40S ribosomal protein S17 OS=Mus musculus GN=Rps17 PE=1 SV=2	Rps17	P63276
Clathrin interactor 1 OS=Mus musculus GN=Clint1 PE=1 SV=2	Clint1	Q99KN9
Ras-related protein Rap-1b OS=Mus musculus GN=Rap1b PE=2 SV=2	Rap1b	Q99JI6
Dedicator of cytokinesis protein 7 OS=Mus musculus GN=Dock7 PE=1 SV=3	Dock7	Q8R1A4
Syntaxin-8 OS=Mus musculus GN=Stx8 PE=1 SV=1	Stx8	O88983
BAG family molecular chaperone regulator 2 OS=Mus musculus GN=Bag2 PE=1 SV=1	Bag2	Q91YN9
Myosin light chain 3 OS=Mus musculus GN=Myl3 PE=1 SV=4	Myl3	P09542
26S protease regulatory subunit 4 OS=Mus musculus GN=Psmc1 PE=1 SV=1	Psmc1	P62192

### C) Proteins belonging to the dataset "In both"

Description	Gene name	Uniprot accession
Ras-related protein Rab-8B OS=Mus musculus GN=Rab8b PE=1 SV=1	Rab8b	P61028
39S ribosomal protein L11, mitochondrial OS=Mus musculus GN=Mrpl11 PE=2 SV=1	Mrpl11	Q9CQF0
Serine/threonine-protein phosphatase PGAM5, mitochondrial OS=Mus musculus GN=Pgam5 PE=2 SV=1	Pgam5	Q8BX10

# Curriculum vitae

## Personal information

**Name, Surname** Luca, Avenali  
**Date and place of birth** 23.10.1986 in Jesi, Italy  
**Nationality** Italian  
**Office address** Somatosensory Signalling Group  
Max Planck Institute of Experimental Medicine  
Hermann-Rein Strasse 3  
D-37075, Göttingen, Germany  
Phone: +49 (0) 551 3899 578  
Email: avenali@em.mpg.de; luca.avenali@gmail.com

## Scientific education

**12/2012 – present** PhD student at Somatosensory Signalling Group  
Max Planck Institute of Experimental Medicine, Göttingen, Germany  
Supervisor: Dr. Manuela Schmidt  
Thesis: “Characterization of protein complexes associated with TRP channels in the context of nociception”

**10/2008 – 07/2010** **Master’s degree in Pharmaceutical Biotechnology**  
University of Camerino, Camerino, Italy  
Grade: Full marks (110/110) with honours  
Thesis: “A novel gold(I)-phosphine complex induces mitochondria-mediated apoptosis in colon cancer cells”

**10/2005 – 10/2008** **Bachelor’s Degree in Biotechnology**  
University of Camerino, Camerino, Italy  
Grade: Full marks (110/110) with honours  
Thesis: “Binding of the potential chemotherapeutic agent Thymoquinone and flavonoids to the acute phase carrier Alpha1-Acid Glycoprotein”

## Awards, stipends

Förderpreis für Schmerzforschung 2015 (1st place) awarded by the Deutsche Schmerzgesellschaft, section of the International Association for the Study of Pain (IASP).

Excellence fellowship from University of Camerino for the years from 2005 to 2010.

## Publications

T. Rouwette, J. Sondermann, **L. Avenali**, D. Gomez-Varela and M. Schmidt. Standardized proteome profiling of mouse dorsal root ganglia provides novel insights into chronic pain. In submission.

T. Rouwette, **L. Avenali**, J. Sondermann, P. Narayanan, D. Gomez-Varela and M. Schmidt (2015). "Modulation of nociceptive ion channels and receptors via protein-protein interactions: implications for pain relief." Channels (Austin) **9**(4): 175-185.

**Avenali, L.**, P. Narayanan, T. Rouwette, I. Cervellini, M. Sereda, D. Gomez-Varela and M. Schmidt (2014). "Annexin A2 regulates TRPA1-dependent nociception." J Neurosci **34**(44): 14506-14516.

Lupidi, G., **L. Avenali**, M. Bramucci, L. Quassinti, R. Pettinari, H. K. Khalife, H. Gali-Muhtasib, F. Marchetti and C. Pettinari (2013). "Synthesis, properties, and antitumor effects of a new mixed phosphine gold(I) compound in human colon cancer cells." J Inorg Biochem **124**: 78-87.

Lupidi, G., E. Camaioni, H. Khalife, **L. Avenali**, E. Damiani, F. Tanfani and A. Scire (2012). "Characterization of thymoquinone binding to human alpha(1)-acid glycoprotein." J Pharm Sci **101**(7): 2564-2573.

Lupidi G, Bramucci M, Quassinti L, Fornari E, **Avenali L**, Khalife H, Gali-Muhtasib H. (2011). "Antiproliferative activities of Artemisia herba-alba ethanolic extract in human colon cancer cell line (HCT116)". Alternative Medicine Studies; volume 1:e14.

## Conference participation

**03/2015** 94th Annual Meeting of the German Physiological Society (talk contribution)

Magdeburg, Germany

**05/2015** Neurizons 2015 (poster contribution)

Göttingen, Germany

**10/2015** Neuroscience 2015: Society for Neuroscience annual meeting (poster contribution)

Chicago, USA